Institute of Clinical and Experimental Trauma Immunology,

Ulm University Hospital

Prof. Dr. med. Markus Huber-Lang

TriFu effectively modulates the complement system activation in a rat xenotransfusion model

Dissertation submitted in partial fulfillment of the requirements for the degree of "Doctor of Philosophy" (PhD) of the International Graduate School in Molecular Medicine Ulm

Susa Savukoski

Born in Alavieska, Finland

2026

Current Dean of the Medical Faculty: Prof. Dr. Thomas Wirth

Current Dean of the Graduate School: Prof. Dr. Bernd Knöll

Thesis Advisory Committee:

1st supervisor: Prof. Dr. Markus Huber-Lang

2nd supervisor: Prof. Dr. Holger Barth

3rd supervisor: Prof. Dr. Kristina Nilsson-Ekdahl

External Reviewers:

Prof. Dr. Michael Kirschfink

Day doctorate awarded: 23.10.2026

Results gained during my doctoral thesis have previously been published in the following journals:

Savukoski S, Dettner AM, Schultze A, Gerber C, Steinberger MS, Halbgebauer R, Melter P, Dopler A, Palmer A, Braun CK, Hafner S, Nilsson B, Ekdahl KN, Mollnes TE, Heller R, Schrezenmeier H, Schmidt CQ, Huber-Lang MS, Mannes M: In vivo evidence of effective complement modulation by TriFu in comparison to C5 inhibition and complement depletion. Blood Adv (2026)

© 2026 American Society of Hematology. Published by Elsevier Inc. Licensed under Creative Commons Attribution-NonCommercial-NoDerivatives 4.0 International (CC BY-NC-ND 4.0), https://creativecommons.org/licenses/by-nc-nd/4.0/legalcode.en

Further publications with my contribution which are not associated with this thesis:

Original articles:

Bauer A, **Savukoski S**, Dettner A, Braun CK, Schultze A, Achatz G, Friemert B, Melnyk M, Mannes M, Huber-Lang M: Early Inflammatory Activation of Platelets and Neutrophils by Volume Resuscitation in a Human Whole Blood Model Mimicking a Severe Trauma-Related Micromilieu. Shock 65:471-80 (2026)

Mannes M, Halbgebauer R, Wohlgemuth L, Messerer DAC, **Savukoski S**, Schultze A, Berger B, Knapp CL, Schmidt CQ, Fürst D, Hillmer M, Siebert R, Eriksson O, Persson B, Nilsson B, Nilsson Ekdahl K, Huber-Lang M: Combined Heterozygous Genetic Variations in Complement C2 and C8B: An Explanation for Multidimensional Immune Imbalance? Journal of Innate Immunity 15:412-27 (2023)

Savukoski S, Mannes M, Wohlgemuth L, Schultze A, Guest PC, Meyer-Lotz G, Dobrowolny H, Relja B, Huber-Lang M, Steiner J: Soluble terminal complement complex blood levels are elevated in schizophrenia. Eur Arch Psychiatry Clin Neurosci 274:1215-22 (2024)

Review articles:

Mannes M, **Savukoski S**, Ignatius A, Halbgebauer R, Huber-Lang M: Crepuscular rays - The bright side of complement after tissue injury. European Journal of Immunology 54:2350848 (2024)

Table of contents

1. Introduction 9
1.1. The complement system 9
1.1.1. Components and activation pathways 9
1.1.2. Effector functions 11
1.1.3. Endogenous regulators 12
1.2. The multifactorial functions of the complement system 13
1.2.1. Homeostatic clearance: Resolution of possible harm 13
1.2.2. Loss of regulatory balance 14
1.2.3. Pathological conditions: Genetic deficiencies 15
1.3. Complement therapeutics 16
1.3.1. Pre-clinical evaluation of complement involvement 16
1.3.2. Clinical success of anti-complement therapies 16
1.3.3. Call for site-directed regulation over systemic inhibition 17
1.3.4. Utilizing endogenous regulatory potential as therapeutic approach ... 18
2. Research hypothesis and aims 20
3. Materials 21
4. Methods 26
4.1. *In vitro* AB/0 mismatch model 26
4.2. Rat Xenotransfusion Model 26
4.2.1. Complement therapeutics 26
4.2.2. Study Protocol 27
4.2.3. Experimental groups 28
4.2.4. Sample collection and storage 28
4.3. Analyses of collected samples 29
4.3.1. Clinical Chemistry 29
4.3.2. Rotational thromboelastometry (ROTEM) 29
4.3.3. Homogenization of tissues 29
4.3.4. Protein concentration determination 29
4.3.5. Rat Cytokine Array 30

4.4. Flow cytometric analysis 31
4.4.1. Rat IgG/IgM antibody detection 31
4.4.2. Quantification of transfused huRBCs 31
4.4.3. Analysis of complement opsonization of huRBCs 32
4.4.4. Analysis of rat granulocytes 32
4.4.5. Inflammatory cytokine panel 33
4.5. Complement protein consumption and activation 33
4.5.1. Commercially available ELISAs 33
4.5.2. In-house developed ELISAs 34
4.6. Western Blot analyses 36
4.7. *In vitro* hemolysis assay 37
4.8. Statistical analysis and figures 37
4.9. Data transparency statement 38
5. Results 39
5.1. Preliminary evaluation of TriFu 39
5.2. Effect of complement modulation on intravascular lysis 40
5.3. Pattern of complement activation 42
5.4. Leukocyte population shifts 45
5.5. Screening of systemic and local inflammation markers 46
5.6. Assessment of thromboinflammation 49
5.7. Evaluation of hemolysis-associated kidney injury 50
5.8. Validation of complement modulation efficacy *in vivo* 52
6. Discussion 57
6.1. Performance of complement modulators *in vivo* 57
6.2. Hemolysis-driven inflammation and organ response 62
6.3. Linking experimental findings to clinical observations 64
6.4. Limitations of study 66
6.5. Conclusions 68
6.6. Future perspectives 69
7. References: 70
8. Appendix 81

List of abbreviations

aHUS	Atypical hemolytic uremic syndrome
AP	Alternative pathway
APC	Allophycocyanin
BSA	Bovine serum albumin
C3G	C3 glomerulopathy
C4BP	C4b-binding protein
CA	Cofactor activity
CFT	Clot formation time
CP	Classical pathway
CR1	Complement receptor 1
CRIg	Complement receptor immunoglobulin
CT	Clotting time
Ctrl	Control
CVF	Cobra venom factor
CXCL1	C-X-C motif chemokine ligand 1
DAF	Decay accelerating factor
DAMP	Damage-associated molecular patterns
EDTA	Ethylenediaminetetraacetic acid
ELISA	Enzyme-linked immunosorbent assay
FH	Factor H
FHL-1	Factor H-like 1
FITC	Fluorescein isothiocyanate
FSC	Forward scatter
GM-CSF	Granulocyte-macrophage colony-stimulating factor
GPI	Glycosylphosphatodylinositol
HRP	Horseradish peroxidase
IFN	Interferon
IgG	Immunoglobulin G

IgM	Immunoglobulin M
IL	Interleukin
LP	Lectin pathway
MAC	Membrane attack complex
MASP	MBL-associated serine protease
MBL	Mannose-binding lectin
MCF	Maximum clot firmness
MCF-t	Maximum clot firmness time
MCP	Membrane cofactor protein
MCP-1	Monocyte chemoattractant protein 1
MFI	Mean fluorescence intensity
mRNA	messenger RNA
NGAL	Neutrophil gelatinase-associated lipocalin
OD	Optical density
OmCI	Ornithodoros moubata complement inhibitor
PFA	Paraformaldehyde
PAMP	Pathogen-associated molecular patterns
PNH	Paroxymal nocturnal hemoglobinuria
PBS	Phosphate-buffered saline
RBC	Red blood cell
ROTEM	Rotational thromboelastometry
RT	Room temperature
SPR	Surface plasmon resonance
SSC	Side scatter
TCC	Terminal complement complex
TNF	Tumor necrosis factor
TriFu	Triple fusion protein

1. Introduction

1.1. The complement system

1.1.1. Components and activation pathways

The complement system is a crucial part of the innate immune system [107]. Components in the fluid phase are proteolytically cleaved into active fragments with effector functions to ensure efficient host defense against invading pathogens. The cascade is composed of more than 50 proteins, some of which function as pattern-recognition molecules (e.g., C1q, MBL), lytic membrane attack complex (MAC; consisting of C5b, C6, C7, C8, and multiple C9), or give rise to effector fragments known as opsonins (e.g., C4b, C3b) or anaphylatoxins (e.g., C3a, C5a) [88]. Most of the complement proteins are synthesized and secreted by liver, although important local production occurs in several tissues, particularly in immune-privileged compartments [79]. Inflammatory conditions can further stimulate complement production by immune cells, thereby replenishing components following their consumption [107].

As intracellular complement pathways are still being elucidated [147], mainly the canonical extracellular activation pathways are described here, including the classical pathway (CP), lectin pathway (LP), and alternative pathway (AP), which are triggered by antibody-antigen complexes, carbohydrate moieties, and foreign or altered surfaces, respectively (Figure 1) [88, 89]. Although these pathways differ in their pattern-recognition mechanisms, they all converge at the central C3, ultimately leading to C5 activation and initiation of the lytic terminal pathway. While AP lacks the target specificity characteristic of the CP and LP, it serves as the major amplification loop of complement activation independent of the initial trigger [107]. Constant low level C3 activation allows formation of AP-specific fluid phase C3 convertase ($C3(H_2O)Bb$). Although relatively inefficient, it can accelerate surface C3b deposition under certain conditions, resulting in generation of membrane-bound C3 convertase (C3bBb) and activation of further C3 [88]. Moreover, along with three canonical activation pathways, non-canonical exogenous complement activation takes place via various serine proteases

of the coagulation system [51, 84], interconnecting these two pathways tightly together [3].

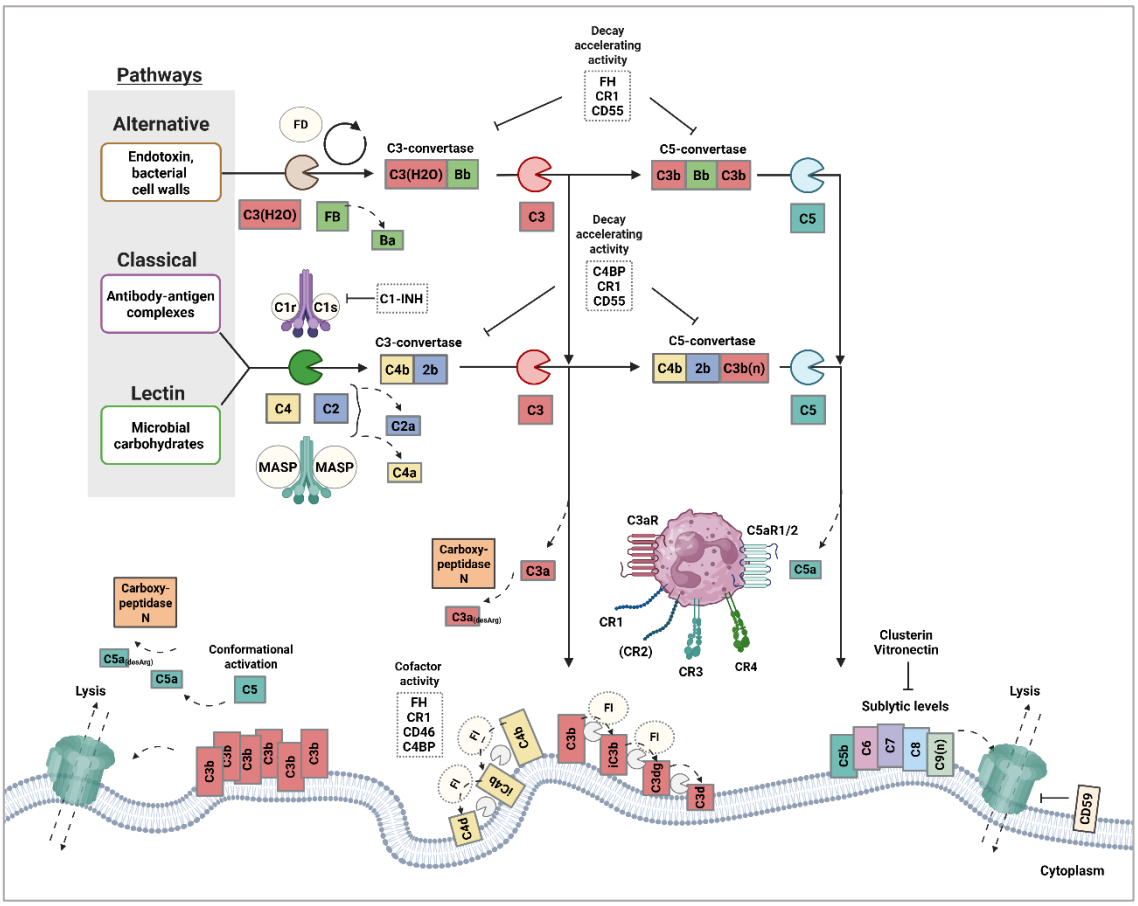


Figure 1. Illustration of the complement system. There are three canonical activation routes: the classical, lectin, and alternative pathway, which are selectively triggered by antibody-antigen complexes, microbial carbohydrates, or foreign surfaces, respectively. Pattern recognition receptors (PRR) such as C1q and MBL interact with their antigens, leading to the enzymatic activation of C2 and C4. Generated C3 convertases (C4b2b/C3Bb) can in turn cleave C3. Subsequent C5 convertases (C4b2b3b/C3bBbC3b) can cleave C5 and initiate the terminal pathway and formation of MAC (C5b-9_n) for lysis. Regulators of both the fluid phase (FH, C4BP, Clusterin, Vitronectin, carboxypeptidase N, C1-INH) and the membrane-bound (CD59, CD55, CR1, CD46) halt excessive activation when not required. Complement receptors (C3aR, C5aR1/2, and CR1/2/3/4) on cell surfaces allow interaction with fluid phase anaphylatoxins (C3a, C5a) and opsonins (C3b/C4b, iC3b/iC4b, etc.) covalently attached on surfaces. C5 activation may also take place on C3b/C4b dense surfaces under strong complement triggers. Figure generated with Biorender.com. Nomenclature: Mannose-binding lectin (MBL), Mannose binding lectin-associated serine protease (MASP), e.g., Factor H (FH), C1-inhibitor (C1-INH), C4b-binding protein (C4BP), Membrane attack complex (MAC).

Taken together, despite the complex and interconnected network of complement cascade systems, all three pathways share a common goal of promoting efficient immune defense although triggered by different antigens. [54, 107]

1.1.2. Effector functions

The complement system can mark foreign cells and particles to be recognized by the immune system. Opsonization by proximal pathway components allows efficient clearance of a wide range of targets, including pathogens, apoptotic cells, and cellular debris [88]. Indeed, evolutionary evidence suggests that opsonization represents the ancestral function of the complement system, predating the emerge of lytic activity [95]. Upon activation, as for C5, C3 releases the soluble C3a molecule; the remaining C3b molecule undergoes a rapid conformational change allowing the exposed thioester bond to covalently attach to nearby surfaces [88]. C3a is able to bind to its receptor, C3aR, found on various cell surfaces, including neutrophils [86]. Although both pro- and anti-inflammatory functions have been proposed for C3a, the conclusions remain controversial and are most likely context-dependent [24, 26, 138, 149, 153].

Along with terminal pathway activity, the complement system is capable of directly killing pathogens, particularly MAC-sensitive Gram-negative bacteria and enveloped viruses with phospholipid membranes [10, 88]. Activation of the terminal pathway yields C5 cleavage into C5b and C5a. C5b interacts with C6 and C7 to form membrane-binding C5b-7 complex [103], followed by recruitment of C8 and polymerization of C9 for pore assembly [88]. Interestingly, metabolically inert cells, like erythrocytes, can be lysed in a one-hit-manner, while metabolically active nucleated cells can resist multiple channels without lysing [64]. In turn, soluble C5a is a highly active anaphylatoxin having the affinity to two major receptors C5aR1 and C5aR2, in which C5aR1 is G-protein coupled, inducing intracellular signaling pathways and activation of the innate immune cells [89]. The major effector functions of C5a include chemoattraction, cellular activation, and subsequent release of inflammatory mediators, production of reactive oxygen species (ROS), or modulation of intracellular and extracellular pH [22, 59].

Consequently, upon pathway activation, stimulated immune cells can further promote the production and proteolytical cleavage of complement components, thereby establishing a positive feedback loop between the fluid phase and cellular compartments that facilitates efficient recognition, processing, and clearance of both external and internal threats [88].

1.1.3. Endogenous regulators

Pathway specificity enables the complement system to respond appropriately to distinct danger signals. In addition, there is a protein family of regulators of the complement activation (RCA), which target components of the CP, LP, and AP, ensuring that complement activation is tightly controlled [97, 155]. Structurally, RCA proteins are composed of repeating complement control protein (CCP) modules (also termed "sushi domains") arranged in tandems and connected by short amino acid linkers [97]. The number of CCP domains varies considerably between family members, ranging from four in the decay-accelerating factor (DAF, also CD55) to as many as 59 in the oligomeric C4b-binding protein (C4BP) complex [124]. The main regulatory activities include decay-accelerating activity (DAA), which promotes dissociation of convertases, and cofactor activity (CFA), enabling Factor I (FI) - mediated proteolytic cleavage of C3b/C4b [97, 124].

Not all complement regulators are members of the RCA family; however, both RCA and non-RCA proteins are functionally important in limiting complement activation and are therefore discussed together here. Soluble complement regulators, such as C1-inhibitor (C1-INH) and C4BP, primarily hinder CP and LP [113], whereas Factor H (FH), FH-like protein 1 (FHL-1) [124], and FH-related proteins predominantly regulate AP [111]. There are also regulators specific for MAC formation, including the soluble regulators vitronectin (S-protein) and clusterin targeting nascent sC5b-7, sC5b-8, sC5b-9 in the fluid phase [55, 56], and CD59 (protectin) found widely in host surfaces interfering with C9 polymerization on C5b-8 complexes at the final stage of complement activation [88, 124, 155].

Opsonins can be inactivated by proteases, primarily by the soluble serine protease FI and locally by less-specific enzymes such as neutrophil elastase, providing additional levels of control over complement activation [140]. Importantly, FI requires cofactors such as FH, CR1 (CD35), CD46 (MCP), or C4BP, to achieve substrate-specific proteolytic activity [88, 99, 118]. C4b and C3b have high affinities for complement receptor 1 (CR1) on immune cells and can be integrated into newly formed convertases C4b2b and C3bBb, respectively [70, 89]. Upon proteolytic cleavage, opsonins are rapidly

trimmed down to iC3b/C3dg and iC4b/C4d, no longer able to form convertases. Furthermore, these downstream products demonstrate stronger affinity to integrin-receptors CR3 and CR4, or CR2, instead of glycoprotein CR1 [89, 124]. The anaphylatoxins C3a and C5a can also be cleaved into C3a(desArg) and C5a(desArg), respectively, mainly by carboxypeptidase N, altering their receptor-binding capacity [16, 148].

Taken together, both soluble and membrane bound regulators direct complement activity towards pathogens while limiting host tissues damage from spillover activation.

1.2. The multifactorial functions of the complement system

1.2.1. Homeostatic clearance: Resolution of possible harm

The central components of the complement system likely emerged more than one billion years ago [95]. Over time, the complement system has acquired vital and diverse roles in development, tissue repair, regeneration, and homeostatic processes, including the clearance of complement-opsonized apoptotic and damaged cells prior to the onset of systemic inflammation [88]. The erythrocyte shuttling system plays an important role in this process by binding opsonized particles and immune complexes, and also, transporting them to the liver and spleen for clearance [19, 42]. This process is primary mediated by CR1, which is abundantly expressed on erythrocytes and certain leukocyte populations [143]. Given the clustering of CR1 on erythrocytes, and the overwhelming abundance of erythrocytes relative to other blood cell types, their prominent role in immune adherence is readily understood [42, 80]. In tissues, the mononuclear phagocyte system (MPS) mediates selective phagocytosis of opsonized material while allowing erythrocytes to re-enter the circulation [19]. Kupffer cells express complement receptors, including CRIg, on their surface, contributing to the non-inflammatory removal of primarily C3b- and iC3b-opsonized particles [41, 143].

As complement receptors are also highly present on circulating phagocytes, they readily participate in removal of particles as part of maintenance of homeostasis [142]. Although the β2-integrins CR3 (CD11b/CD18) and CR4 (CD11c/CD18) are considered the principal phagocytotic complement receptors, CR1 can also contribute to phagocytosis-associated processes [27, 90, 143]. Moreover, upon inside-put signaling, β2-integrins undergo conformational activation that enables high-affinity interactions with

additional ligands, including endothelial ICAM-1 and ICAM-2, thereby promoting leukocyte adhesion and transmigration into affected tissues [69, 72].

Taken together, complement receptors are crucial for maintaining homeostasis by capturing and engulfing complement-opsonized particles either from the circulation or inflamed tissues.

1.2.2. Loss of regulatory balance

In contrast to homeostasis, severe injury can overwhelm innate immune regulatory mechanisms, resulting in a shift from protective inflammation toward uncontrolled and pathogenic immune responses [50]. At this stage, the complement system no longer transmits its protective effects for clearance of PAMPs and DAMPs but rather reflects an overshooting towards all directions without a specific aim, accompanied and supported by systemic cellular activation [50]. In a cohort of critical polytrauma patients, complement activation products increased rapidly after trauma, whereas hemolytic complement activity (CH50) was markedly reduced during the first 24 h, indicating consumption of complement proteins during trauma [15]. In parallel, the key complement regulatory proteins C4BP and FI were significantly depleted early after injury. Interestingly, CH50 and C4BP and FI recovered within 5-10 days post-trauma, suggesting compensatory restoration of complement function [15]. Moreover, polytrauma in humans induces early alterations in leukocyte complement regulatory protein expressions, including upregulation of CD55 and CD59. These data suggest the development of early trauma-induced complementopathy [4].

In sepsis, excessive complement activation and subsequent consumption of immune mediators are associated with poor clinical outcomes [146]. Experimental studies further demonstrated that excessive generation of C5a impairs neutrophil function, resulting in defective bacterial clearance and increased mortality [20, 52, 108, 146, 150, 151], suggesting that therapeutic inhibition of C5a may be beneficial in systemic hyperinflammation. However, given the essential role of C5a in cellular recruitment and antimicrobial sensitivity [22, 59], careful consideration is required when targeting C5a systemically. It has been further suggested that excessive systemic exposure of neutrophils to C5a before bacterial encounter may prematurely impair their phagocytotic

capacity, whereas temporally and spatially restricted C5a generation at sites of infection is likely required for effective antimicrobial responses [150].

1.2.3. Pathological conditions: Genetic deficiencies

Genetic complement deficiencies are rare, with a combined estimated prevalence of 0.03% in the general population [14]. The main clinical manifestations include recurrent infections, autoimmune responses (e.g., systemic lupus erythematosus; SLE), renal disorders (e.g., atypical hemolytic syndrome; aHUS and C3 glomerulopathy; C3G), and eye diseases (e.g., age-related macular degeneration; AMD) [14]. Complement deficiencies account for approximately 5% of all primary immunodeficiencies. Mutations leading to the absence or dysfunctional C1q [116] are often causative for the loss of self-tolerance and development of autoimmunity, as has also described for other proximal pathway components [89]. Interestingly, among complement deficiencies, C2 deficiency is the most prevalent and is generally associated with relatively mild clinical manifestations compared with other complement deficiencies [25].

Regarding various pathological conditions, the kidney relies heavily on local complement regulation to prevent complement deposition on blood-exposed surfaces. In fact, around 50% to 60% of patients with atypical hemolytic syndrome (aHUS) have abnormalities in genes regulating AP, with the highest prevalence in FH, followed by FI, and FB [14]. When the complement system is not properly regulated, activation on endothelial cells leads to platelet activation and microthrombus formation, as well as entrapment and lysis of RBCs, ultimately resulting in kidney injury [60, 124]. Although less frequently than in aHUS, complement deficiencies are associated with C3G, in which fluid phase complement activation and C3 deposition within the glomeruli drive the disease progression [39]. Lastly, regarding another pathology called age-related macular degeneration (AMD), the leading cause of blindness in elderly people [28], the progressive accumulation of drusen between Bruch's membrane and the retinal pigment epithelium promotes complement activation and amplifies the ongoing retinal injury [31].

Beyond the tissue-specific manifestations of complement dysregulation described above, the loss of adequate complement regulatory proteins on host cell surfaces

represents another critical pathogenic mechanism [46]. Loss of the glycosylphosphatidylinositol (GPI)-anchored membrane proteins CD55 and CD59, caused by somatic mutations in phosphatidylinositol glycan class A (PIGA) in hematopoietic stem cells, lead to the rare hemolytic disorder paroxysmal nocturnal hemoglobinuria (PNH) [45]. Erythrocytes are particularly susceptible to complement-mediated lysis, and therefore the primary targets of deficiency, in contrast to other blood cells that possess mechanisms to resist and shed off MAC [64]. Intravascular hemolysis releases free hemoglobin, which scavenges nitric oxide (NO), promoting endothelial dysfunction, platelet activation, and prothrombotic state that contributes substantially to morbidity [13].

1.3. Complement therapeutics

1.3.1. Pre-clinical evaluation of complement involvement

To experimentally demonstrate the involvement of complement in disease processes, cobra venom factor (CVF) has been, and continues to be, widely used as a complement depleting agent in animal models since 1970s [17], particularly in situations where specific pharmacological complement inhibitors are not yet available [93]. Mechanistically, CVF strongly activates the AP because of its structural and functional similarity to C3b [2], enabling binding to FB and formation of stable C3 and C5 convertases that are resistant to FH-mediated regulation [65]. Although efforts have been directed toward the preclinical evaluation of complement-targeted therapies in experimental animal models [92, 101], CVF remains a widely used and standardized tool for investigating the role of complement in diverse disease settings.

1.3.2. Clinical success of anti-complement therapies

As a complement-model disease, PNH is the first disease being treated with anti-complement therapy starting from 2007 by introducing the anti-C5 antibody Eculizumab (Soliris) [123]. The treatment greatly prolonged the survival of patients by blocking the continuous lysis of CD55- and CD59-deficient RBCs and thereby, the consequent fatal thrombotic events [43]. After its great success, research in the field of complement therapeutics increased rapidly. At present, several complement proteins are specifically targeted by therapeutic inhibitors, including C5, C3, C1s, factor D, factor B, and

C5a receptor (C5aR1), with C5 remaining the most established and widely targeted component [106].

The current alternatives to Eculizumab are Ravulizumab and Crovalimab, providing enhanced durability and greater cost-effectiveness making C5-inhibition more accessible to patients [106]. However, the burden of illness still occurs in patients treated with most C5-inhibiting agents, including residual intra- and extravascular lysis on cells, encouraging further development of therapeutic approaches [23]. The next generation therapeutics are formulated differently and constructed as peptides (Zilucoplan), small recombinant proteins (Nomacopan, same as Coversin) or small interfering RNAs (Cemdisiran) address current issues related to incomplete inhibition by Eculizumab [6, 125, 139]. Moreover, combination therapy of FD and Eculizumab or Ravulizumab has been approved for treatment of PNH patients, showing improved hematological parameters by addressing also extravascular clearance of RBCs in clinical trials [71].

By blocking C3, all complement activation pathways can be simultaneously halted [88] giving rise to both concerns about the function of host defence [25] and an opportunity to halt all complement activation pathways and C3 mediated functions simultaneously [32, 68]. Small peptides of the Compstatin family prevent C3 activation by convertases and work efficiently both locally and systemically [68]. In 2021, a PEGylated form of the peptide against C3 (Pegcetacoplan) was introduced to address residual extravascular clearance of C3 opsonized RBCs in PNH patients treated with C5-inhibition [74]. No major adverse effects of systemic C3 inhibition were seen, and more stable haemoglobin counts were observed in patients treated with a C3-inhibitor than with C5-inhibitor [48]. Moreover, the indication spectrum of Pegcetacoplan is not only restricted to PNH treatment, but also include the treatment of the “dry” form of age-related macular degeneration (AMD, more precisely GA), given as intravitreal injection into the eye [106].

1.3.3. Call for site-directed regulation over systemic inhibition

Complement-targeted therapies have achieved significant clinical success over the past 20 years, and growing insight into their applications has driven the development of new agents [106]. There are several reasons to expand the current repertoire of

therapeutics: 1) current anti-complement therapies provide limited or no control over immune-privileged sites such as the brain and the eye, due to protective barriers or systemic drug consumption [77]; 2) when soluble components are neutralized in a stoichiometric manner, high doses are required due to their abundance and high turnover; 3) the risk of certain infections remain, even with prophylactic vaccinations [87]; and 4) when a cascade is inhibited at a specific level, upstream components may remain active, potentially leading to an imbalance between newly generated activation fragments versus potential regulatory capacity [37, 144].

1.3.4. Utilizing endogenous regulatory potential as therapeutic approach

In fact, nature has developed various mechanisms to dampen excessive complement activation by offering cofactor activity (CFA), decay-accelerating function (DAF), host cell targeting, and terminal pathway blockade [124, 155]. By utilizing these modules in therapeutic components, one can achieve more physiological approaches for complement control [77]. As example, within several approaches, mini-FH, an engineered construct composed of selected domains of FH1-4 and FH19-20, exhibited promising *in vitro* AP-inhibitory function [122]. Furthermore, mini-FH revealed *in vivo* efficacy in a periodontitis model [73], due to the combined function of CFA, DAA, and host recognition derived from FH.

To achieve a broad regulatory control over all three complement pathways with a tissue-targeting approach, a molecule called Triple-Fusion-Protein (TriFu) was designed and engineered by Prof. Christoph Schmidt at Ulm University, Germany. The molecule contains the following CCP domains included in human RCAs: four N-terminal domains of DAF, CCP19-20 of FH, and CCP15-17 of CR1, connected with polyglycine linkers (Figure 2). Together, TriFu provides decay acceleration function to all convertases, cofactor activity, and recognition and targeting of sialic acids, glycosaminoglycans, and late-stage C3 opsonins [132]. TriFu has functionality in human serum, but also cross reactivity towards other species, such as the rat (unpublished data). As conclusion, TriFu brings complement regulatory activity at the site where it is required, while it does not neutralize total proteins in the fluid phase, and thereby prevent immune functions.

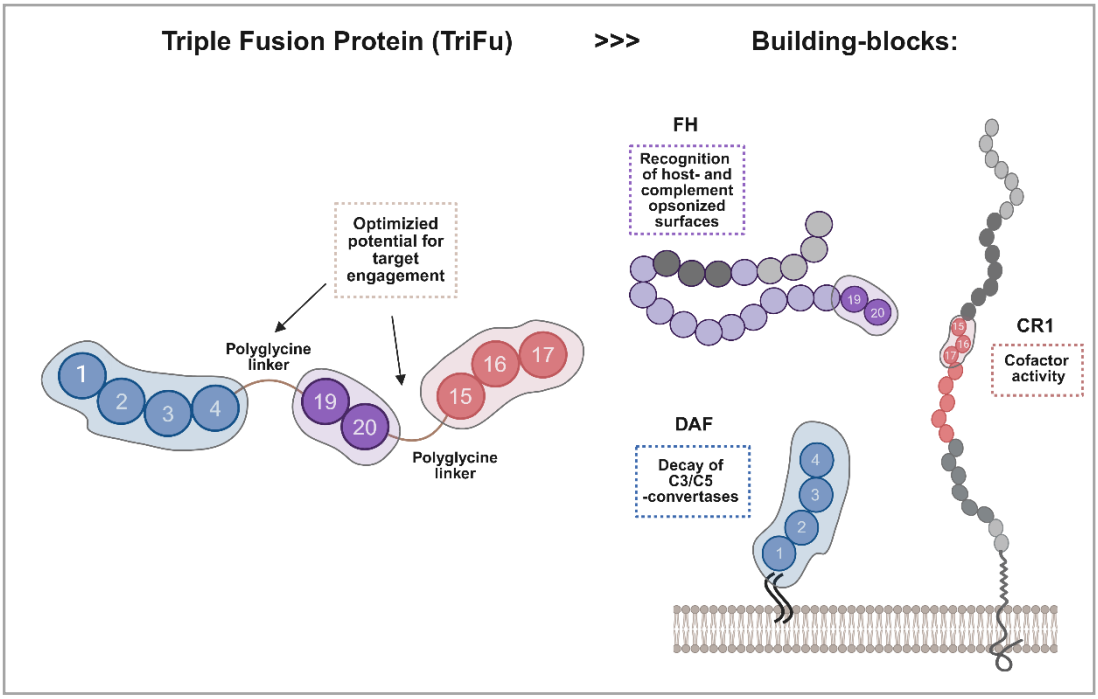


Figure 2. Representation of Triple Fusion protein, TriFu. Engineered fusion protein combining parts of three naturally occurring complement regulators linked together with two polyglycine linkers. TriFu contains decay accelerating activity (DAA) from DAF(1-4), host recognition from FH(19-20), and cofactor activity (CA) from CR1(15-17). Figure generated with Biorender.com, based on Sonnentag et al., 2024 [88].

Of note, TriFu has been extensively characterized *in vitro* [132]; however, *in vivo* validation is still lacking. Its enzyme-like mode of action may offer advantages over stoichiometric inhibitors in terms of dosing amount and frequency. Moreover, its ability to inhibit all three pathways provides wider inhibitory capacity than most of the agents in the pipeline [77]. This may mitigate effector functions mediated by covalently deposited proximal pathway opsonins and cleavage products of C3 and C4, as these are either prevented or inactivated by TriFu, respectively [132].

2. Research hypothesis and aims

I hypothesized that complement regulation by TriFu is superior to stoichiometric single C5-inhibition strategy by OmCI due to its more physiological enzyme-like control of C3 activation, opsonin processing, and binding properties to complement targeted huRBC surfaces.

To answer our research aims, a model of strong classical pathway activation was applied in Wistar rats evaluating the survival of transfused huRBCs, hemolysis-induced inflammation, and general well-being.

The following points were addressed:

- To study the complement regulatory efficacy of TriFu for the first time *in vivo*.
- To compare the regulatory potential of TriFu over known stoichiometric C5-inhibition (OmCI) and complement depletion strategy (CVF).
- To understand how circulating immune cell functions are affected based on differential complement opsonization patterns and/or lysis.

In addition, further focus points were set on:

- Safety, tolerance, and plasma clearance of TriFu administered.
- Availability of modulators (OmCI and TriFu) across the experimental timeline.
- Characterization of the effectiveness of complement (OmCI), regulation (TriFu), and depletion (CVF) in animals across experimental timeline.

3. Materials

Consumables

Reaction tubes: 0.5 ml, 1.5 ml, 2 ml	Eppendorf, Hamburg, Germany
Falcon 15ml, 50ml	Sarstedt, Nümbrecht, Germany
Filter (0.2 µm)	GE Healthcare, Freiburg, Germany
96 Well Plate	Thermo Fisher Scientific, Waltham, USA
Nunc™ MaxiSorp™ 96-Well ELISA plate	NUNC A/S, Roskilde, Denmark
ELISA Sealing Tape	Thermo Fisher Scientific, Waltham, USA
Ethanol	Sigma-Aldrich, Steinheim, Germany
BD FACS Flow	BD Biosciences, Heidelberg, Germany
BD FACS Clean	BD Biosciences, Heidelberg, Germany
Cup & Pin mini	Werfen, Munich, Germany
Anesthesia chamber	Föhr Medical Instruments (FMI), Seeheim-Jugenheim, Germany
Polyethylene catheter (0.62 mm)	Föhr Medical Instruments GmbH, Seeheim/Ober-Beerbach, Germany
Syringe, 1 ml	BD Biosciences, Heidelberg, Germany
Serum S-Monovette®	Sarstedt, Nümbrecht, Germany
Citrate Monovette®	Sarstedt, Nümbrecht, Germany
Heparin Monovette®	Sarstedt, Nümbrecht, Germany
EDTA Monovette®	Sarstedt, Nümbrecht, Germany
Ceramic beads (innuSPEED Lysis Tube P)	Analytik Jena, Germany
Pre-cast stain-free gel (4-15 %)	BioRad Laboratories, Hercules, California, USA
Amersham Hybond PVDF Blotting-Membrane (0.45µm)	GE Healthcare, Freiburg, Germany

Solutions and buffers

Aqua dest	Fresenius Kabi, Bad Homburg, Germany
Sterile water	B. Braun, Melsungen, Germany
Dulbecco's Phosphate-Buffered Saline w/o Ca2+/Mg2+; DPBS -/-)	Gibco BRL, Grand Island, USA
Dulbecco's Phosphate-Buffered Saline with Ca2+/Mg2+; DPBS +/+)	Gibco BRL, Grand Island, USA
Sodium chloride solution (0.9%)	Fresenius Kabi, Bad Homburg, Germany
ELISA coating buffer	BioLegend, San Diego, USA

Reagents and chemicals

FACS Lysing Solution	BD Biosciences, Heidelberg, Germany
CountBright™ Plus Absolute Counting Beads	Invitrogen, Carlsbad, USA
Paraformaldehyde (PFA) powder	Sigma Life Sciences, St. Louis, USA
Ethylenediaminetetraacetic acid (EDTA)	Sigma Life Sciences, St. Louis, USA
Milk powder	Sigma-Aldrich, St. Louis, USA
SDS	Gibco BRL, Grand Island, USA
TEMED	Fresenius Kabi, Bad Homburg, Germany
TBS	Sigma-Aldrich, St. Louis, USA
Tween-20	Sigma-Aldrich, St. Louis, USA
Laemmli buffer	BioRad Laboratories, Hercules, California, USA
Bovine Serum Albumin	Sigma-Aldrich, St. Louis, USA
β-Mercaptoethanol	Sigma-Aldrich, St. Louis, USA
Ex-tem	Werfen, Munich, Germany
Star-tem	Werfen, Munich, Germany
Protease Inhibitor (PI) cocktail	Sigma-Aldrich, St. Louis, USA
Triton X-100	Sigma-Aldrich, St. Louis, USA
Streptavidin-APC conjugate	BioLegend, San Diego, USA
Western ECL solution	BioRad Laboratories, Hercules, USA
Precision protein streptactin HRP-conjugate	BioRad Laboratories, Hercules, USA
Streptavidin-Horseradish Peroxidase (HRP)	Thermo Fisher Scientific, Waltham, USA
TMB substrate solution	BD Biosciences, Heidelberg, Germany
0.5 M H_2SO_4 stop solution	Self-prepared
A recombinant fusion construct comprising OmCI (FH8-15-OmCI)	Self-prepared

Antibodies

Anti-rat IgM, APC-conjugated	StemCell Technologies
Anti-rat IgG, Alexa-Fluor Plus 488 -conjugated	Invitrogen, Carlsbad, USA
Anti-human CD59, APC-conjugated	Invitrogen, Carlsbad, USA
Goat anti-rat C3	Invitrogen, Carlsbad, USA
Rabbit anti-rat C4d	Self-produced and purified

Anti-human CD59, PE-conjugated	eBioscience™, Thermo Fisher Scientific, Waltham, USA
Anti-human CD59, APC-conjugated	eBioscience™, Thermo Fisher Scientific, Waltham, USA
Donkey anti-goat, Alexa Fluor 647-conjugated	Thermo Fisher Scientific, Waltham, USA
Goat anti-rabbit, Alexa Fluor 488-conjugated	Thermo Fisher Scientific, Waltham, USA
Anti-rat CD11b/c, APC-conjugated	BioLegend, San Diego, USA
Anti-rat CD62L, PE-conjugated	BioLegend, San Diego, USA
Biotinylated anti-rat CD61	Invitrogen, Carlsbad, USA
Anti-rat CD62, PE-conjugated	BioLegend, San Diego, USA
Streptavidin-APC conjugate	BioLegend, San Diego, USA
Rabbit anti-human C5a	Calbiochem Inc., San Diego, USA
Anti-rabbit $F(ab')_2$, HRP-conjugated	GE Healthcare, Freiburg, Germany
Anti-goat IgG, HRP-conjugated	R&D Systems, Minneapolis, USA
Anti-rabbit IgG, HRP-conjugated	BioRad Laboratories, Hercules, USA
Anti-human Factor H	Thermo Fisher Scientific, Waltham, USA
Anti-human CD55	Thermo Fisher Scientific, Waltham, USA
Anti-rabbit IgG	Abcam, Cambridge, UK
Rabbit anti-OmCI	Generated by Davids Biotechnology, Regensburg, Germany
Goat anti-rat C3	Thermo Fisher Scientific, Waltham, USA
Rabbit anti-rat C5	Thermo Fisher Scientific, Waltham, USA
Factor H antibody	Thermo Fisher Scientific, Waltham, USA
Anti-human CD55 antibody	Thermo Fisher Scientific, Waltham, USA
Anti-rabbit IgG, HRP-conjugated	Abcam, Cambridge, UK

Injection solutions and medications

Natriumchlorid (NaCl) 0,9%	B. Braun, Melsungen, Deutschland
Sevofluran (Sevorane™)	Abbott, Wiesbaden, Germany
Buprenorphine (Temgesic®)	Boehringer, Mannheim, Germany
Cobra Venom Factor (CVF)	Quidel Ortho, San Diego, USA
OmCI	Prof Dr. Christoph Schmidt, University of Ulm, Germany
TriFu	Prof Dr. Christoph Schmidt, University of Ulm, Germany

Blood Products

Sheep red blood cells	Fiebig Nährstofftechnik GbR, Idstein, Germany
Rabbit anti-sheep serum	Colorado Serum Company, Denver, USA
Purified human C5	Quidel Ortho, San Diego, USA
Purified human C5a	Complement Technology, Inc., Tyler, TX, USA
Human AB-RBCs	Prof. Dr. Schrezenmeier, German Red Cross, Ulm, Germany

Immunoassays

Anti-rat C3 ELISA	Abcam, Cambridge, UK
Anti-rat C3a ELISA	Abbexa, Cambridge, UK
Anti-rat TCC ELISA	Hycultec, Beutelsbach, Germany

Devices

Anesthesia vaporizer (Vapor 2000)	Dräger, Lübeck, Germany
Temperature control system	ATC2000; World Precision Instruments, Sarasota, USA
ChemiDoc XRS+	BioRad Laboratories, Hercules, USA
Roller Mixer SRT1	Stuart Scientific, Staffordshire, UK
Sunrise Plate Reader	Tecan, Männedorf, Schweiz
Trans-Blot Turbo Transfer System	BioRad Laboratories, Hercules, USA
ThermoMixer C	Eppendorf, Hamburg, Deutschland
Homogenizer (Speadmill Plus)	Analytik Jena, Germany
ROTEM® delta	Werfen, Munich, Germany
Nanodrop	Thermo Fisher Scientific, Waltham, USA

Kits

Pierce™ BCA Protein Assay Kit	Thermo Fisher Scientific, Waltham, USA
Proteome Profiler Rat XL Cytokine Array	R&D Systems, Minneapolis, USA
LEGENDplex™ Rat Inflammation Panel (13-Plex)	BioLegend, San Diego, USA

Softwares

FlowJo software (version 10.10.0).	FlowJo, LLC, Ashland, USA
Cytolution	Cytolytics, Tubingen, Germany
GraphPad Prism (v.10)	GraphPad Software, San Diego, USA
LEGENDplex™ Data Analysis Software Suite	BioLegend, San Diego, USA
ImageJ	National Institutes of Health, Bethesda, USA

4. Methods

4.1. *In vitro* AB/0 mismatch model

In accordance with the ethical approval (#370/24; Local Independent Ethics Committee of Ulm University), all healthy blood donors provided written informed consent for the use of their blood. Peripheral blood was collected via venipuncture into Hirudin-monovette® collection tubes (#04.1959.001, Sarstedt). Human AB red blood cells (huRBC) concentrates were obtained from the German Red Cross (Deutsches Rotes Kreuz, DRK, Ulm, Germany) and kept at 4 °C until use.

A preliminary *in vitro* experiment employing a human mismatch model was conducted to test functionality of OmCI and TriFu. Human AB-RBC were washed three times with PBS-/- at 2,000 x g for 5 min, at 4 °C. A set concentration of OmCI (0.3, 3.3, or 33 µg/mL) and TriFu (2.5, 25, or 250 µg/mL) were mixed with type 0 human whole blood (including natural anti-A/B antibodies) and pre-incubated for 5 min to allow target binding. Next, washed AB-RBCs were mixed with blood followed by incubation for 30 min, at 37 °C under shaking conditions (700rpm). To stop further complement activation, 5 mM EDTA was added, and supernatants were collected by centrifuging at 2,200 x g for 3 min, at 4 °C. Hemolysis was quantified by measuring plasma absorbance at 405 nm (OD_{405}) using a spectrophotometer (Tecan Sunrise).

4.2. Rat Xenotransfusion Model

4.2.1. Complement therapeutics

The C5-inhibitor OmCI and complement regulator TriFu were recombinantly expressed in *Pichia pastoris* similarly as previously described for FH [122, 132]. Following production and purification, recombinant proteins were tested for potential endotoxin contamination which was kept below the critical value for *in vivo* examination. Complement C3 and C5 depleting agent Cobra venom factor (CVF) was derived originally from *Naja naja kaouthia* and was commercially available (#A600; Quidel Ortho, San Diego, CA).

4.2.2. Study Protocol

The animal model was performed as previously described [130] (Figure 3). The study protocol was approved by the regulatory authority (Regierungspräsidium Tübingen, approval number TVA1542), and all experiments were conducted by trained personnel in accordance with institutional and governmental guidelines. For complement depletion, CVF was injected intraperitoneally 24 h prior to the start of the experiment. During the experimental day, animals received a single dose of buprenorphine (0.05 mg/kg) prior to instrumentation. Anesthesia was induced with 3.5–4.0 % sevoflurane at the beginning of the experiment and maintained as needed based on physiological responses. A catheter was placed in the femoral vein allowing administration of either buffer (PBS) or complement modulator (OmCI or TriFu) 5 min prior to the transfusion of huRBCs.

Preparation of human AB-RBCs included two washing cycles with 50 ml PBS at 2,500 x g for 15 min, at RT, and adjustment into a hematocrit of 80 %. The cell density was adjusted based on absorbance at 405 nm (OD_{405}) after adding 10 µl of this suspension to 2.5 ml of water, leading to 100% lysis. The cell suspension was kept at RT until transfusion. After preparation, 1ml of prepared huRBCs was transfused slowly over a period of 5 min, to which end marked as the experimental start.

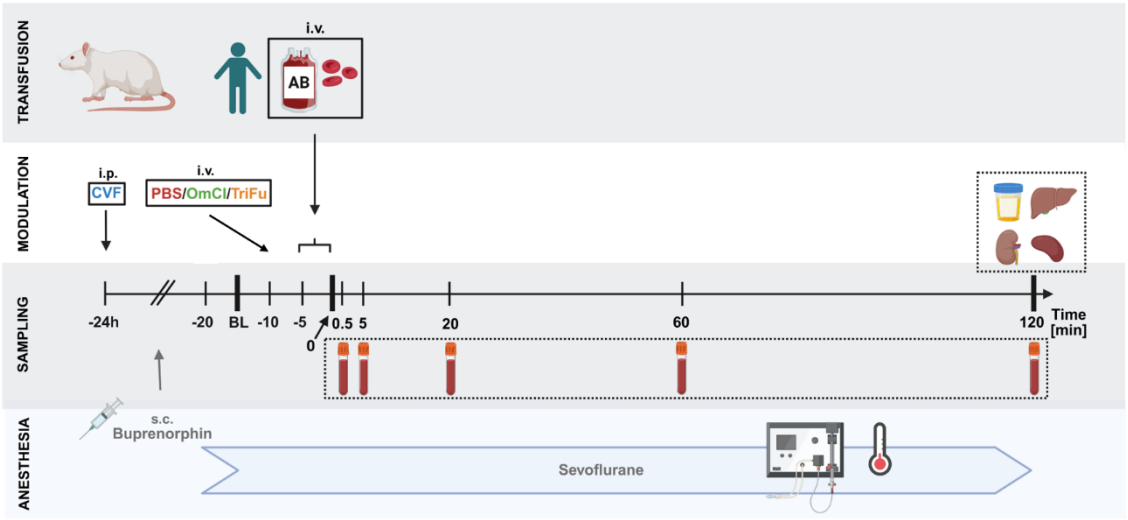


Figure 3. Study design of rat xenotransfusion. Wistar rats were transfused with human AB-RBCs triggering strong CP activation and intravascular lysis. CVF was applied 24h prior transfusion to allow successful complement depletion, while buffer (PBS), C5-inhibitor OmCI and complement regulator TriFu was applied 5min prior transfusion. Blood samples were collected from the tail vein at 0.5, 5, 20, 60, and 120-min timepoint, and organs were harvested at the experimental endpoint. All animals received an injection of Buprenorphin before the experiment was initiated and were under general anesthesia (Sevoflurane). Temperature was monitored throughout the experiment.

4.2.3. Experimental groups

The study included five experimental groups; negative control (n=10), positive control (n=10), OmCI-treated (660 µg, n=10), TriFu-treated (5,000 µg, n=10), and CVF-treated (130 µg, n=8) animals described in the table below (Table 1). The concentrations of OmCI and TriFu was adjusted based on previous unpublished work, scaled to a blood volume of 300 g rat (mean weight 310 g, ranging from 244 to 470 g). To ensure sustained inhibition, an excess factor was applied to the estimated dose. Regarding CVF dosing, small excess was applied to previously applied amount [67].

Groups	Transfusion	Target	Description
neg-Ctrl	(-)	(-)	No response
pos-Ctrl	(+)	(-)	Response, no intervention
OmCI	(+)	C5	Modulated response, stoichiometric C5-inhibition
CVF	(+)	C3, C5	Modulated response, complement depletion
TriFu	(+)	Various	Modulated response, CP/LP/AP regulation

Table 1. Included study groups. Animals without transfusion served as neg-Ctrls while transfused animals without complement modulation represented as pos-Ctrls responding with a strong complement activation towards huRBCs. Modulation strategies included C5-inhibition (OmCI), complement depletion (CVF) and complement regulation (TriFu).

4.2.4. Sample collection and storage

Blood samples were collected from the tail vein at baseline and 0.5, 5, 20, 60, and 120 min after huRBC transfusion. In detail, 16 µl of blood was immediately mixed with 2 µl EDTA (50 mM), yielding a final EDTA concentration of 10 mM to prevent sample clotting. At the experimental endpoint, animals were euthanized via heart puncture under deep anesthesia. Blood was collected from the abdominal aorta and anticoagulated with either citrate (1.2 ml monovette), heparin (1.2 ml monovette) or EDTA (2 X 2.7 ml monovettes). Unless used as whole blood, serum and plasma were generated by centrifuging at 2,200 × g for 15 min at 4 °C to separate cells from supernatant. For serum preparation, blood was allowed to clot for 15-30 min prior to centrifugation. Samples were aliquoted and stored at –80 °C until further use. Organs (liver, spleen, and adrenal glands) were harvested and snap-frozen in liquid nitrogen.

4.3. Analyses of collected samples

4.3.1. Clinical Chemistry

Heparin- or EDTA-anticoagulated blood and urine samples were collected at the experimental endpoint and analyzed by the routine clinical laboratory of Ulm University Medical Center. Analysis included the following readouts from blood: cell counts, hemoglobin, hematocrit, LDH, AST, and ALT, and from urine: albumin, creatinine, and total protein.

4.3.2. Rotational thromboelastometry (ROTEM)

To evaluate the hemostatic properties following transfusion and hemolytic events in the rats, a rotational thromboelastometry (ROTEM) analysis was performed for a subgroup of animals. Citrated blood from the experimental endpoint was examined. In detail, evaluation of extrinsic pathway of the coagulation system was initiated by applying 1:1 of star-tem (#503-01, Rotem) and ex-tem (#503-05, Rotem) reagents mixed briefly with 105µl of citrated blood. The samples were added into Cup&Pin mini cuvettes (#400492, Werfen, Rotem) allowing reduction of the sample volume. The read-outs included parameters of clotting time (CT), clot formation time (CFT), maximum clot firmness (MCF), MCF time (MCF-t), and the angle of clot polymerization rate (α-angle).

4.3.3. Homogenization of tissues

Collected tissues of rat liver, and spleen, were treated with a protease inhibitor cocktail (#P8340, Sigma) and homogenized by using ceramic beads (innuSPEED Lysis Tube P, #845-CS-1020100, Analytik Jena) and a homogenizer (Speadmill Plus, Analytik Jena, Germany) run with the soft tissue program II (2 x 30 sec shredder). Afterwards, 1 % (v/v) Triton X-100 was added to each sample, mixed thoroughly, and incubated at -80 °C for 1 h. Later, frozen samples were thawed on ice and centrifuged at 10,000 x g for 5min at 4 °C for protein concentration determination and proteome profiling.

4.3.4. Protein concentration determination

The protein amount of tissue lysates was analyzed by using Pierce™ BCA Protein Assay Kit (#23225, Thermo Scientific). Shortly, the centrifuged cell lysates were diluted 1:40 in sterile water. Working reagent was prepared by diluting Reagent B to A in 1:50 ratio.

BSA Standard concentration row was performed according to the manufacturer's protocol. Next, 10µl of each sample or standard was added to a 96-well plate in duplicates. Working Reagent was added to each well and the plate was incubated for 30 min, at 37 °C. Afterwards, the absorbance was measured at 562 nm by spectrophotometer (Tecan Sunrise). The protein quantity was interpolated from the standard curve constructed from the standard samples and considering the dilution factor applied.

4.3.5. Rat Cytokine Array

Rat serum, and tissue homogenates of the liver and spleen were analyzed by Proteome Profiler Rat XL Cytokine Array (#ARY030, R&D Systems, Minneapolis, USA). First, the membranes were placed into individual plastic containers and blocked with Array Buffer 6 for 1 h, at RT, on a shaker. All subsequent incubation and washing steps were performed with gentle shaking to allow homogeneous reagent distribution. After blocking, 150 µl of serum or 200 µg of tissue homogenates were added in 0.5 ml of Array Buffer 4 and required amount of Array Buffer 6 to reach 1.5 ml. Samples were incubated on the membrane overnight, at 4°C. The next day, membranes were washed three times with 1 x Wash buffer for 10 min. Biotinylated detection antibodies were diluted 1:50 in Array Buffer 6 and incubated on membranes for 1 h, at RT. After consequent washing, Streptavidin-HRP was diluted 1:2,000 in Array Buffer 6, and added to the membranes for 30min, at RT. After washing, membranes were carefully placed on the plastic sheet protector with the identification number facing up. Next, 1 ml of 1:1-diluted Chemi reagent mix was added evenly on the membranes and incubated for 1 min. Excess reagent was removed with paper towels, and the membranes were covered with plastic wrap. Imaging was performed by ChemiDoc XRS+ device (BioRad) with Chemi Hi Sensitive program with multiple exposure times to obtain the best signal-to-noise ratio for integrated optical densities (IOD). For data analysis, Image J was used. Raw dot intensities were background-subtracted and normalized to the negative control. To ensure mathematical symmetry between up- and down-regulated proteins, normalized values were transformed into $\log_2$ fold changes.

4.4. Flow cytometric analysis

Flow cytometry was used to analyze individual cells in suspension. This laser-based technique measures light-scattering properties and fluorescence signals emitted by labelled particles, enabling the identification and characterization of distinct populations [1]. Depending on the subsequent experimental approach, appropriate gating strategies were applied. Typically, the analysis included the exclusion of debris and doublets, followed by the discrimination of cell populations based on the expression of specific surface markers.

4.4.1. Rat IgG/IgM antibody detection

To assess the presence and possible *in vivo* consumption of endogenous rat antibodies against human AB-RBCs, an *in vitro* analysis was performed on a subgroup of animals (n = 5 per group for neg- and pos-Ctrls). Shortly, human AB blood was collected from a healthy blood donor, and RBCs were pelleted and washed in PBS -/- at 2,200 × g for 15 min at 4 °C until the supernatant appeared clear. Before initiation of the assay, the 96-well plate wells were pre-coated with 1% BSA in PBS -/- for 15 min, RT to prevent adhesion of the cells to the well bottom during procedure. Afterwards, pre-diluted washed cells were exposed to 1:2.5-diluted rat EDTA-plasma (collected at the experimental endpoint) for 15 min, at 37 °C under shaking conditions (700 rpm). Next, samples were centrifuged down at 2,200 × g for 2 min, washed, and incubated with either goat anti-rat IgM (5 µg/ml, #60140AZ, APC-conjugated, StemCell Technologies) or anti-rat IgG (20µg/ml, #A48626, Alexa-Fluor Plus 488 -conjugated, Invitrogen) antibodies for 20 min, at RT in darkness. Followed by washing, samples were analyzed by flow cytometry. Negative controls included samples (RBCs) without plasma exposure.

4.4.2. Quantification of transfused huRBCs

The number of circulating transfused huRBCs was assessed at all time points using a small volume of the EDTA-anticoagulated tail blood. Samples were stained with anti-human CD59 antibody (2.5 µg/ml, APC-conjugated, #17-0596-42, clone: OV9A2, Invitrogen) for 15 min, at RT. Subsequently, CountBright™ Plus Absolute Counting Beads (8 beads/µL, #C36995, Invitrogen) were added to each sample. Flow cytometric measurements were performed immediately after staining. Data acquisition was stopped

upon detection of 50 events within the counting bead gate. This stopping criterion ensured a standardized acquisition volume across samples, enabling the quantification of huRBCs at each time point. For analysis, huRBCs were identified as CD59+ events, and their number was normalized to the total number of singlet events acquired.

4.4.3. Analysis of complement opsonization of huRBCs

For analysis of the complement opsonins, residual huRBCs were stained with either a commercially available goat anti-rat C3 antibody (0.9 mg/mL; #PA1-29715, polyclonal, Invitrogen) or a self-produced rabbit anti-rat C4d antibody (polyclonal, affinity purified). For gating purposes, an anti-human CD59 antibody conjugated with either PE (0.25 µg/ml, #12-0596-42, clone: OV9A2, eBioscience) or APC (0.25 µg/ml, #17-0596-42, clone: OV9A2, eBioscience) was applied. Secondary antibodies included donkey anti-goat Alexa Fluor 647-conjugated (20 µg/ml, #A32849TR, ThermoFisher Scientific) and goat anti-rabbit Alexa Fluor 488-conjugated (10 µg/ml, #A-11034, ThermoFisher Scientific) antibodies, used against the primary C3 and C4 antibodies, respectively. Antibody labelling was performed for 10 min at RT, and washing by PBS was done before and after antibody incubation at 2,200 x g for 2 min, at RT. Negative controls included samples stained without primary antibodies for C3 and C4. For flow cytometric data, FSC-files were analyzed using FlowJo software (version 10.10.0).

4.4.4. Analysis of rat granulocytes

Whole blood collected at the experimental endpoint was stained with anti-rat CD11b/c (3.3 µg/ml, APC-conjugated, #201809, clone OX-42, BioLegend) and anti-rat CD62L (3.3 µg/ml, PE-conjugated, #202912, clone OX-85, BioLegend) antibodies for 15 min, at 37 °C. Next, samples were fixed with FACS Lysing (1:10 pre-diluted in demineralized water, #349202, BD Biosciences) for 30 min, at RT. Following centrifugation at 340 x g for 5 min, pellet was resuspended in 1% PBS-BSA solution and analyzed by flow cytometry. Rat neutrophils were gated based on characteristic FSC and SSC parameters and mean fluorescence intensity (MFI) values were determined by FlowJo software (version 10.10.0). Raw data were further analyzed using an automated multidimensional analysis platform (Cytolytics, Tubingen, Germany) to identify potential subpopulations within the rat granulocytes. This next-generation, cloud-based analysis software

allows simultaneous assessment of all included parameters: FSC, SSC, PE, and APC, using machine learning-driven workflows.

4.4.5. Inflammatory cytokine panel

Plasma inflammatory cytokine levels were assessed using the LEGENDplex™ Rat Inflammation Panel (13-Plex, Version 02, #741396, BioLegend) following instructions provided by the supplier. The bead-based multiplex assay included the following 13 analytes: IL-1α, IL-1β, IL-6, IL-10, IL-12p70, IL-17A, IL-18, IL-33, CXCL1 (KC, human IL-8 analogue), CCL2 (MCP-1), GM-CSF, IFN-γ, and TNF-α. In short, rat EDTA plasma was diluted 1:3 in buffer, and exposed to fluorescently labeled capture beads overnight, at 4 °C. To avoid bead sedimentation during each incubation step, the foil-wrapped plate was placed on a plate shaker (800 rpm). After washing, biotinylated antibodies were added for 1 h, at RT. Later, signal development was achieved by adding Streptavidin-phycoerythrin for 30 min, at RT. After washing, samples were measured by flow cytometry in a 96-well plate by acquiring 3,000 beads for both populations at medium flow rate. Data were analyzed using the LEGENDplex™ Data Analysis Software Suite (BioLegend). Cytokine concentrations were calculated based on standard curves generated with recombinant protein standards.

4.5. Complement protein consumption and activation

4.5.1. Commercially available ELISAs

For the evaluation of the complement system activity in rats, C3 (#ab157731, Abcam), C3a (#abx155279, Abbexa) and TCC (#HK106, HycultBiotech) Sandwich ELISAs were performed according to the protocol provided by the manufacturer. EDTA-plasma samples (collected at the experimental end point) were diluted in 1:10,000, 1:15, and 1:100, for the assessment of C3, C3a, and sC5b-9, respectively. Shortly, all experiments included sample incubation, detection utilizing biotinylated tracer antibodies followed by HRP-based detection system, TMB substrate, and 0.5 M H_2SO_4 stop solution. The generated color intensity was measured at 450 nm (OD_{450}) using a spectrophotometer (Tecan Sunrise). The protein quantity was interpolated from the standard curve determined from the standard samples and considering the dilution factor applied.

4.5.2. In-house developed ELISAs

To ensure complement modulation success by TriFu, OmCI, and depletion by CVF, multiple retrospective *in vitro* analyses were conducted. Since there were no commercially available detection method for intact C5, unbound free OmCI, and TriFu, self-assembled sandwich ELISAs were established and validated in our lab (**Figure 4**).

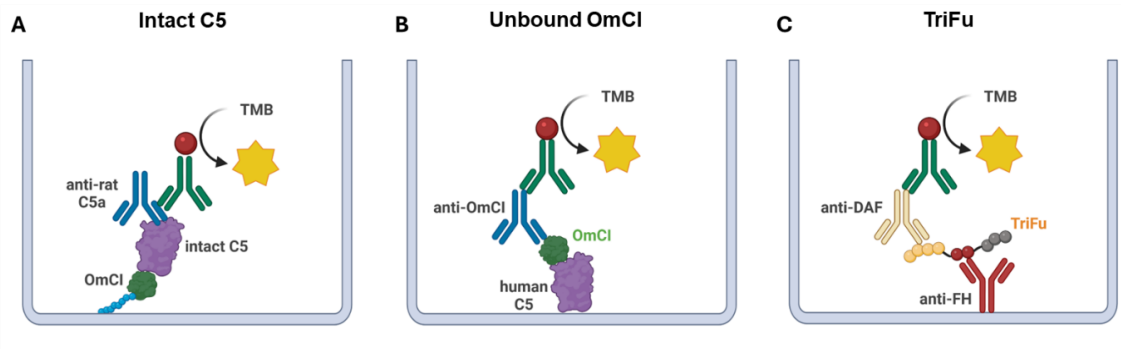


Figure 4. **Self-assembled ELISAs.** Detection method of rat A) intact plasma C5, B) unbound plasma OmCI, and C) plasma TriFu. Savukoski et al., (2026) [121], CC BY-NC-ND 4.0, https://creativecommons.org/licenses/by-nc-nd/4.0/legalcode.en

Intact rat C5 ELISA

To confirm that rat C5 is bound by OmCI or depleted by CVF, plasma samples collected either at the experimental baseline or endpoint were analyzed using in-house assembled ELISA (Figure 4A). The assay selectively detects free C5 based on the binding site availability: C5 molecules complexed with OmCI *in vivo* lack accessible binding site availability and are therefore not captured by OmCI used as a capture reagent in the assay. Briefly, 200 µg/ml of a recombinant fusion construct comprising OmCI (FH8-15-OmCI, self-produced) was coated onto a 96-well MaxiSorp plate (#446612, ThermoFisher Scientific) overnight at 4 °C. Plates were washed with 0.05 % PBS-T and blocked with 2 % PBS-BSA. Diluted rat plasma samples were added and incubated for 45 min at RT. After washing, a rabbit anti-rat C5a antibody (5 µg/ml, #PA5-78891, polyclonal, Invitrogen) was applied and incubated for 1 h at RT. This antibody binds to a site opposite to the OmCI binding site, allowing detection of captured C5 molecules. Following an additional wash, an HRP-conjugated anti-rabbit $F(ab')_2$ fragment (1:250-dilution; #NA9340, GE Healthcare) was added for 30 min at RT. Signal detection was achieved using TMB substrate (#555214, BD Biosciences), and the reaction was stopped with 0.5 M H_2SO_4. Absorbance was measured at 450 nm (OD_{450}).

Unbound OmCI ELISA

Unbound OmCI molecules were detected via our established sandwich ELISA (Figure 4B). The principle of capturing solely free OmCI depends on the binding site availability: OmCI, bound to C5 molecule *in vivo*, has no available binding site for additional C5 used here as a capture reagent. Wells of a 96-well MaxiSorp plate (#446612, ThermoFisher Scientific) were coated with 12 µg/ml of purified human C5 (#A403, Quidel Ortho) overnight at 4 °C. The following day, wells were washed five times with 200 µl PBS-T and blocked with 2 % PBS-BSA for 1 h, at RT. Diluted rat plasma samples were added and incubated for 30 min at RT, followed by five washes with PBS-T. To detect captured OmCI molecules, a polyclonal rabbit anti-OmCI antibody (2 µg/mL; generated by Davids Biotechnology, Regensburg, Germany) was applied for 30 min, at RT. After five additional washes with PBS-T, an HRP-linked anti-rabbit IgG (0.1 µg/ml, #AB97051, Abcam) was added for 30 min at RT. Following the final washing step, signal detection was performed as indicated above (in section *"Intact rat C5 ELISA"*).

TriFu ELISA

To detect TriFu molecules in plasma, a novel sandwich ELISA was established utilizing antibodies recognizing domains derived from the respective regulatory proteins; CD55 and FH (Figure 4C). Shortly, 96-well MaxiSorp plates (#446612, ThermoFisher Scientific) were coated with an anti-human Factor H antibody (0.23 µg/ml, #GAU-018-03-02, clone C18/3, ThermoFisher Scientific) diluted in a coating buffer (1.59 g/l Na2CO3, 2.93 g/l NaHCO3, pH 9.6, #421701, Biolegend) and incubated overnight at 4 °C. The next day, plates were washed 4 times with PBS-T and blocked with 2 % PBS-BSA for 1 h at RT, followed by 4 additional washes with PBS-T. Samples and standards (TriFu in PBS-/-) were added and incubated for 2 h, at RT under shaking conditions (700 rpm). After 5 washes with PBS-T, an anti-human CD55 antibody (0.1 µg/ml, #MA5-29118, clone O28, ThermoFisher Scientific) was added for 1 h, at RT. Following another 5 washes, an HRP-linked anti-rabbit IgG (0.1 µg/ml, #AB97051, Abcam) was added for another 30 min, at RT. Plates were washed 8 times, and signal detection was performed as indicated above (in section *"Intact rat C5 ELISA"*).

4.6. Western Blot analyses

Rat C3 and C5

Rat plasma samples collected at the experimental endpoint were treated in reducing conditions. Shortly, 1,5 µl of plasma samples were mixed with 2 x Laemmli sample buffer (#1610737, BioRad) containing ß-mercaptoethanol and boiled for 4 min at 95 °C. Afterwards, samples were run on a pre-cast stain-free gel (4-15 %, 4568086, Bio-Rad) for 45 min at 210 V. Next, proteins were transferred into Amersham hybond membrane (#10600023, GE Healthcare) by a 7-min blotting program for mixed-molecular weight proteins. Blocking was performed in 5 % dry skim milk for 2 h, at RT. Primary antibodies included goat anti-C3 (1:1000-diluted, #PA1-29715, ThermoFisher Scientific) and anti-C5a (1:1,000-diluted, #PA5-78891, ThermoFisher Scientific) incubated overnight at 4 °C under rolling conditions. Polyclonal anti-C3 antibody is defined to identify C3, C3a, C3b, and C3c of multiple species, while anti-C5a antibody is raised against a synthetic peptide corresponding to the N-terminal sequence of rat C5a. Secondary antibodies included an HRP-linked anti-goat IgG (for C3) (1:1,000-diluted, #HAF017, R&D systems) and HRP-linked anti-rabbit IgG (for C5) (1:4,000-diluted, #1721019, BioRad) antibody for 1 h, at RT. A protein ladder was visualized by using Precision Protein StrepTactin-HRP Conjugate (1:15,000-diluted, #1610380, BioRad). After washing twice in TBS-T and once in TBS for 10 min, the blot was developed with Clarity Western ECL Substrate (#170-5061, BioRad) for 40 sec, after which a chemiluminescence picture was taken using the ChemiDoc XRS+ system (BioRad).

Human C5a

To determine the sensitivity of C5a detection by western blot, variable amounts of native human C5a (1, 10, or 100 ng, #A144, Complement Technologies Inc.) were applied in gel. Moreover, to determine possible serum matrix effect, 10 ng of C5a were mixed with 0,5 µl of human serum. Prepared samples were treated in reducing conditions and transferred to Amersham hybond membrane as stated above (in section *"Rat C3 and C5"*). The membrane was blocked in 5 % dry skim milk (70166, Sigma-Aldrich) for 1 h, at RT. Primary antibody of rabbit anti-human C5a (1:1,000-diluted, #204889, CalbioChem) was applied on the membrane overnight at 4 °C under rolling conditions. The

details of an epitope recognized by the antibody is not defined by the supplier, however, is known to bind human C5a and is supplied as a form of serum. Following three washing steps in TBS-T for 15 min, HRP-linked anti-rabbit antibody (1:4,000-diluted, #1721019, BioRad) was applied for 1 h, at RT. The washing and membrane detection was done as indicated above (in section *"Rat C3 and C5")*

4.7. *In vitro* hemolysis assay

To assess residual hemolytic activity in serum at the experimental endpoint, a classical pathway-based assay was performed in accordance with a standardized protocol [33]. Briefly, shRBCs (Fiebig Nährstofftechnik GbR, Idstein, Germany) were washed with 5 mM PBS-EDTA at 2,200 x g for 2 min until clear supernatant was obtained. The cells were coated with antibodies using rabbit anti-sheep serum (1:4000 dilution, #C51162, Colorado Serum Company, Denver, CO) for 20 min at 37 °C under shaking conditions (700 rpm). After washing, the cells were resuspended in PBS +/+ and incubated with 10 % rat serum for 1 h at 37 °C under shaking conditions (700 rpm). The reaction was terminated by addition of 10 mM PBS-EDTA, and hemolysis was quantified by measuring the absorbance of the supernatant at 405 nm (OD_{405}) using a spectrophotometer. The negative control was supplemented with 10 mM Mg-EGTA, capturing the required calcium-ions for CP activation. Results were normalized to shRBC in water (100%).

4.8. Statistical analysis and figures

Due to relatively small sample number (reaching n ≤10 per group), normality tests were not applied. All data sets were analyzed using non-parametric tests and presented as medians with interquartile ranges. To compare two groups, the Mann-Whitney test was applied. For comparison for more than two groups, Kruskal–Wallis tests followed by Dunn's multiple comparisons post-hoc tests were applied. For repeated-measures time-course data, Friedman tests were used. Correlation analyses included non-parametric Spearman correlation. To illustrate data trends, a simple linear regression line was included.

Statistical significance is indicated as $p \leq 0.05$ (*), $p \leq 0.01$ (**), $p \leq 0.001$ (***), $p \leq 0.0001$ (****). Values of $p > 0.05$ were considered as non-significant (ns) and were not

displayed in graphs for clarity. All statistical analyses and graphical representations of data were performed using GraphPad Prism (v10). For illustrative purposes, elements from Biorender.com have been used for figure generation.

4.9. Data transparency statement

To adhere to the 3Rs principles (Replacement, Reduction and Refinement) for animal experiments, a few preliminary analyses, including a small subset of rats (n = 5 / group), are part of a previously published study (Mannes et al., 2023; [82]) and Doctoral Medical Dissertation (Steinberger, 2024; [134]) pursuing a completely different research hypotheses. The entire experimental groups of TriFu and CVF are not included in the previous studies [82] and [134], respectively.

5. Results

5.1. Preliminary evaluation of TriFu

As a proof-of-concept experiment, the functionality of TriFu was first demonstrated *in vitro* using an AB/0 mismatch setup. Hemolysis of human AB-RBCs was prevented by pre-incubation with either 25 µg/ml TriFu or 33 µg/ml OmCI in heathy type 0 blood (Figure 5A), demonstrating an effective complement modulation by both agents.

Subsequently, as this study represents the first *in vivo* evaluation of TriFu, the assessment of acute tolerability and potential adverse effects in animals was included as an exploratory objective. Body temperature and requirements of anesthesia supply over the course of the experiment did not differ markedly between groups, although some variability was observed (Figure 5B-C). Accordingly, an area under the curve (AUC) analysis revealed no statistically significant differences between the groups for either of the monitored parameters (Suppl. Figure 1A-B).

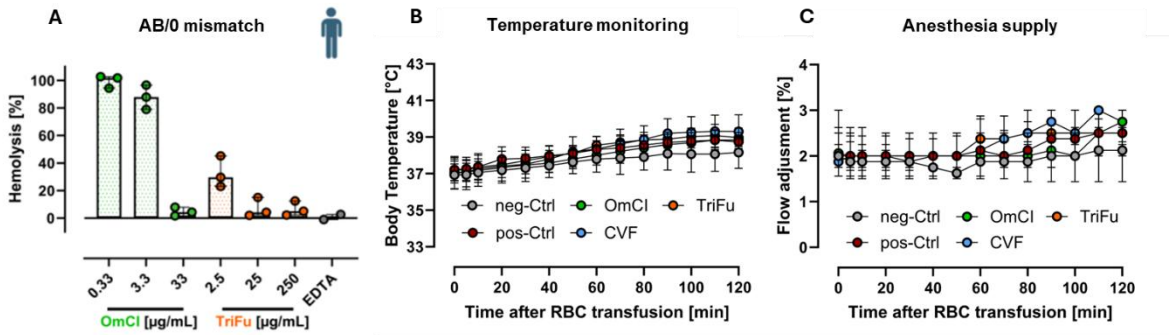


Figure 5. Preliminary experiment and animal monitoring parameters. A) *In vitro* human AB/0 mismatch experiment. Blood was pre-incubated with OmCI (0.33, 3.3, 33 µg/ml) and TriFu (2.5, 25, 250 µg/ml) to demonstrate effective inhibition of lysis of human AB-RBCs (%) measured by the release of hemoglobin. EDTA was used as negative control while 100% lysis was achieved by incubating cells in water. *In vivo* monitoring parameters of B) body temperature and C) anesthesia flow adjustment (%) in all animals after RBC transfusion (min). Median with interquartile range is shown. As author partially adapted from Savukoski et al., (2026) [121], CC BY-NC-ND 4.0, https://creativecommons.org/licenses/by-nc-nd/4.0/legalcode.en

5.2. Effect of complement modulation on intravascular lysis

Quantification of huRBCs

To demonstrate the effect of different complement modulation strategies on intravascular clearance of transfused cells, flow cytometric quantification of huRBCs was performed at each time point (Figure 6). Data were analyzed as the degree of clearance (%) relative to the 5-min time point, which was defined as the baseline representing an even distribution of circulating huRBCs. Pos-Ctrl and OmCI-treated animals exhibited the lowest numbers of remaining huRBCs across all time points pos-transfusion. A significantly slower decrease in huRBCs was observed in TriFu-treated animals compared with OmCI-treated animals at the 20-min time point, and in CVF-treated animals compared with both pos-Ctrl and OmCI-treated animals at 120-min time point. Although not reaching statistical significance and observed only descriptively, CVF- and TriFu-treated animals exhibited a comparable reduction in huRBC counts across all examined time points.

Analysis of total rat RBC count, hemoglobin, and hematocrit

In addition to huRBC analysis, the total rat erythrocyte count was analyzed to observe potential residual cumulative effect of RBCs in the circulation at the experimental endpoint. Based on clinical chemistry data, no differences in the total erythrocyte count were seen between the experimental groups 120 min after transfusion (Figure 6B), although the transfused huRBCs corresponded to an approximate 9-10 % increase in the total RBC count at the start of the experiment, calculated according to a previously described method [67]. Moreover, no major differences were observed in hematocrit [L/L] or hemoglobin values [G/dL] between the experimental groups (Figure 6C-D).

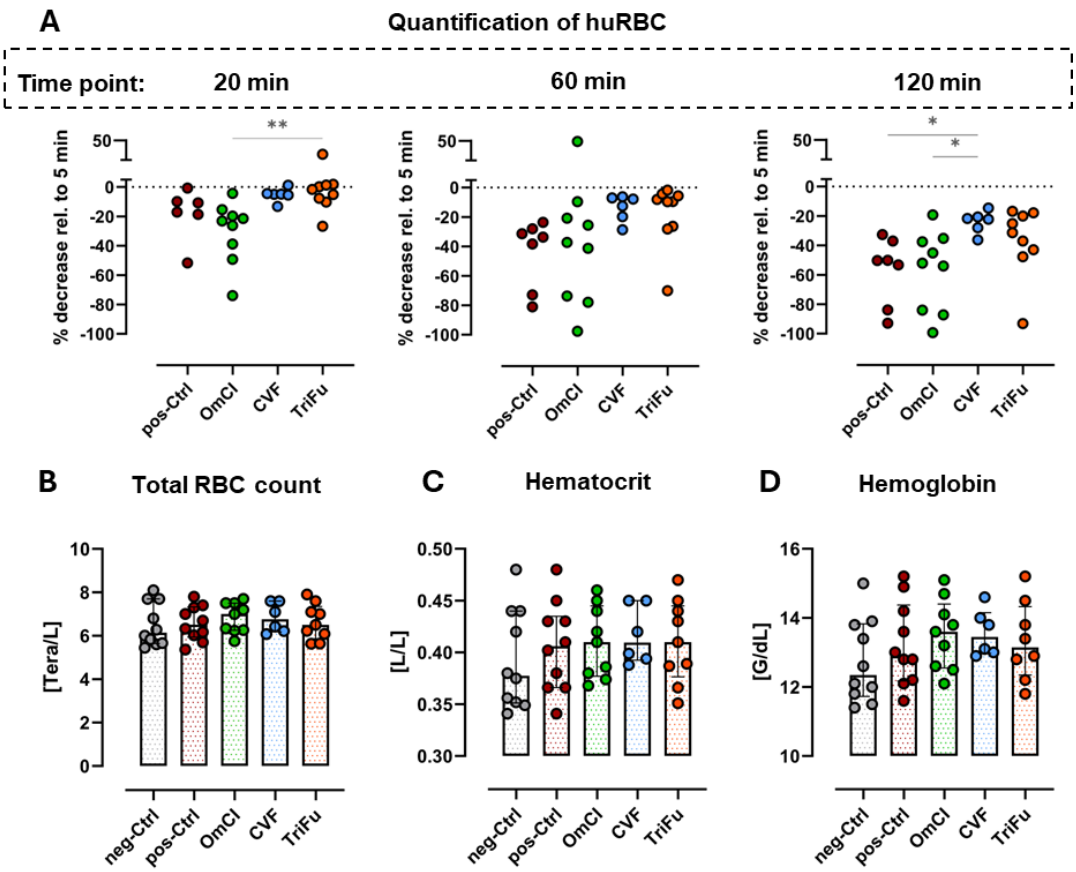


Figure 6. Analysis of huRBC count and total rat erythrocytes. A) Count of huRBCs after transfusion at 20-, 60-, and 120-min time point normalized to the count at 5-min time point (%). Clinical chemistry parameters of B) total rat RBC count, hematocrit (L/L), and hemoglobin (G/dL) at the experimental endpoint (120 min). Median with interquartile range is shown. Only statistically significant differences are indicated: $p \leq 0.05$ (*), $p \leq 0.01$ (**), $p \leq 0.001$ (***), $p \leq 0.0001$ (****). As author partially adapted from Savukoski et al., (2026) [121], CC BY-NC-ND 4.0, https://creativecommons.org/licenses/by-nc-nd/4.0/legalcode.en

Assessment of intravascular lysis parameters

Markers of intravascular hemolysis, including LDH, free plasma hemoglobin, and AST, were significantly elevated in pos-Ctrl and OmCl-treated animals when compared to neg-Ctrl animals, whereas no significant increase was observed in CVF- or TriFu-treated animals (Figure 7A-C). In fact, CVF-treated animals exhibited significantly lower levels of LDH and AST compared with the pos-Ctrl animals. To identify whether the elevation in AST reflected possible liver inflammation or injury rather than intravascular lysis, ALT levels were included in the analysis. No alterations in the ALT levels were observed in any of the experimental groups (Figure 7D).

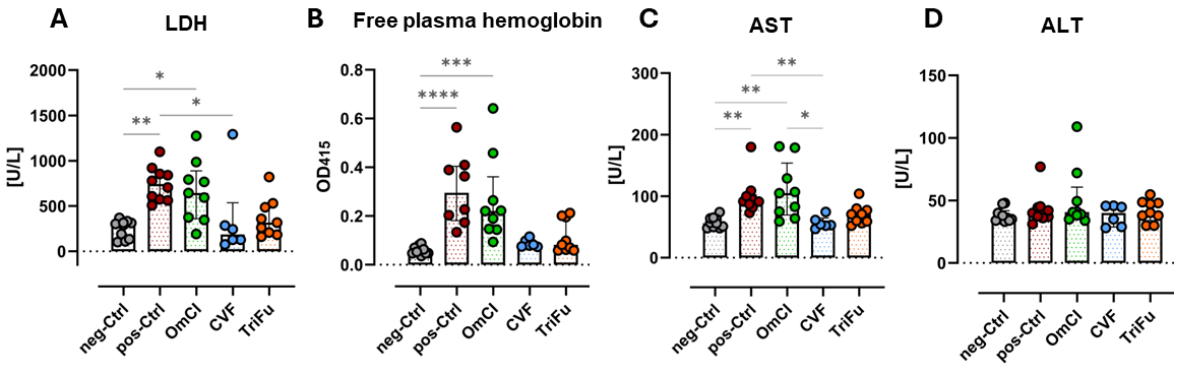


Figure 7. Markers of intravascular lysis and alanine aminotransferase. Parameters of A) lactate dehydrogenase (LDH; U/L), B) free plasma hemoglobin (OD415), C) aspartase aminotransferase (AST; U/L), and D) alanine aminotransferase (ALT; U/L). Median with interquartile range is shown. Only statistically significant differences are indicated: $p \leq 0.05$ (*), $p \leq 0.01$ (**), $p \leq 0.001$ (***), $p \leq 0.0001$ (****). As author partially adapted from Savukoski et al., (2026) [121], CC BY-NC-ND 4.0, https://creativecommons.org/licenses/by-nc-nd/4.0/legalcode.en

5.3. Pattern of complement activation

Opsonization of C3/C4 cleavage fragments on huRBCs

If not lysed by the complement system, cells can be used to assess complement activation through the detection of covalently bound opsonins. Therefore, the remaining huRBCs were analyzed by flow cytometry with anti-C4 and C3 antibodies at each time point of sample collection. Regarding C3 opsonization, pos-Ctrl and OmCI-treated animals exhibited the highest levels of opsonization peaking at the 20-min time point. In contrast, minimal C3 opsonization was observed for CVF- and TriFu-treated animals (Figure 8A). Regarding C4 opsonization, all experimental groups revealed detectable levels that increased over time. A trend toward higher C4 opsonization of huRBCs was observed in CVF- and TriFu-treated animals, particularly at 20-min time point, compared to both pos-Ctrl and OmCI-treated animals (Figure 8B).

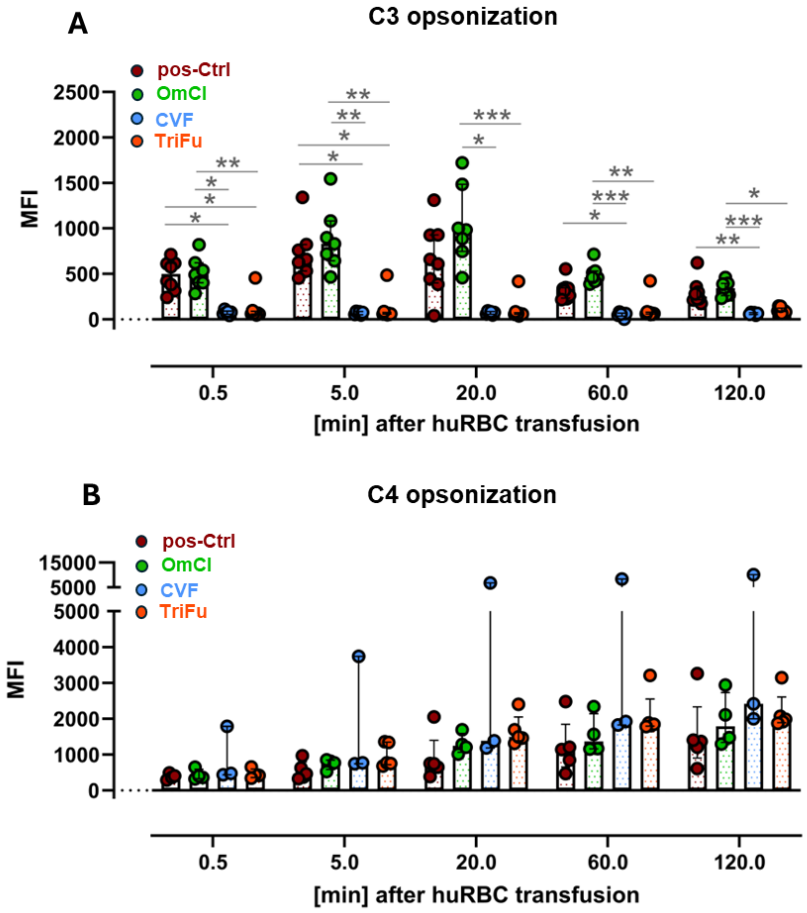


Figure 8. Opsonization of huRBCs. Flow cytometric analysis of A) C3 (MFI) and B) C4 (MFI) on the surface of remaining huRBCs after 0.5, 5, 20, 60, and 120-min of transfusion. Median with interquartile range is shown. Only statistically significant differences are indicated: $p \leq 0.05$ (*), $p \leq 0.01$ (**), $p \leq 0.001$ (***), $p \leq 0.0001$ (****). As author partially adapted from Savukoski et al., (2026) [121], CC BY-NC-ND 4.0, https://creativecommons.org/licenses/by-nc-nd/4.0/legalcode.en

Systemic complement activation

To determine whether complement activation leads to detectable depletion of systemic C3, plasma C3 levels were assessed (Figure 9A). As expected, CVF-treated animals revealed significant drop in the C3 plasma levels when compared to the other experimental groups. There was no clear reduction of C3 plasma levels in any other experimental groups. However, when C3a generation was evaluated, a significant increase in systemic C3a levels was observed in pos-Ctrl and OmCI-treated animals compared with neg-Ctrl animals, whereas CVF- and TriFu-treated animals exhibited levels comparable with neg-Ctrl animals (Figure 9B). Interestingly, only CVF-treated animals demonstrated a significant increase in the sC5b-9 levels at the experimental endpoint (Figure 9C), aligning with the data of effective C3 depletion (Figure 9A).

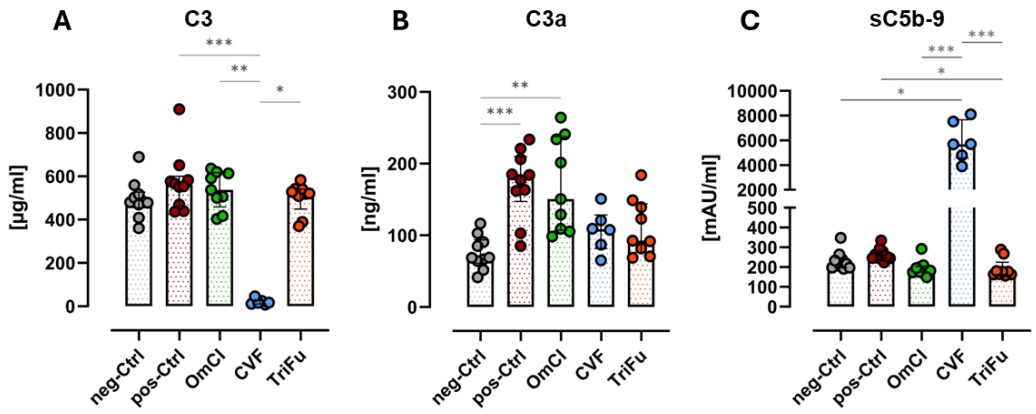


Figure 9. Assessment of systemic complement activation. Measurement of plasma A) C3 protein (µg/ml), B) C3a (ng/ml), and C) sC5b-9 (mAU/ml) at the experimental endpoint measured by ELISA. Median with interquartile range is shown. Only statistically significant differences are indicated: $p \leq 0.05$ (*), $p \leq 0.01$ (**), $p \leq 0.001$ (***), $p \leq 0.0001$ (****). As author partially adapted from Savukoski et al., (2026) [121], CC BY-NC-ND 4.0, https://creativecommons.org/licenses/by-nc-nd/4.0/legalcode.en

Analysis of complement activating endogenous rat antibodies

To demonstrate the *in vivo* trigger of complement activation, *a* retrospective *in vitro* analysis was conducted by using plasma samples collected at the experimental endpoint. In this exploratory analysis, washed human AB-RBCs were bound predominantly by rat IgM, although with variable levels irrespective of the experimental group (Figure 10A), whereas rat IgG was detected only to a limited extent, mainly in neg-Ctrl animals (Figure 10B).

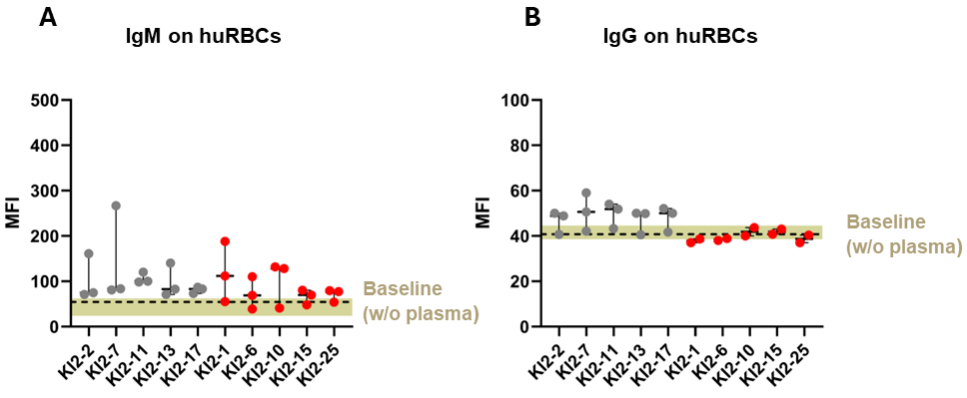


Figure 10. Binding of rat antibodies on huRBCs. Subgroup analysis of rat plasma A) IgM (MFI) and B) IgG (MFI) binding to washed human-AB RBCs. Measurement included five neg-Ctrl (in grey) and pos-Ctrl (in red) animals performed in triplicates. Baseline value was adapted based on signal on huRBCs without plasma exposure. Median with interquartile range is shown.

5.4. Leukocyte population shifts

Cellular composition post-transfusion

The observed intravascular hemolysis and complement activation can theoretically cause major changes in leukocyte population shifts as a sign of ongoing inflammation. Therefore, cell counts (Giga/L) were quantified by clinical chemistry and assessed across all experimental groups at the experimental endpoint (Figure 11). There was a significant increase in leukocytes in pos-Ctrl and OmCI-treated animals in comparison to neg-Ctrl animals (Figure 11A). CVF-treated animals also demonstrated significantly higher leukocyte, lymphocyte, and monocyte counts in comparison to neg-Ctrl animals (Figure 11A-C). Importantly, an almost 4-fold increase in absolute neutrophil counts was detected for pos-Ctrl and OmCI-treated animals when compared to neg-Ctrl animals, while neutrophil counts were found significantly lower in TriFu-treated animals when compared to either pos-Ctrl or OmCI-treated animals (Figure 11D). No statistically significant difference was found for eosinophil or basophil counts between the experimental groups (Figure 11E-F).

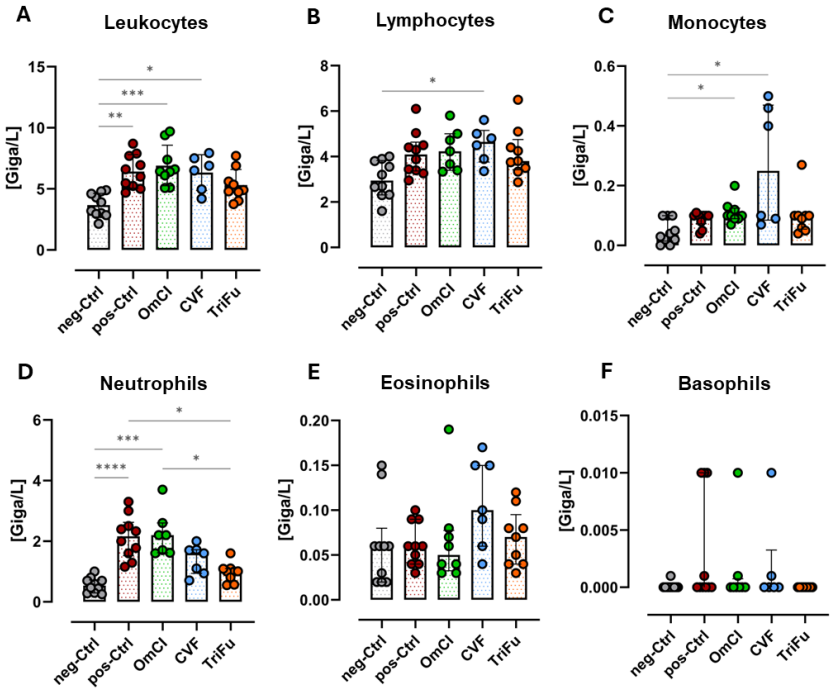


Figure 11. Cellular composition. Clinical chemistry results of cell numbers (shown as Giga/L) for A) total leukocytes, B) lymphocytes, C) monocytes, D) neutrophils, E) eosinophils, and F) basophils at the experimental endpoint. Median with interquartile range is shown. Only statistically significant differences are indicated: $p \leq 0.05$ (*), $p \leq 0.01$ (**), $p \leq 0.001$ (***), $p \leq 0.0001$ (****). As author partially adapted from Savukoski et al., (2026) [121], CC BY-NC-ND 4.0, https://creativecommons.org/licenses/by-nc-nd/4.0/legalcode.en

Analysis of neutrophil activation and potential subgroups

To describe the neutrophil population in more detail, their activation state was assessed by combining markers for CD11b (integrin αM) and CD62L (L-selectin). Upon cellular activation, their expression increases and decreases, respectively. Although a tendency of lower CD11b and higher CD62L expressions was found in pos-Ctrl and OmCI-treated animals, no statistical difference was seen between the groups (Suppl. Fig 2A-B). As a lower activation status could potentially point towards immaturity of cells, a machine learning-based software platform for automated cluster analysis was performed based on FSC, SSC, APC (CD11b), and PE (CD62L) parameters (Suppl. Fig 2D). Differential clusters were obtained, in which neutrophils of positive control animals appeared different from the ones of neg-Ctrl animals and TriFu-treated animals (Suppl. Fig 2E-F), including enrichment of larger neutrophils (Suppl. Fig 2G). However, this descriptive sub-analysis does not permit definitive conclusions regarding cellular phenotype, functionality, or maturation state.

5.5. Screening of systemic and local inflammation markers

Cytokine screening of neg-Ctrl and pos-Ctrl animals

To explore trends in systemic and local inflammation post-transfusion, a membrane-based sandwich immunoassay for rat cytokines and chemokines was conducted. The analyses included one pos-Ctrl and neg-Ctrl animal for serum samples and liver homogenates, and two pos-Ctrl and neg-Ctrl animals for spleen homogenates, thus, the experiments were conducted for solely screening purposes. First, representative membrane images demonstrated visible differences in some serum proteins between pos-Ctrl and neg-Ctrl animals (Figure 12). Following densitometric analysis, including background signal subtraction, normalization to neg-Ctrl values, and $\log_2$-transformation, some notably upregulated and downregulated proteins were identified (Figure 13).

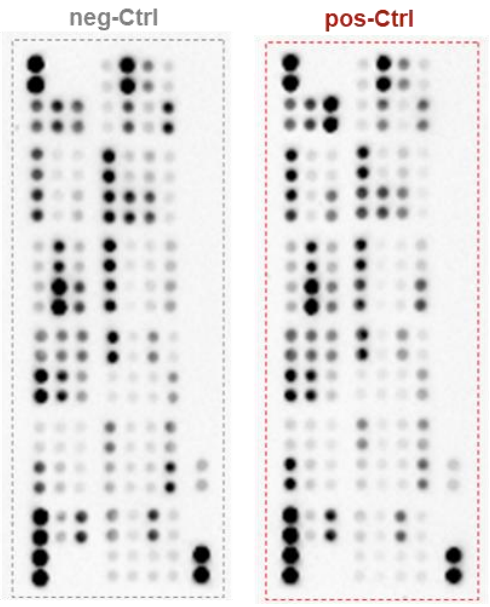


Figure 12. Screening array for cytokines and chemokines. Image of proteome membranes incubated with neg-Ctrl or pos-Ctrl serum samples collected at the experimental endpoint.

For serum, higher than two-fold increase was found for three proteins: GDF-15 (gdf15), Galecting-3 (lgals3), and Serpin E1 (serpine 1), while greater than two-fold decrease was found for six proteins: Hepassocin (Hps), IL-1ra (Il1rn), PDGF-BB (Pdgfb), TWEAK (Tnfsf12), IL-22 (Il22), and LIF (Lif) (Figure 13A). In the liver, higher than two-fold increase was found for six proteins: NGAL (Lcn2), IGFBP-3 (Igfbp3), Adiponectin (Adipoq), CXCL7 (Ppbp), IGFBP-5 (Igfbp5), and VCAM-1 (Vcam1), while no proteins were seen greatly downregulated (Figure 13B). In spleen, there were multiple upregulated proteins identified: Serpin E1 (Serpine1), MCP-1 (Ccl2), IGFBP-2 (Igfbp2), NT-3 (Ntf3), and IL-13 (Il13), Fibulin-3 (Efemp1), IL17A (Il17a), IGF-1 (Igf1), SCF (Kitl), FGF-21 (Fgf21), CCN3 (Nov), CD10 (Mme), CCL3/4 (Ccl3/4), IL-6 (Il6), CCN1 (Ccn1), KIM-1 (Havcr1), and NT-4 (Ntf5), and a few downregulated: Flt-3 Ligand (Flt3l) and VCAM-1 (Vcam1) (Figure 13C). The relative protein levels of all measured cytokines and chemokines in serum, liver, and spleen are represented in the supplementary material as heatmaps (Suppl. Fig 3A-C).

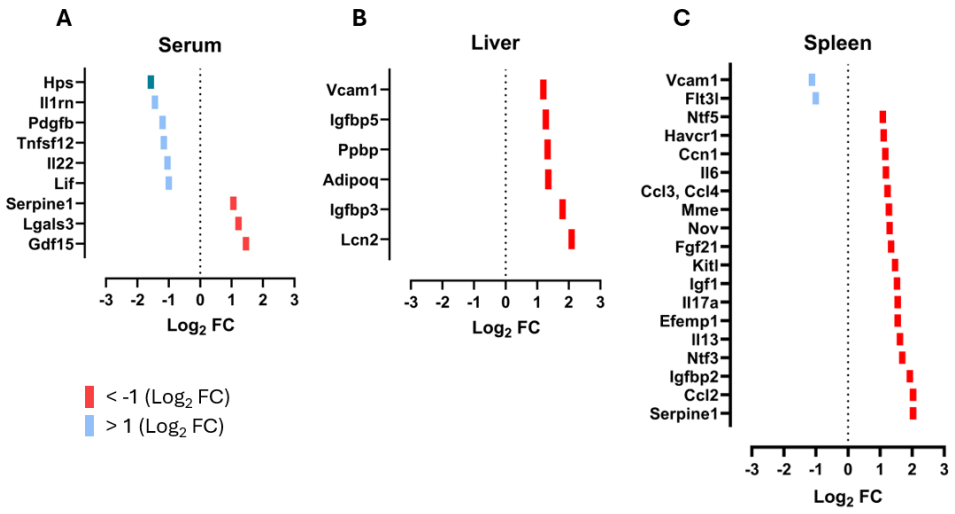


Figure 13. Relative cytokine and chemokine levels in pos-Ctrl animals. Following semi-quantitative analysis and normalization to neg-Ctrl samples, upregulated and downregulated proteins were identified. Proteins showing a ≥2-fold increase (in red; Log_2 fold change of ≥1) and a ≥2-fold decrease (in blue, Log_2 fold change of ≤-1) of A) serum, B), liver homogenates, and C) spleen homogenates.

Association of neutrophil counts with markers of hemolysis, complement and inflammation

As the greatest increase was observed in neutrophil counts, their association with measured analytes of hemolysis, complement activation, and inflammation was investigated. First, there was a significant positive correlation between neutrophil counts and free plasma hemoglobin levels, complement C3 deposition on transfused cells (at 20-min timepoint), and plasma C3a generation (Figure 14A-B).

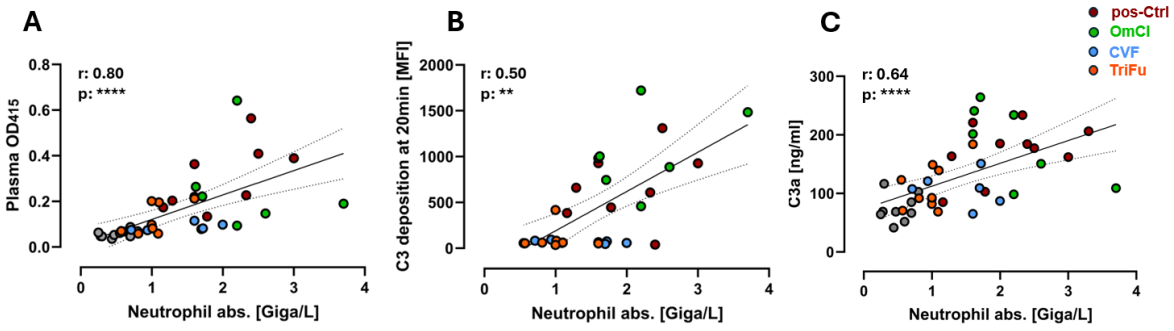


Figure 14. Correlation of neutrophil counts to hemolysis and complement markers. Association of neutrophils to A) free plasma hemoglobin (r:0.80, p****), B) C3 deposition on huRBCs (r:0.50, p**), and C) C3a in plasma (r:0.64; p****). Spearman correlation with illustrative simple linear regression line set for all data points. Only statistically significant differences are indicated: p ≤ 0.05 (*), p ≤ 0.01 (**), p ≤ 0.001 (***), p ≤ 0.0001 (****)

In addition to the descriptive screening analysis of rat proteins in serum, liver, and spleen, comprehensive analysis of rat cytokines and chemokines in plasma was conducted in all animals by using bead-based multiplex analysis (Legendplex, BioLegend). Based on these analyses, neutrophil counts were correlated with significantly altered markers of IL-6, TNF-α, and MCP-1, revealing significant positive associations across all examined parameters (Figure 15A-C).

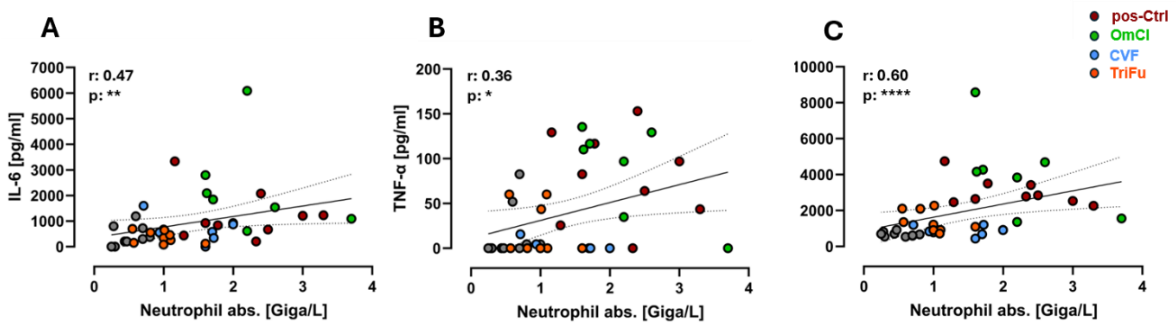


Figure 15. Correlation of neutrophils counts to pro-inflammatiory plasma cytokines and chemokines measured by Legendplex. Association of neutrophils (Giga/L) to A) IL-6 (pg/ml) (r:0.47; p**), B) TNF-a (pg/ml) (r:0.36, p*), and C) MCP-1 (pg/ml) (r:0.60, p****). Spearman correlation with illustrative simple linear regression line for all data points. Only statistically significant differences are indicated: p ≤ 0.05 (*), p ≤ 0.01 (**), p ≤ 0.001 (***), p ≤ 0.0001 (****)

5.6. Assessment of thromboinflammation

As hemolytic events frequently coincide with major pro-thrombotic events (61), descriptive analysis of thrombocyte counts and the viscoelastic properties of whole blood clot formation over time were conducted. First, no statistically significant differences were seen in the thrombocyte counts between the experimental groups, although a drop in count was seen in a few pos-Ctrl animals (Figure 16A).

To assess the functional consequences of hemolysis on clot formation, which integrates the contributions of platelets, coagulation factors, and fibrinogen, ROTEM analysis was included. The following parameters were analyzed: the initial time of clot formation (CT, [s]), clot propagation time (CTF, [s]) and kinetics (α-angle [°]), maximum overall clot strength (MCF, [mm]), and time required to form maximum clot firmness (MCF-T, [s]) (Figure 16B). Analysis included the activation of the extrinsic pathway of the coagulation cascade by addition of tissue factor (EXTEM). Briefly, no statistically significant difference was seen in any of the parameters measured (Figure 16C-G).

However, high inter-individual variability and the limited sample size were noted, limiting the power of the analysis.

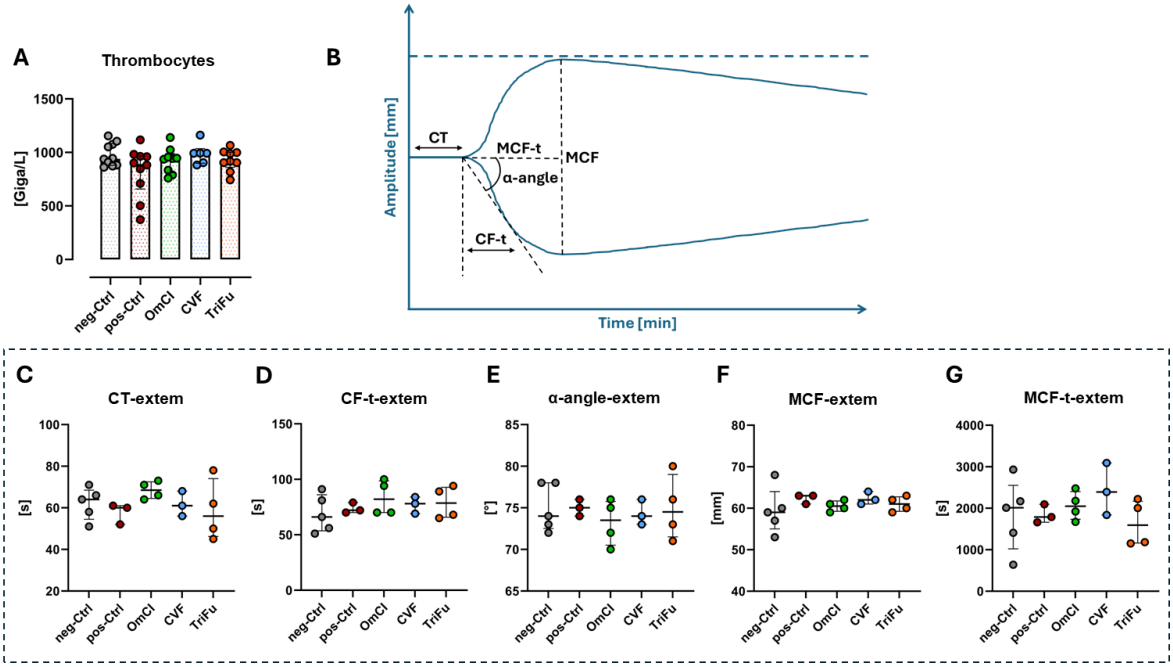


Figure 16. Subgroup analysis of hemostatic properties post-transfusion. A) Thrombocyte count (Giga/L) measured by clinical chemistry. B) Diagram of rotational thromboelastometry (ROTEM) including explanation of different parameters acquired over time (y=amplitude, x=time). Results of subgroup analysis of C) clotting time (CT), D) clot formation time (CF-t), E) alpha-angle of clot, F) maximum clot firmness (MCF), and maximum clot firmness time (MCF-t) for extrinsic pathway of coagulation. Median with interquartile range is shown. As author partially adapted from Savukoski et al., (2026) [121], CC BY-NC-ND 4.0, https://creativecommons.org/licenses/by-nc-nd/4.0/legalcode.en

5.7. Evaluation of hemolysis-associated kidney injury

A subgroup analysis was conducted to evaluate the response to huRBC transfusion in animals, including five neg-Ctrl animals and five pos-Ctrl animals. Urine samples collected at the experimental endpoint exhibited a darker color in some transfused animals, whereas this was absent in all neg-Ctrl animals (Figure 17A). After quantification, significantly higher hemoglobin levels (OD_{413}) were detected in pos-Ctrl animals, indicative of major hemolytic events due to mismatched transfusion (Figure 17B).

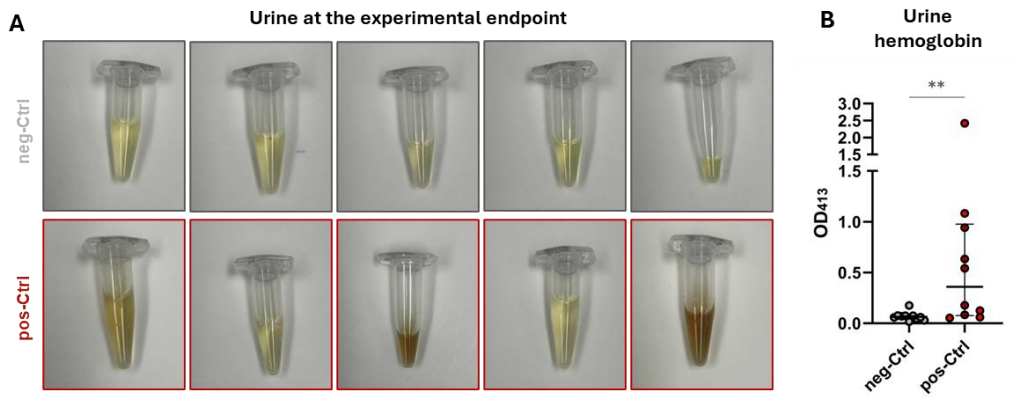


Figure 17. Assessment of urine hemoglobin. A) Pictures of comparing the color of urine collected from neg-Ctrl and pos-Ctrl animals at the experimental endpoint (120-min). B) Quantification of urine hemoglobin measured by spectrophotometry at OD413nm. Median with interquartile range is shown. Only statistically significant differences are indicated: $p \leq 0.05$ (*), $p \leq 0.01$ (**), $p \leq 0.001$ (***), $p \leq 0.0001$ (****)

Beyond hemolysis-induced systemic inflammation, free hemoglobin and heme can contribute to substantial renal injury, given that the kidney's primary role is to constantly filter by-products. Based on our results, there was an increase (although not significant) in total protein and albumin content in the urine of pos-Ctrl animals in comparison to neg-Ctrl animals (Figure 18A-B). Both parameters were significantly lower in CVF-treated animals when compared to the pos-Ctrl animals, while urine albumin content was significantly lower in TriFu-treated animals in comparison to the pos-Ctrl animals. Urine total protein significantly correlated with urine albumin levels (Figure 18C), and to free urine hemoglobin levels (Figure 18D). To study the possible alterations of the glomerular filtration rate (GFR) of the kidney, creatinine levels were measured. No major differences in serum creatinine or urine creatinine were observed between the experimental groups (Suppl. Fig 4A-B). Moreover, when urine albumin was normalized to urine creatinine, the pattern was similar to urine albumin levels (Figure 18B); pos-Ctrl and OmCI-treated animals demonstrated higher levels (although not significant), while TriFu-treated animals had significantly lower levels compared with pos-Ctrl animals (Suppl. Fig 4C).

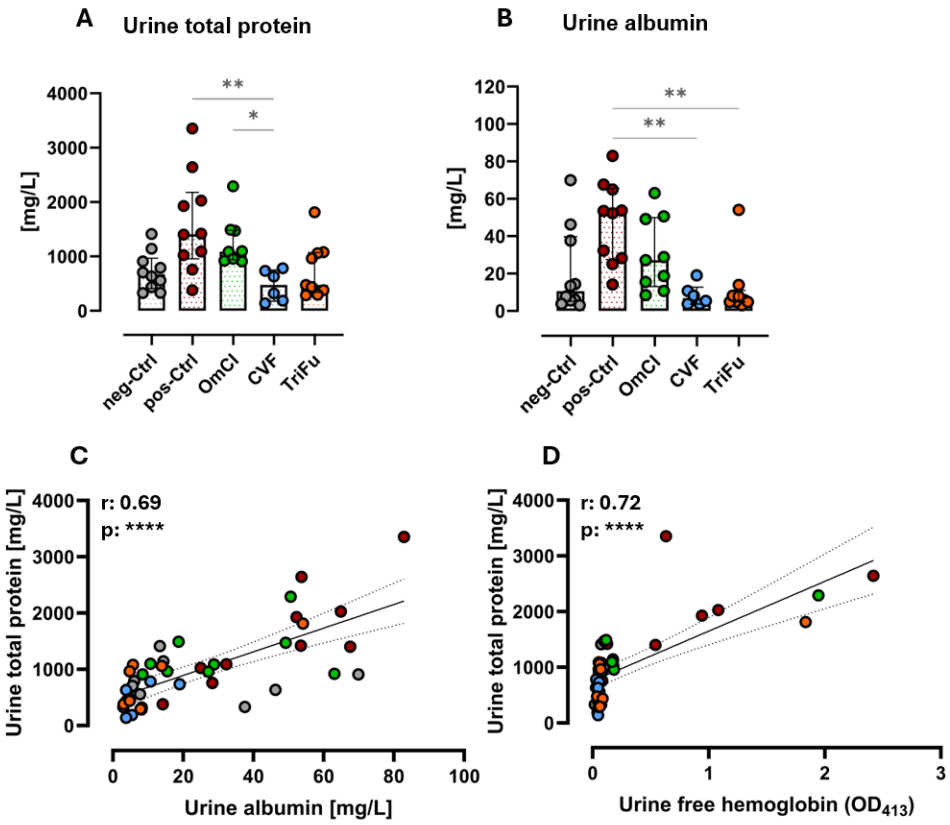


Figure 18. Analysis of hemoglobinuria. A) Total protein (mg/ml) and B) albumin (mg/ml) content in urine at 120-min post-transfusion. Correlation of urine total protein (mg/ml) to C) urine albumin (mg/ml) and D) urine hemoglobin (OD413). Median with interquartile range is shown. Spearman correlation with illustrative simple linear regression line set for all data points. Only statistically significant differences are indicated: $p \leq 0.05$ (*), $p \leq 0.01$ (**), $p \leq 0.001$ (***), $p \leq 0.0001$ (****). As author partially adapted from Savukoski et al., (2026) [121], CC BY-NC-ND 4.0, https://creativecommons.org/licenses/by-nc-nd/4.0/legalcode.en

5.8. Validation of complement modulation efficacy *in vivo*

To validate the *in vivo* efficacy and availability of the complement modulators OmCI, CVF, and TriFu, various retrospective *in vitro* analyses were conducted. For this purpose, plasma/serum samples from individual animals were examined in respect of complement functionality, concentration of modulators, or intact proteins.

As a summary of the subsequent comprehensive retrospective analyses, the following animals were excluded from the study: CVF-2, CVF-5, OmCI-9, and TriFu-1. These analyses validated successful complement modulation in all other animals, allowing confident comparison between the experimental groups.

Residual hemolytic activity of serum

First, to confirm the *in vivo* functional activity of the complement modulators, the residual hemolytic activity of the serum collected at the experimental endpoint was analyzed *in vitro*. The assay followed a standardized classical pathway activation assay using hemolysin-treated shRBCs and 10 % individual rat serum, performed in triplicates (Figure 19A). The results showed that all neg-Ctrl and pos-Ctrl animals demonstrate hemolytic activity ranging from approximately 60-80% as mean values (Figure 19B-C) Among complement modulated animals, only previously identified animals; OmCI-9, CVF-2, CVF-5, and TriFu-1 represented high hemolytic activity, comparable to control animals (Figure 19D-F). While other OmCI- and CVF-treated animals had no hemolytic activity left, some hemolytic activity was left for TriFu-treated animals, ranging from approximately 20-40 %.

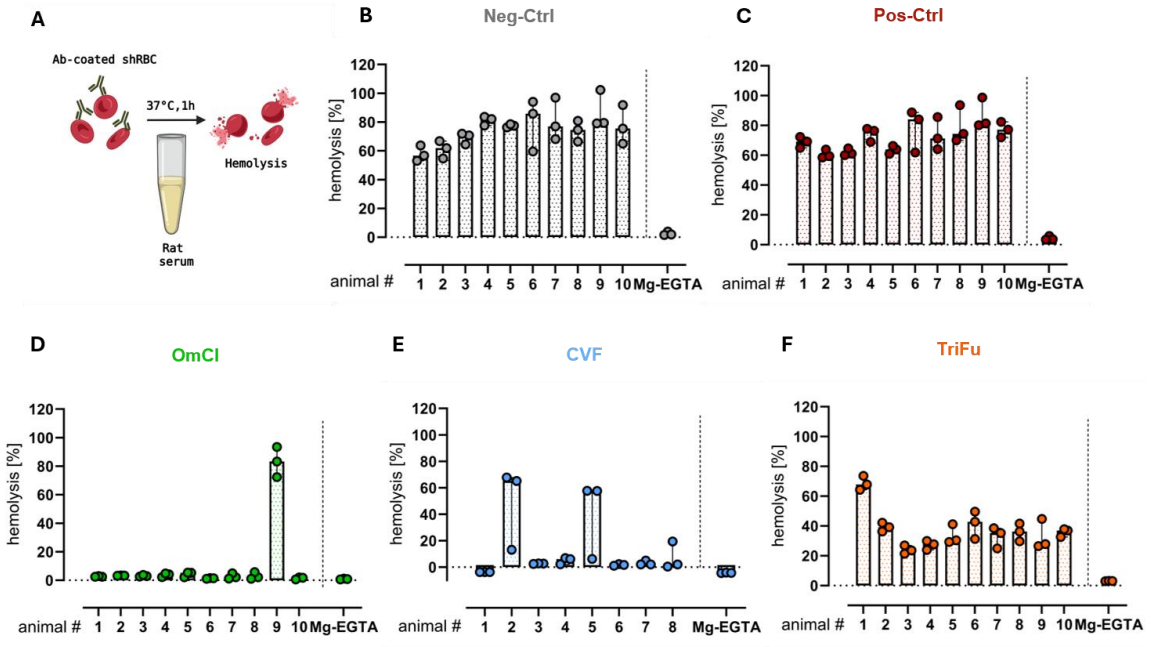


Figure 19. Hemolytic function of rat serum collected at the experimental endpoint. A) Illustration of classical pathway hemolytic assay conducted with antibody-opsonized sheep RBCs (shRBCs) exposed to 10 % rat serum. This leads to RBC lysis in the case of intact complement activity. Hemolysis (%; normalized to 100 % lysis with water) in B) neg-Ctrl, C) pos-Ctrl, D) OmCI-treated, E) CVF-treated, and F) TriFu-treated individual animals measured in triplicates. Serum incubated with mg-EGTA served as negative control, while cells in water represented full lysis. Median with interquartile range is shown. As author partially adapted from Savukoski et al., (2026) [121], CC BY-NC-ND 4.0, https://creativecommons.org/licenses/by-nc-nd/4.0/legalcode.en

Availability of OmCI and TriFu in vivo

To identify appropriate administration and clearance of OmCI and TriFu in individual animals, novel in-house ELISAs were established to measure unbound OmCI, intact C5, and TriFu levels. The results demonstrated successful administration of OmCI in all animals except OmCI-9, resulting in excess plasma levels of OmCI throughout the 120-min experimental timeline (Figure 20A). Effective C5 blockade was further confirmed by the low levels of intact C5 detected at the experimental endpoint in all animals except OmCI-9 (Figure 20B).

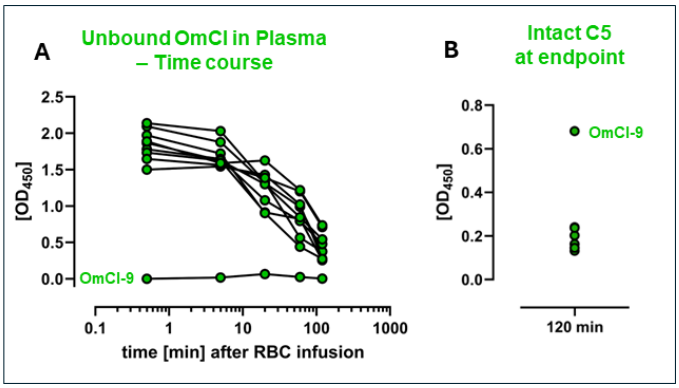


Figure 20. Retrospective analyses of plasma OmCI and intact C5. A) The presence of free OmCI at the course of the experiment (time (min) after RBC transfusion) measured using a novel self-made ELISA (450 nm). B) Intact C5 at 120-min timepoint (450 nm). As author partially adapted from Savukoski et al., (2026) [121], CC BY-NC-ND 4.0, https://creativecommons.org/licenses/by-nc-nd/4.0/legalcode.en

Similarly, TriFu was detected in the plasma of all treated animals throughout the experimental timeline, except for one TriFu animal (TriFu-1), which exhibited almost no detectable TriFu at the experimental endpoint (Figure 21A-B).

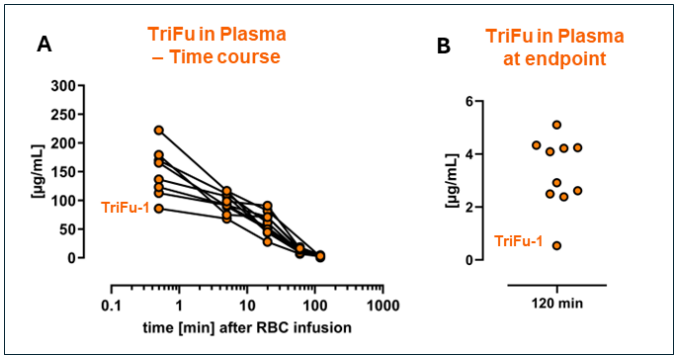


Figure 21. Retrospective analyses of plasma TriFu. A) Concentration of TriFu (µg/ml) at the course of the experiment (time (min) after RBC transfusion) and zoomed-in to the experimental endpoint (at 120-min) (µg/ml). Measurement was performed using a novel in-house developed ELISA. As author partially adapted from Savukoski et al., (2026) [121], CC BY-NC-ND 4.0, https://creativecommons.org/licenses/by-nc-nd/4.0/legalcode.en

Effectiveness of complement depletion by CVF

Moreover, the success of complement depletion by CVF was assessed by detecting C3 and C5 proteins, as well as their cleavage fragments, in plasma collected at the experimental endpoint. Western blot analysis showed depletion of plasma C3 (α-chain in reducing conditions; ~110,000 Da) in all other CVF animals except CVF-5 and CVF-2 (Figure 22A). To validate this observation, a pos-Ctrl animal was included as a control, which exhibited a similar C3 band observed in the two non-responsive CVF-treated animals. Furthermore, unbound plasma C5 levels of CVF-5 and CVF-2 were comparable to levels detected prior OmCI administration (baseline plasma samples), indicating a lack of effective C5 depletion in these animals (Figure 22B). Subsequent gel electrophoresis analysis of plasma samples (Suppl Fig 4A) and Western Blot analysis of C5 (α-chain in reducing conditions; ~110,000 Da) (Suppl. Fig 5B) further confirmed the inadequate C5 depletion in CVF-5 and CVF-2 animals, while other CVF-treated animals demonstrated clear reduction in C5 levels (Suppl. Fig 5-B).

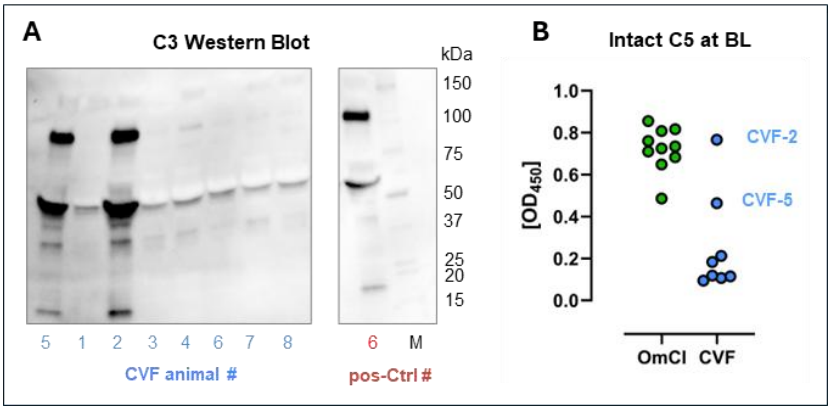


Figure 22. Analysis of complement C3 and C5 depletion by CVF. A) Western blot analysis of C3 in all CVF-treated animals. A pos-Ctrl animal was used as a control. B) Measurement of intact C5 (OD450) at baseline (BL) in CVF-treated animals and OmCI-treated animals that functioned as pos-Ctrl for C5 (baseline prior C5-inhibition but 24 h after administration of CVF). As author partially adapted from Savukoski et al., (2026) [121], CC BY-NC-ND 4.0, https://creativecommons.org/licenses/by-nc-nd/4.0/legalcode.en

Based on Western Blot analysis, rat C5a was not detectable in plasma samples, despite the use of a suitable antibody against rat C5a (Suppl. Fig 5A-B). Therefore, the sensitivity of the method was further evaluated using human C5a in a subsequent analysis. Purified human C5a was titrated at different concentrations (1, 10, and 100 ng), as well as at 10 ng in the presence of human serum to assess a possible matrix effect (Suppl. Fig 5C-D). Interestingly, human C5a was detectable only at concentrations of

10 ng or higher. This amount of C5a is difficult to achieve from small plasma volumes of the rats, indicating inherited assay-related limitations to detect rat C5a by Western Blot (Suppl. Fig 5A-B).

6. Discussion

The current thesis included the evaluation of the efficacy of engineered complement regulator TriFu in protection of transfused huRBCs susceptible to strong classical complement pathway activation, lysis, and lysis-associated adverse effects in Wistar rats. Inspired by naturally occurring complement regulation processes, TriFu combines decay-acceleration and cofactor activity with recognition of host surfaces and presence of late-stage complement opsonins offering enzyme-like performance on halting each complement pathway activity [132]. As seen in certain clinical reports, current stoichiometric complement C5-inhibitors demonstrate challenges in inhibiting terminal pathway activity under strong complement activating conditions [37, 45, 49, 61, 128] raising a need of multifunctional and -focal modulation approach avoiding sole systemic neutralization of target molecule. Thus, it was hypothesized that TriFu offers advantageous protection of huRBCs over a single C5-inhibition strategy by OmCI, based on its physiological characteristic, integrating three different natural complement regulatory proteins.

Briefly, based on the measures of prolonged survival of huRBCs, dampened C3 activation, and attenuated hemolysis-mediated detrimental effects, TriFu performed comparable to prior complement depletion and superiorly to C5-inhibition by OmCI, providing the first *in vivo* evidence of efficient complement modulation by TriFu.

6.1. Performance of complement modulators *in vivo*

As previously described, Wistar rats have endogenous antibodies against human AB-RBCs capable of selectively lysing cells via the classical pathway [5, 130]. In the present work, retrospective analyses revealed variable levels of IgM in rat plasma, whereas IgG was largely undetectable with the applied method. This is consistent with the greater complement-fixing capacity of IgM compared to IgG antibodies [30], and the presence of primary IgM type anti-AB antibodies in the human system [137].

To confidently compare the effects of the applied complement modulators, extensive retrospective *in vitro* analyses were performed to assess their *in vivo* efficacy. Conclusively, four animals had to be excluded from the study, including two animals that exhibited an insufficient complement depletion response, one animal with inadequate

plasma levels of OmCI, and one animal with inadequate plasma levels of TriFu. The remaining animals exhibited sufficient inhibitor levels, confirming appropriate treatment exposure and thereby ensuring valid and unbiased comparison between the experimental groups.

Complement activation patterns

Covalently bound cleavage fragments of C4 and C3 accurately reflect complement activation pattern on transfused huRBCs. As these cells are also susceptible to complement-mediated lysis [64], time-course assessment of opsonization was beneficial to understand the dynamics and impact of complement activation. C4 products seemed to accumulate gradually reaching the highest levels at the experimental endpoint in all animals receiving huRBCs. TriFu- and CVF-treated animals exhibited in trend higher deposition of C4 fragments than pos-Ctrl and OmCI-treated animals. This could be potentially explained purely by the lack of C3 products on surfaces, enabling more fixation sites for C4 fragments or their antibody detection, as C3 opsonins may sterically hinder antibody access [9, 126].

In fact, no C3 fragments were observed on huRBCs in TriFu- and CVF-treated animals, as expected on their inherited mechanism of function. Only a minimal increase in C3 products was detected at the experimental endpoint in TriFu-treated animals, potentially reflecting pharmacokinetic limitation of TriFu. In comparison, a pattern of C3 fragment accumulation could be demonstrated in pos-Ctrl and, even slightly more so, in OmCI-treated animals peaking at 20-min timepoint post-transfusion. This could be predicted because terminal pathway inhibition does not block proximal pathway activation and accumulation of opsonins [106]. At later timepoints, lesser C3 fragments were observed on huRBCs, indicating susceptible lysis or extravascular clearance of heavily C3-dense cells, both mechanisms that have been described in the literature [75, 109, 131].

Regarding systemic levels, significantly elevated C3a concentrations were measured in pos-Ctrl and OmCI-treated animals, but not in TriFu- or CVF-treated animals. This data is in line with the C3 opsonization data for TriFu. However, in CVF-treated animals, depletion of plasma C3 is expected to cause a major increase in C3a levels, but not in

surface-bound C3b. It is postulated that the increase in C3a could be seen in pos-Ctrl and OmCI-treated animals due to a shorter activation period of completement system (2 h), but not in CVF-treated animals due to the longer time period of de-complementation (26 h). Anaphylatoxins can be undetectable in plasma because of their rapid binding to C3aR and C5aR1/2 or overall renal clearance [96, 129]. Another explanation for the insufficient detection of C3a-des(Arg) with the commercially available ELISA. This could explain why we see ongoing active C3a generation in pos-Ctrl and OmCI-treated samples, but no longer in the CVF-treated animals. However, since C3a-des(Arg) is generated within minutes from C3a and they differ only in their terminal arginine residue [16, 148], it is quite unlikely that the antibody is directed solely against C3a.

While there was a detectable elevation of C3a at the nanogram-level in the pos-Ctrl and OmCI-treated animals, this was not associated with any change in total C3 concentration, which remained at the microgram level. Only CVF-treated animals exhibited a clear reduction in the total C3 levels, confirming de-complementation. Of note, a slight trend toward higher plasma C3 concentration was observed in both pos-Ctrl and OmCI-treated animals, possibly reflecting an acute inflammatory response [35, 58, 119]. However, given the short experimental timeframe, this increase is more likely driven by local complement production rather than *de novo* hepatic synthesis of C3 [35, 79].

Considering terminal pathway activation, the applied method was unable to detect potential residual C5a generation by Western blot analysis in CVF-treated animals. As it applies to C3a, it is possible that C5a is not free and available for detection [16, 148], especially after 26-h of de-complementation. However, assay sensitivity limitations were confirmed in a separate experiment using a purified human C5a concentration series. Regarding sC5b-9, high levels were observed in CVF-treated animals, whereas no differences could be seen in other experimental groups. Based on the documented plasma half-life of sC5b-9 in rabbits (30-50-min) [53], it is quite surprising that sC5b-9 remains as greatly elevated until the experimental endpoint in the CVF-treated animals. In comparison to systemic de-complementation, local complement activation on lysis-sensitive huRBCs did not cause significant alterations in plasma sC5b-9

levels. It is tempting to speculate that observed albuminuria in pos-Ctrl and OmCI-treated animals may have contributed to accelerated sC5b-9 clearance, although this remains without experimental evidence for now.

Protection of huRBCs

In terms of circulating huRBC, TriFu-treated animals revealed significantly higher counts at the 20-min timepoint than OmCI-treated animals. This is in line with the C3 opsonization data showing highest opsonization at early time points, possibly accounting for the removal of highly opsonized cells, prevented by TriFu. In comparison to C5-inhibitors, TriFu has the inherent ability to bring complement regulation to sialic acid-rich huRBCs [120, 132] preventing terminal pathway activation where it is required [77, 132]. Although there was not a statistically significant difference between the TriFu-treated and OmCI-treated groups regarding the huRBC counts at later timepoints, a trend of higher counts in TriFu-treated animals was observed. Thus, the absence of C3 activation by TriFu and CVF can slow down the removal of transfused cells especially in the early time-points after transfusion.

Regarding of the later timepoint post-transfusion, because the huRBC stock was stored at 4 °C for up to three weeks and underwent extensive *ex vivo* washing prior transfusion, a proportion of altered or storage-damaged huRBCs may have been cleared extravascularly independent of complement-mediated mechanisms, as reported previously in mouse models [76, 117]. Moreover, capture of antibody-opsonized cells is expected to occur in the liver or spleen [67, 76, 130, 133]. Nevertheless, the transfusion of severely damaged or lysed huRBCs was avoided by confirming a clear supernatant following the washing steps daily prior to administration in rats. The time-dependent effect of TriFu on the entrapment of huRBCs in tissues remains to be examined in future studies.

To point out whether intravascular lysis is causative for the drop of huRBC count, markers of intravascular lysis were assessed. OmCI-treated and pos-Ctrl animals had significantly increased levels of LDH, free plasma hemoglobin, and AST, markers which are found in high amounts inside of intact RBCs [85]. This increase was not detectable in TriFu- or CVF-treated animals, supporting our previous conclusions about possibility

of extravascular entrapment of huRBCs, as also demonstrated for CVF-treated animals in previous xenotransfusion study [130].

To confidently discuss the reason for improper protection of huRBC by OmCI, it was crucial to demonstrate the efficacy of C5-inhibition since a minor free C5 in blood could have the potential to lyse RBCs [38, 64]. Our retrospective *in vitro* analyses demonstrated clearly no hemolytic activity in the serum of OmCI-treated animals. Furthermore, an excess of unbound OmCI and correspondingly, the lack of free C5 in plasma, was confirmed. The differential outcome of *in vivo* and *in vitro* hemolysis assessment could be explained by the lower C3 densities obtained from 10% serum, limiting C5 conformational activation occurring in higher serum concentrations or *in vivo*. In line with our statement, previous AP-based experiments performed with 25% serum with excess amount of Eculizumab or OmCI demonstrated a remaining residual hemolytic activity of 30-40% [37]. Conclusively, there were no pharmacokinetic issues of the OmCI administration in the animals, and the difference in hemolytic potential *in vitro* and *in vivo* stems from the initial capacity of the complement system activation.

Regarding the efficacy of TriFu *in vivo*, there was some residual hemolytic activity left in the serum collected from TriFu-treated animals at the experimental endpoint. The initial administration dose of TriFu was chosen and adjusted based on previous *in vitro* CP and AP hemolysis assays utilizing 50% of rat serum (unpublished data). Here, we could observe a time-dependent clearance of TriFu during the experimental course, representing low plasma levels at the 2-h timepoint. In concordance with low TriFu plasma concentrations at the experimental endpoint, a slight elevation in C3 deposition on huRBCs was seen at 120-min time point. Therefore, it is only postulated that by increasing the TriFu availability throughout the experimental timeline, a complete CP inhibition would have maintained until the experimental endpoint, making the protection of huRBCs even more pronounced by TriFu. However, from another perspective, since only a minor C3 activation occurred at the experimental endpoint and C3b deposition can, in theory, enhance complement regulation by TriFu on huRBCs surfaces [132], the insufficient C3 activation control may not initially cause detrimental effects to transfused cells.

6.2. Hemolysis-driven inflammation and organ response

Since hemolysis can cause damage by the release of DAMPs and activation of complement cascade, further exploratory analyses of released cytokines and chemokines in both fluid phase and in tissues were conducted together with assessment of systemic inflammation, blood hemostatic properties, and the kidney response.

Descriptive proteome analysis of liver and spleen

Certain alterations in cytokine and chemokine levels from liver and spleen samples were detected for pos-Ctrl animals. In general, a trend toward increased levels of proteins related to inflammation, leukocyte recruitment, and tissue repair was observed, including NGAL [91, 112], IL-6 [36], MCP-1 [78], and IGF-1 [145]. The alteration most probably stems from activated immune cells within the site, not from time-consuming acute phase protein synthesis [105]. For example, higher levels of platelet-derived protein CXCL7 could potentially indicate platelet entrapment and activation in the liver [11], where upregulation of VCAM-1 as activation marker of endothelial cells was seen [21]. However, since the proteome analysis was rather observatory and hypothesis-driven with very limited sample sizes, no definitive conclusions can be drawn here.

Inflammation and cellular infiltration

Systemically, hemolysis-associated inflammation was characterized by increased neutrophil counts. Free plasma hemoglobin, C3b deposition, and C3a generation were all associated with higher neutrophils counts, consistent with established role of C3a in neutrophil recruitment in Wistar rats [104]. However, given that heme has been reported to exert chemotactic effects on murine neutrophils [102], and that IL-6, TNF-α, and MCP-1 likewise correlated with neutrophil counts, these findings suggest a complex, interconnected network of mediators, in which the causal roles in neutrophil recruitment cannot be clearly defined here.

Related to neutrophil function, no evidence of cellular activation was observed based on CD11b and CD62L expression, although circulating cytokines themselves are potent neutrophil activators [141, 149]. However, to explore potential subpopulations within the approximately three-fold increased total neutrophil population, automated

cluster analysis incorporating forward scatter (FSC) and side scatter (SSC) parameters as proxies for cellular size and granularity, respectively, was performed. As stated in the literature, the presence of bigger neutrophils with lower CD11b expression could potentially implicate immaturity of cells in positive control animals [29]. However, since this aspect was not the primary objective of the present work, no definitive conclusion regarding neutrophil maturation status can be drawn.

No sign of major thromboinflammation

As reported in clinical studies of PNH, thrombotic events are closely associated with hemolytic activity and represent major complications [46], and were significantly reduced by C5 inhibition [43, 47, 49, 62]. Although the underlying mechanistic reasons for thrombosis are multifactorial, particularly, the release of hemoglobin and NO scavenging from damaged RBCs are considered key drivers of downstream thrombocyte activation [40]. Thrombocyte depletion is commonly interpreted as marker of overt or subclinical thrombus formation [83, 152]. Here, apart from few pos-Ctrl animals, no clear consumption of thrombocytes was detected. Furthermore, based on our descriptive analysis the global hemostatic function appeared mainly preserved, although high intergroup variability and limited samples size limit the robustness of these conclusions.

Indication of kidney damage

Extensive intravascular hemolysis is often associated with kidney injury due to the massive release of hemoglobin from lysed RBCs [34, 63, 94]. If free hemoglobin is not scavenged by haptoglobin and remains longer in the circulation, it is more prone to glomerular infiltration and consequent damage [7, 34]. Briefly, hemoglobin is oxidized to methemoglobin with a ferric (Fe^{3+}) state, which is poor at carrying oxygen and more prone to heme dissociation. Heme itself, if not bound by hemopexin, is cytotoxic molecule that promotes oxidative stress both in the fluid phase and upon insertion into lipid membranes via its hydrophobic porphyrin ring, where it can drive membrane damage [8, 63].

As expected, animals undergoing huRBC transfusion and complement-mediated hemolysis exhibited elevated urinary concentrations of free hemoglobin, total protein, and albumin. In case of alterations of the glomerular basement membrane and change of its physical integrity, large and/or negatively charged plasma proteins like albumin can be present in urine [127]. There was seemingly less albumin detected in the urine of CVF- and TriFu-treated animals, demonstrating a protective effect of kidney by complement depletion and regulation, respectively. To avoid possible "dilution effects" of the urine in these animals, normalization of albumin to creatinine, a marker representative of glomerular filtration rate (GFR) [135], was determined with similar results. However, due to the limited assessment of markers of kidney function and injury, only observatory conclusions can be made.

6.3. Linking experimental findings to clinical observations

The aim was to demonstrate the beneficial effect of an alternative approach to complement modulation by TriFu compared with current stoichiometric therapeutic strategies. Over the past two decades, clinical studies have provided valuable insights into the mechanisms of the complement system under terminal pathway inhibition [106, 123]. PNH was the first clinical pathology treated with complement therapeutics, specifically with the humanized anti-C5 monoclonal antibody Eculizumab [106, 115]. Terminal pathway inhibition markedly improved patient's quality of life and has nearly normalized life expectancy. Although complement therapeutics have since been expanded to treat other diseases, PNH remains the best-characterized clinical model, supported by extensive clinical experience and long-term clinical evidence [45, 49, 106, 123].

In the past decade, structural insights into C5 regulation [57] and functional studies of terminal pathway activity under C5-inhibition have been reported [38, 81]. Evidence from these studies supports that C5 can be conformationally activated in C3b-dense surfaces with reduced dependency on canonical trimolecular C5 convertases [81]. These significant *in vitro* findings are consistent with reports of so-called "breakthrough" hemolysis in PNH patients treated with Eculizumab, particularly under conditions of strong complement amplifying conditions [37, 44, 109]. Therefore, although

there is a significant improvement in LDH and hemoglobin values in PNH patients, they often fail to normalize [37, 49, 61, 114, 128]. Although our xenotransfusion model does not recapitulate the pathology of PNH, our findings demonstrate that OmCI mediates incomplete terminal pathway inhibition under strong complement activation trigger, closely reflecting clinical observations in patients with PNH.

Interestingly, double C5-inhibition targeting of distinct and opposite regions of the C5-molecule enhances “C5 freezing”, more effectively stabilizing C5 conformation, and thereby preventing terminal pathway activity on densely C3b-opsonized RBCs [81]. In the current work, it is postulated that since OmCI failed to protect transfused and highly C3-opsonized huRBCs from lysis, combination with another C5-inhibitor targeting an opposite site of C5 molecule would have provided advantageous protection of transfused cells. However, to date, double-C5 inhibition strategy has not progressed beyond preclinical evaluation [18].

In turn, an add-on therapy of FD with Eculizumab is approved for the treatment of PNH and has shown improvement in halting C5 activation due to the lack of AP-mediated amplification of the proximal pathway and C3b deposition [71]. However, although FD combination therapy and double C5 inhibition could potentially provide advantages on halting both intravascular and extravascular clearance, they were not implemented in the current study. This is because the primary aim of the study was to compare complement regulation by TriFu to a stoichiometric single C5-inhibitor, which remains as the standard-of-care backbone therapy in PNH and continues to dominate the established market for complement inhibition [12, 98, 106].

Regarding other complement inhibition strategies, C3 inhibition by Pegcetacoplan was approved for PNH in 2021. Pegcetacoplan treatment has shown superiority over Eculizumab revealing more stable hemoglobin values in patients by also addressing extravascular clearance of cells [48, 110]. However, importantly, although numerically reduced, some remaining breakthrough events were more severe under C3-inhition than under C5-inhibition [48]. The molecular mechanisms for strong breakthrough hemolytic events under C3-inhibition are still obscure but can be related to an enhanced PNH-clone size affected by occasional strong triggers for complement activation [48,

110]. This could lead to excessive C4b deposition and subsequent C5 activation, referred to C3-bypass activation, demonstrated both *in vitro* and *in vivo* [81, 154]. We demonstrated that TriFu effectively blocked C3 activation *in vivo*. Moreover, although C4 activation is not inhibited by TriFu, cofactor activity could allow effective inactivation of C4b-dense surfaces and suppression of a C3-bypass effect on C5. This could potentially halt terminal pathway activity in CP/LP-driven pathologies, while AP-driven pathologies are not inherently relying on C4 from the start with.

6.4. Limitations of study

To answer our research questions, the established model of acute and systemic complement activation was utilized to compare different complement modulation strategies. As blockade of all activation pathways by TriFu was expected, and time-dependent examination of hemolysis could be conducted, the model was well suited as a starting point for upcoming *in vivo* studies with TriFu. However, the study holds some inherent limitations discussed below.

Dosing of TriFu

Considering administration of TriFu in the following studies, it would be advantageous to adjust doses of TriFu based on the weight of the individual animals. Here, a constant dose of 5,000 µg was assigned to all animals, irrespectively of the body weight variations ranging from 244 to 470 grams, laying in average as 310 grams. The *in vivo* approximated concentration of TriFu was ranging from 110 to 220 µg/ml, averaged as 160 µg/ml, which was theoretically calculated to reach 250 µg/ml in regards of 20 ml blood. Although the level was lower than anticipated, TriFu plasma concentration reached theoretically, and based on previous *in vitro* evaluation (not published data), sufficient levels for full CP inhibition in all animals at the experimental start due to calculated safety factor. Regardless, detailed follow-up studies regarding pharmacokinetic profile of TriFu should focus on normalizing dosing based on the body weight.

Cofactor activity of TriFu

Further, we did not address the state of C4 inactivation by incorporating cofactor activity of TriFu. Previous *in vitro* work has demonstrated good binding affinity of 50 nM for

C3b, while it was 17-fold weaker for C4b [132]. It would be important to explore the C4 opsonization profile achieved after application of TriFu, since it might have some clinically relevant protective functions over stoichiometric C3-inhibitors. The rational is that C4b-dense surfaces can activate C5 *in vitro* [81], which might become a clinical challenge in complement amplifying conditions under C3-inhibition. Moreover, as shown in the literature, C4 opsonins may become sufficient alone for phagocytotic clearance when C3 is lacking [100]. This could permit remaining homeostatic function of complement in clearance of apoptotic or foreign cells. However, the proportion of which inactivated C4d is generated by TriFu, and to which extent these opsonins play a role in intra- and extravascular clearance, remains to be determined.

Inherent limitations of study design

Accordingly, the primary focus was on intravascular clearance of huRBCs with tissue analysis limited to a single static endpoint. However, because heavily complement-opsonized cells are cleared within minutes to hours [136], assessing tissue sequestration at a 2-h time point is unlikely to capture major differences mediated by different complement-modulating strategies. The short experimental timeline presents another limitation in our study, restricting expression analyses to mostly cytokines and chemokines released from activated cells [11, 105], without going into detail about tissue responses and long-term repair mechanisms.

The intrinsic limitation of the study aligns with the challenges to compare clinical C5 inhibitors to tick-derived OmCI. Although involved in clinical studies, OmCI is different from humanized antibodies applied in patients. However, because effective single C5-inhibitors for rodents were not available at the time of study design, OmCI was chosen based on its well-established functional activity *in vivo* [66, 125].

6.5.Conclusions

Taken together, TriFu successfully modulated the complement system, examined for the first time here *in vivo*. TriFu provided efficient protection of huRBCs from complement C3 opsonization, thereby prolonging their circulation time and improving hematological parameters, whereas even sufficient dosing of C5-inhibitor OmCI failed to adequately control terminal pathway activation (Figure 19).

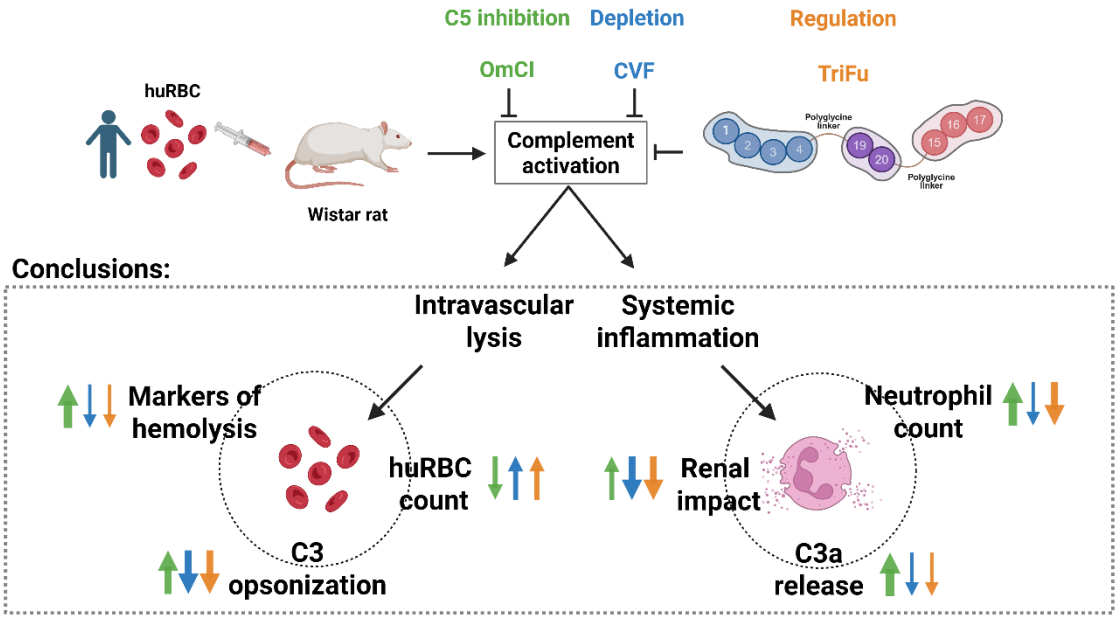


Figure 19. Graphical summary. Complement inhibition by OmCI, depletion by CVF, and regulation by TriFu was compared in a rat xenotransfusion model. The transfusion of human AB-RBCs induces a strong classical pathway activation and subsequent complement-mediated intravascular lysis. While TriFu and CVF prolonged survival of transfused cells, attenuated markers of intravascular lysis (including free hemoglobin, LDH, AST), and prevented C3 activation, OmCI-treated animals did not show these protective effects. As a sign of systemic inflammation, neutrophil counts were significantly elevated in OmCI-treated animals, while greatly lower in TriFu-treated animals. Similarly, markers of systemic inflammation (including IL-6, TNF-α, MCP-1) as well as C3a generation were higher in OmCI-treated animals. TriFu and CVF appeared to protect the kidney from hemolysis-mediated injury based on the urine protein analysis, whereas OmCI-treated animals exhibited albuminuria. Thus, TriFu performance, evaluated here for the first time *in vivo*, was comparable to that of prior complement depletion. In contrast, even efficient dosing of C5-inhibitor OmCI could not protect huRBCs from complement-mediated damage. The thickness of the arrows represents significance of the difference. As author partially adapted from Savukoski et al., (2026) [121], CC BY-NC-ND 4.0, https://creativecommons.org/licenses/by-nc-nd/4.0/legalcode.en

6.6. Future perspectives

Regarding future perspectives, TriFu offers great potential for further *in vivo* studies. First, it would be advantageous to investigate the pharmacokinetic profile of TriFu in animal models. This would enable optimization of the TriFu dosing and dosing intervals and, if necessary, allow for modifications of the protein structure, e.g., coupling it to the stable plasma protein albumin, to prolong its half-life. Pharmacokinetic investigation will become especially important with experimental models that are extended beyond 2 h time frame used here.

Second, as C3 activation has been shown to be effectively abolished *in vivo*, it will be important in future studies to assess also cofactor activity. Addressing the clearance mechanisms of C4-opsonized cells or particles under stoichiometric C5- and C3-inhibitors in comparison to the effect of TriFu would be novel and mechanistically interesting. Thus, TriFu not only provides therapeutic potential, but also serves as an experimental tool to better understand the complex role of inactivated opsonins in their recognition and dynamic clearance.

Third, as TriFu has intrinsic potential to protect host tissues, this function could be furthermore extensively explored in future *in vivo* models, as it represents one of its main advantages compared to complement therapeutics in current clinical practice. An optimal model would combine AP-driven pathology localized in tissues such as the kidney. As the kidney is highly sensitive to complement-mediated damage and heavily relies of FH availability [155], the integrated FH19-20 domain within TriFu molecule may provide an effective means of enhancing complement regulation in renal tissues.

Taken together, the first *in vivo* evidence of TriFu effectiveness encourages *further in vivo* characterization and the use of more tissue-targeted approaches.

7. References:

1. Adan A, Alizada G, Kiraz Y, Baran Y, Nalbant A: Flow cytometry: basic principles and applications. Crit Rev Biotechnol 37:163-76 (2017)
2. Alper CA, Balavitch D: Cobra venom factor: evidence for its being altered cobra C3 (the third component of complement). Science 191:1275-6 (1976)
3. Amara U, Flierl MA, Rittirsch D, Klos A, Chen H, Acker B, Brückner UB, Nilsson B, Gebhard F, Lambris JD, Huber-Lang M: Molecular intercommunication between the complement and coagulation systems. J Immunol 185:5628-36 (2010)
4. Amara U, Kalbitz M, Perl M, Flierl MA, Rittirsch D, Weiss M, Schneider M, Gebhard F, Huber-Lang M: Early expression changes of complement regulatory proteins and C5a receptor (CD88) on leukocytes after multiple injury in humans. Shock 33:568-75 (2010)
5. Aptekman PM, Bogden AE: Characterization of the natural hemagglutinins in normal rat serum associated with a negative phase following tumor implantation. Cancer Res 16:216-21 (1956)
6. Badri P, Jiang X, Borodovsky A, Najafian N, Kim J, Clausen VA, Goel V, Habtemariam B, Robbie GJ: Pharmacokinetic and Pharmacodynamic Properties of Cemdisiran, an RNAi Therapeutic Targeting Complement Component 5, in Healthy Subjects and Patients with Paroxysmal Nocturnal Hemoglobinuria. Clinical Pharmacokinetics 60:365-78 (2021)
7. Baek JH, D'Agnillo F, Vallelian F, Pereira CP, Williams MC, Jia Y, Schaer DJ, Buehler PW: Hemoglobin-driven pathophysiology is an in vivo consequence of the red blood cell storage lesion that can be attenuated in guinea pigs by haptoglobin therapy. J Clin Invest 122:1444-58 (2012)
8. Belcher JD, Beckman JD, Balla G, Balla J, Vercellotti G: Heme degradation and vascular injury. Antioxid Redox Signal 12:233-48 (2010)
9. Bernth Jensen JM, Laursen NS, Jensen RK, Andersen GR, Jensenius JC, Sørensen UBS, Thiel S: Complement activation by human IgG antibodies to galactose-α-1,3-galactose. Immunology 161:66-79 (2020)
10. Bhakdi S KG, Muhly M, Fromm S, Seibert G, Parrisius J: Formation of transmural complement pores in serum-sensitive Escherichia coli. Infect Immun 55:206-10 (1987)
11. Blair P, Flaumenhaft R: Platelet alpha-granules: basic biology and clinical correlates. Blood Rev 23:177-89 (2009)
12. Bodó I, Amine I, Boban A, Bumbea H, Kulagin A, Lukina E, Piekarska A, Zupan IP, Sokol J, Windyga J, Cermak J: Complement Inhibition in Paroxysmal Nocturnal Hemoglobinuria (PNH): A Systematic Review and Expert Opinion from Central Europe on Special Patient Populations. Advances in Therapy 40:2752-72 (2023)
13. Brodsky RA: Paroxysmal nocturnal hemoglobinuria. Blood 124:2804-11 (2014)
14. Brodszki N, Frazer-Abel A, Grumach AS, Kirschfink M, Litzman J, Perez E, Seppänen MRJ, Sullivan KE, Jolles S: European Society for Immunodeficiencies (ESID) and European Reference Network on Rare Primary Immunodeficiency, Autoinflammatory and Autoimmune Diseases (ERN RITA) Complement Guideline: Deficiencies, Diagnosis, and Management. Journal of Clinical Immunology 40:576-91 (2020)

15. Burk AM, Martin M, Flierl MA, Rittirsch D, Helm M, Lampl L, Bruckner U, Stahl GL, Blom AM, Perl M, Gebhard F, Huber-Lang M: Early complementopathy after multiple injuries in humans. Shock 37:348-54 (2012)
16. Campbell WD, Lazoura E, Okada N, Okada H: Inactivation of C3a and C5a octapeptides by carboxypeptidase R and carboxypeptidase N. Microbiol Immunol 46:131-4 (2002)
17. Cochrane CG, Müller-Eberhard HJ, Aikin BS: Depletion of Plasma Complement in Vivo by a Protein of Cobra Venom: Its Effect on Various Immunologic Reactions. The Journal of Immunology 105:55-69 (1970)
18. Conversano E, Vivarelli M: Advances in Complement Inhibitory Strategies for the Treatment of Glomerular Disease: A Rapidly Evolving Field. J Clin Med 14 (2025)
19. Cornacoff JB, Hebert LA, Smead WL, VanAman ME, Birmingham DJ, Waxman FJ: Primate erythrocyte-immune complex-clearing mechanism. J Clin Invest 71:236-47 (1983)
20. Czermak BJ, Sarma V, Pierson CL, Warner RL, Huber-Lang M, Bless NM, Schmal H, Friedl HP, Ward PA: Protective effects of C5a blockade in sepsis. Nat Med 5:788-92 (1999)
21. Deem TL, Cook-Mills JM: Vascular cell adhesion molecule 1 (VCAM-1) activation of endothelial cell matrix metalloproteinases: role of reactive oxygen species. Blood 104:2385-93 (2004)
22. Denk S, Neher MD, Messerer DAC, Wiegner R, Nilsson B, Rittirsch D, Nilsson-Ekdahl K, Weckbach S, Ignatius A, Kalbitz M, Gebhard F, Weiss ME, Vogt J, Radermacher P, Köhl J, Lambris JD, Huber-Lang MS: Complement C5a Functions as a Master Switch for the pH Balance in Neutrophils Exerting Fundamental Immunometabolic Effects. The Journal of Immunology 198:4846-54 (2017)
23. Dingli D, Matos JE, Lehrhaupt K, Krishnan S, Yeh M, Fishman J, Sarda SP, Baver SB: The burden of illness in patients with paroxysmal nocturnal hemoglobinuria receiving treatment with the C5-inhibitors eculizumab or ravulizumab: results from a US patient survey. Annals of Hematology 101:251-63 (2022)
24. Ehrengruber MU GT, Deranleau DA: Activation of human neutrophils by C3a and C5A Comparison of the effects on shape changes, chemotaxis, secretion, and respiratory burst. FEBS Letters 346:181-4 (1994)
25. El Sissy C, Rosain J, Puel M, Gonnin C, Frémeaux-Bacchi V: Complement deficiencies and infections. Current Opinion in Immunology 98:102711 (2026)
26. Elsner J, Oppermann M, Czech W, Kapp A: C3a activates the respiratory burst in human polymorphonuclear neutrophilic leukocytes via pertussis toxin-sensitive G-proteins. Blood 83:3324-31 (1994)
27. Fällman M, Andersson R, Andersson T: Signaling properties of CR3 (CD11b/CD18) and CR1 (CD35) in relation to phagocytosis of complement-opsonized particles. J Immunol 151:330-8 (1993)
28. Fleckenstein M, Keenan TDL, Guymer RH, Chakravarthy U, Schmitz-Valckenberg S, Klaver CC, Wong WT, Chew EY: Age-related macular degeneration. Nature Reviews Disease Primers 7:31 (2021)
29. Francis WR, Ireland RE, Spear AM, Jenner D, Watts SA, Kirkman E, Pallister I: Flow Cytometric Analysis of Hematopoietic Populations in Rat Bone Marrow. Impact of Trauma and Hemorrhagic Shock. Cytometry A 95:1167-77 (2019)

30. Garson JA, Quindlen EA, Kornblith PL: Complement fixation by IgM and IgG autoantibodies on cultured human glial cells. J Neurosurg 55:19-26 (1981)
31. Geerlings MJ, de Jong EK, den Hollander AI: The complement system in age-related macular degeneration: A review of rare genetic variants and implications for personalized treatment. Molecular Immunology 84:65-76 (2017)
32. Gerber GF, Brodsky RA: Pegcetacoplan for paroxysmal nocturnal hemoglobinuria. Blood 139:3361-5 (2022)
33. Giclas PC: Classical Pathway Evaluation. Current Protocols in Immunology 9:13.1.1-.1.26 (1994)
34. Gladwin MT, Kanias T, Kim-Shapiro DB: Hemolysis and cell-free hemoglobin drive an intrinsic mechanism for human disease. J Clin Invest 122:1205-8 (2012)
35. Goldberger G, Bing DH, Sipe JD, Rits M, Colten HR: Transcriptional regulation of genes encoding the acute-phase proteins CRP, SAA, and C3. The Journal of Immunology 138:3967-71 (1987)
36. Graw JA, Mayeur C, Rosales I, Liu Y, Sabbisetti VS, Riley FE, Rechester O, Malhotra R, Warren HS, Colvin RB, Bonventre JV, Bloch DB, Zapol WM: Haptoglobin or Hemopexin Therapy Prevents Acute Adverse Effects of Resuscitation After Prolonged Storage of Red Cells. Circulation 134:945-60 (2016)
37. Harder MJ, Höchsmann B, Dopler A, Anliker M, Weinstock C, Skerra A, Simmet T, Schrezenmeier H, Schmidt CQ: Different Levels of Incomplete Terminal Pathway Inhibition by Eculizumab and the Clinical Response of PNH Patients. Front Immunol 10:1639 (2019)
38. Harder MJ, Kuhn N, Schrezenmeier H, Höchsmann B, von Zabern I, Weinstock C, Simmet T, Ricklin D, Lambris JD, Skerra A, Anliker M, Schmidt CQ: Incomplete inhibition by eculizumab: mechanistic evidence for residual C5 activity during strong complement activation. Blood 129:970-80 (2017)
39. Heiderscheit AK, Hauer JJ, Smith RJH: C3 glomerulopathy: Understanding an ultra-rare complement-mediated renal disease. American Journal of Medical Genetics Part C: Seminars in Medical Genetics 190:344-57 (2022)
40. Helms CC, Marvel M, Zhao W, Stahle M, Vest R, Kato GJ, Lee JS, Christ G, Gladwin MT, Hantgan RR, Kim-Shapiro DB: Mechanisms of hemolysis-associated platelet activation. Journal of Thrombosis and Haemostasis 11:2148-54 (2013)
41. Helmy KY, Katschke KJ, Jr., Gorgani NN, Kljavin NM, Elliott JM, Diehl L, Scales SJ, Ghilardi N, van Lookeren Campagne M: CRIg: a macrophage complement receptor required for phagocytosis of circulating pathogens. Cell 124:915-27 (2006)
42. Hess C, Schifferli JA: Immune adherence revisited: novel players in an old game. News Physiol Sci 18:104-8 (2003)
43. Hill A, Kelly RJ, Hillmen P: Thrombosis in paroxysmal nocturnal hemoglobinuria. Blood 121:4985-96 (2013)
44. Hill A, Rother RP, Arnold L, Kelly R, Cullen MJ, Richards SJ, Hillmen P: Eculizumab prevents intravascular hemolysis in patients with paroxysmal nocturnal hemoglobinuria and unmasks low-level extravascular hemolysis occurring through C3 opsonization. Haematologica 95:567-73 (2010)
45. Hillmen P, Hall C, Marsh JC, Elebute M, Bombara MP, Petro BE, Cullen MJ, Richards SJ, Rollins SA, Mojcik CF, Rother RP: Effect of eculizumab on hemolysis and transfusion requirements in patients with paroxysmal nocturnal hemoglobinuria. N Engl J Med 350:552-9 (2004)

46. Hillmen P, Lewis SM, Bessler M, Luzzatto L, Dacie JV: Natural history of paroxysmal nocturnal hemoglobinuria. N Engl J Med 333:1253-8 (1995)
47. Hillmen P, Muus P, Dührsen U, Risitano AM, Schubert J, Luzzatto L, Schrezenmeier H, Szer J, Brodsky RA, Hill A, Socié G, Bessler M, Rollins SA, Bell L, Rother RP, Young NS: Effect of the complement inhibitor eculizumab on thromboembolism in patients with paroxysmal nocturnal hemoglobinuria. Blood 110:4123-8 (2007)
48. Hillmen P, Szer J, Weitz I, Röth A, Höchsmann B, Panse J, Usuki K, Griffin M, Kiladjian J-J, de Castro C, Nishimori H, Tan L, Hamdani M, Deschatelets P, Francois C, Grossi F, Ajayi T, Risitano A, Peffault de Latour R: Pegcetacoplan versus Eculizumab in Paroxysmal Nocturnal Hemoglobinuria. N Engl J Med 384:1028-37 (2021)
49. Hillmen P, Young NS, Schubert J, Brodsky RA, Socié G, Muus P, Röth A, Szer J, Elebute MO, Nakamura R, Browne P, Risitano AM, Hill A, Schrezenmeier H, Fu CL, Maciejewski J, Rollins SA, Mojcik CF, Rother RP, Luzzatto L: The complement inhibitor eculizumab in paroxysmal nocturnal hemoglobinuria. N Engl J Med 355:1233-43 (2006)
50. Huber-Lang M, Lambris JD, Ward PA: Innate immune responses to trauma. Nat Immunol 19:327-41 (2018)
51. Huber-Lang M, Sarma JV, Zetoune FS, Rittirsch D, Neff TA, McGuire SR, Lambris JD, Warner RL, Flierl MA, Hoesel LM, Gebhard F, Younger JG, Drouin SM, Wetsel RA, Ward PA: Generation of C5a in the absence of C3: a new complement activation pathway. Nature Medicine 12:682-7 (2006)
52. Huber-Lang MS, Younkin EM, Sarma JV, McGuire SR, Lu KT, Guo RF, Padgaonkar VA, Curnutte JT, Erickson R, Ward PA: Complement-Induced Impairment of Innate Immunity During Sepsis. The Journal of Immunology 169:3223-31 (2002)
53. Hugo F, Berstecher C, Krämer S, Fassbender W, Bhakdi S: In vivo clearance studies of the terminal fluid-phase complement complex in rabbits. Clin Exp Immunol 77:112-6 (1989)
54. Janeway CA. The complement system and innate immunity. Immunobiology: The Immune System in Health and Disease. 5 ed: New York: Garland Science; 2001.
55. Jenne D, Stanley KK: Molecular cloning of S-protein, a link between complement, coagulation and cell-substrate adhesion. Embo j 4:3153-7 (1985)
56. Jenne DE, Tschopp J: Molecular structure and functional characterization of a human complement cytolysis inhibitor found in blood and seminal plasma: identity to sulfated glycoprotein 2, a constituent of rat testis fluid. Proc Natl Acad Sci U S A 86:7123-7 (1989)
57. Jore MM, Johnson S, Sheppard D, Barber NM, Li YI, Nunn MA, Elmlund H, Lea SM: Structural basis for therapeutic inhibition of complement C5. Nature Structural & Molecular Biology 23:378-86 (2016)
58. Julen N, Davrinche C, Ozanne D, Lebreton JP, Fontaine M, Ripoche J, Daveau M: Differential modulation of complement factor H and C3 expression by TNF-alpha in the rat. In vitro and in vivo studies. Mol Immunol 29:983-8 (1992)
59. Karasu E, Demmelmaier J, Kellermann S, Holzmann K, Köhl J, Schmidt CQ, Kalbitz M, Gebhard F, Huber-Lang MS, Halbgebauer R: Complement C5a Induces Pro-inflammatory Microvesicle Shedding in Severely Injured Patients. Frontiers in Immunology 11:1789 (2020)

60. Kavanagh D, Goodship TH, Richards A: Atypical hemolytic uremic syndrome. Semin Nephrol 33:508-30 (2013)
61. Kelly RJ, Hill A, Arnold LM, Brooksbank GL, Richards SJ, Cullen M, Mitchell LD, Cohen DR, Gregory WM, Hillmen P: Long-term treatment with eculizumab in paroxysmal nocturnal hemoglobinuria: sustained efficacy and improved survival. Blood 117:6786-92 (2011)
62. Kokoris S, Polyviou A, Evangelidis P, Grouzi E, Valsami S, Tragiannidis K, Gialeraki A, Tsakiris DA, Gavriilaki E: Thrombosis in Paroxysmal Nocturnal Hemoglobinuria (PNH): From Pathogenesis to Treatment. International Journal of Molecular Sciences 25:12104 (2024)
63. Kokoris SI, Gavriilaki E, Miari A, Travlou A, Kyriakou E, Anagnostopoulos A, Grouzi E: Renal involvement in paroxysmal nocturnal hemoglobinuria: an update on clinical features, pathophysiology and treatment. Hematology 23:558-66 (2018)
64. Koski CL, Ramm LE, Hammer CH, Mayer MM, Shin ML: Cytolysis of nucleated cells by complement: cell death displays multi-hit characteristics. Proceedings of the National Academy of Sciences 80:3816-20 (1983)
65. Krishnan V, Ponnuraj K, Xu Y, Macon K, Volanakis JE, Narayana SV: The crystal structure of cobra venom factor, a cofactor for C3- and C5-convertase CVFBb. Structure 17:611-9 (2009)
66. Kuhn N, Schmidt CQ, Schlapschy M, Skerra A: PASylated Coversin, a C5-Specific Complement Inhibitor with Extended Pharmacokinetics, Shows Enhanced Anti-Hemolytic Activity in Vitro. Bioconjugate Chemistry 27:2359-71 (2016)
67. Kumar PS, Pallera HK, Hair PS, Rivera MG, Shah TA, Werner AL, Lattanzio FA, Cunnion KM, Krishna NK: Peptide inhibitor of complement C1 modulates acute intravascular hemolysis of mismatched red blood cells in rats. Transfusion 56:2133-45 (2016)
68. Lamers C, Mastellos DC, Ricklin D, Lambris JD: Compstatins: the dawn of clinical C3-targeted complement inhibition. Trends Pharmacol Sci 43:629-40 (2022)
69. Lamers C, Plüss CJ, Ricklin D: The Promiscuous Profile of Complement Receptor 3 in Ligand Binding, Immune Modulation, and Pathophysiology. Frontiers in Immunology Volume 12 - 2021 (2021)
70. Law SK, Dodds AW: The internal thioester and the covalent binding properties of the complement proteins C3 and C4. Protein Sci 6:263-74 (1997)
71. Lee JW, Griffin M, Kim JS, Lee Lee LW, Piatek C, Nishimura J-i, Carrillo Infante C, Jain D, Liu P, Filippov G, Sicre de Fontbrune F, Risitano A, Kulasekararaj AG, Barcellini W, Barraco F, Beneitez Pastor D, Capra M, Chew LP, Chrysavgi L, De Castro C, de la Tour RP, De Oliveira MM, Di Bona E, Forcade E, Fu C-L, Furha C, Gaya Valls A, Giannouli S, Gonzalez-Fernandez A, Griffin M, Gural A, Gutierrez EO, Hernández-Rodríguez I, Ibrahim I, Iori AP, Ishida T, Jang JH, Kim J-A, Kim JS, Kitano T, Kosugi H, Kreiniz N, Kulasekararaj A, Lee JW, Lee Lee LW, Mayer J, Mitchell L, Mori Y, Nishiwaki K, Notaro R, Nunez R, Obara N, Oliva EN, Patriquin C, Pessoa V, Piatek C, Piekarska A, Raza S, Risitano AM, Rojnuckarin P, Samuel D, Shammo J, Tadmor T, Takami A, Tamari R, Terriou L, Uchiyama H, Vannucchi AM, Yamaguchi H: Addition of danicopan to ravulizumab or eculizumab in patients with paroxysmal nocturnal haemoglobinuria and clinically significant extravascular haemolysis (ALPHA): a double-blind, randomised, phase 3 trial. The Lancet Haematology 10:e955-e65 (2023)

72. Li R, Xie J, Kantor C, Koistinen V, Altieri DC, Nortamo P, Gahmberg CG: A peptide derived from the intercellular adhesion molecule-2 regulates the avidity of the leukocyte integrins CD11b/CD18 and CD11c/CD18. J Cell Biol 129:1143-53 (1995)
73. Li X, Wang H, Schmidt CQ, Ferreira VP, Yancopoulou D, Mastellos DC, Lambris JD, Hajishengallis G: The Complement-Targeted Inhibitor Mini-FH Protects against Experimental Periodontitis via Both C3-Dependent and C3-Independent Mechanisms. J Immunol 211:453-61 (2023)
74. Lin Z, Schmidt CQ, Koutsogiannaki S, Ricci P, Risitano AM, Lambris JD, Ricklin D: Complement C3dg-mediated erythrophagocytosis: implications for paroxysmal nocturnal hemoglobinuria. Blood 126:891-4 (2015)
75. Lindorfer MA, Pawluczkowycz AW, Peek EM, Hickman K, Taylor RP, Parker CJ: A novel approach to preventing the hemolysis of paroxysmal nocturnal hemoglobinuria: both complement-mediated cytolysis and C3 deposition are blocked by a monoclonal antibody specific for the alternative pathway of complement. Blood 115:2283-91 (2010)
76. Litvack ML, Post M, Palaniyar N: IgM promotes the clearance of small particles and apoptotic microparticles by macrophages. PLoS One 6:e17223 (2011)
77. Liu F, Wawersik S, Tomlinson S, Thurman JM, Holers VM: Tissue-targeted regulators of complement for amelioration of human disease: rationale and novel therapeutic strategies. The Journal of Immunology 214:2138-49 (2025)
78. Liu Y, Shayo S, Su S, Bao W, Zhong H, Murakhovskaya I, Lobo CA, An X, Manwani D, Shi PA, Yazdanbakhsh K: Heme-induced activation of the TLR3/TRIF-IFN-I-CCL2 pathway contributes to kidney injury in sickle cell disease. Blood 147:1624-33 (2026)
79. Lubbers R, van Essen MF, van Kooten C, Trouw LA: Production of complement components by cells of the immune system. Clinical and Experimental Immunology 188:183-94 (2017)
80. Madi N, Paccaud JP, Steiger G, Schifferli JA: Immune complex binding efficiency of erythrocyte complement receptor 1 (CR1). Clin Exp Immunol 84:9-15 (1991)
81. Mannes M, Dopler A, Zolk O, Lang SJ, Halbgebauer R, Höchsmann B, Skerra A, Braun CK, Huber-Lang M, Schrezenmeier H, Schmidt CQ: Complement inhibition at the level of C3 or C5: mechanistic reasons for ongoing terminal pathway activity. Blood 137:443-55 (2021)
82. Mannes M, Pechtl V, Hafner S, Dopler A, Eriksson O, Manivel VA, Wohlgemuth L, Messerer DAC, Schrezenmeier H, Ekdahl KN, Nilsson B, Jacobsen EM, Hoenig M, Huber-Lang M, Braun CK, Schmidt CQ: Complement and platelets: prothrombotic cell activation requires membrane attack complex-induced release of danger signals. Blood Adv 7:6367-80 (2023)
83. Marchetti M, Zermatten MG, Bertaggia Calderara D, Aliotta A, Alberio L: Heparin-Induced Thrombocytopenia: A Review of New Concepts in Pathogenesis, Diagnosis, and Management. Journal of Clinical Medicine 10:683 (2021)
84. Markiewski MM, Nilsson B, Nilsson Ekdahl K, Mollnes TE, Lambris JD: Complement and coagulation: strangers or partners in crime? Trends in Immunology 28:184-92 (2007)

85. Marques-Garcia F: Methods for Hemolysis Interference Study in Laboratory Medicine - A Critical Review. Ejifcc 31:85-97 (2020)
86. Martin U, Bock D, Arseniev L, Tornetta MA, Ames RS, Bautsch W, Köhl J, Ganser A, Klos A: The Human C3a Receptor Is Expressed on Neutrophils and Monocytes, but Not on B or T Lymphocytes. Journal of Experimental Medicine 186:199-207 (1997)
87. McNamara LA, Topaz N, Wang X, Hariri S, Fox L, MacNeil JR: High Risk for Invasive Meningococcal Disease Among Patients Receiving Eculizumab (Soliris) Despite Receipt of Meningococcal Vaccine. American Journal of Transplantation 17:2481-4 (2017)
88. Merle NS, Church SE, Fremeaux-Bacchi V, Roumenina LT: Complement System Part I - Molecular Mechanisms of Activation and Regulation. Front Immunol 6:262 (2015)
89. Merle NS, Noe R, Halbwachs-Mecarelli L, Fremeaux-Bacchi V, Roumenina LT: Complement System Part II: Role in Immunity. Front Immunol 6:257 (2015)
90. Mevorach D, Mascarenhas JO, Gershov D, Elkon KB: Complement-dependent clearance of apoptotic cells by human macrophages. J Exp Med 188:2313-20 (1998)
91. Mishra J, Mori K, Ma Q, Kelly C, Barasch J, Devarajan P: Neutrophil gelatinase-associated lipocalin: a novel early urinary biomarker for cisplatin nephrotoxicity. Am J Nephrol 24:307-15 (2004)
92. Mollnes TE, Kirschfink M: Strategies of therapeutic complement inhibition. Molecular Immunology 43:107-21 (2006)
93. Morgan BP, Harris CL: Complement therapeutics; history and current progress. Molecular immunology 40 2-4:159-70 (2003)
94. Nath KA, Vercellotti GM, Grande JP, Miyoshi H, Paya CV, Manivel JC, Haggard JJ, Croatt AJ, Payne WD, Alam J: Heme protein-induced chronic renal inflammation: Suppressive effect of induced heme oxygenase-11. Kidney International 59:106-17 (2001)
95. Nonaka M, Kimura, A: Genomic view of the evolution of the complement system. Immunogenetics 58:701-13 (2006)
96. Norda R, Schött U, Berséus O, Akerblom O, Nilsson B, Ekdahl KN, Stegmayr BG, Knutson F: Complement activation products in liquid stored plasma and C3a kinetics after transfusion of autologous plasma. Vox Sang 102:125-33 (2012)
97. Ojha H, Ghosh P, Singh Panwar H, Shende R, Gondane A, Mande SC, Sahu A: Spatially conserved motifs in complement control protein domains determine functionality in regulators of complement activation-family proteins. Commun Biol 2:290 (2019)
98. Padilla Kelley T, King H, Malhotra A, DeLoughery TG, Martens K, Shatzel JJ: Advancements in complement inhibition for PNH and primary complement–mediated thrombotic microangiopathy. Blood Advances 9:3937-45 (2025)
99. Pangburn MK, Schreiber RD, Müller-Eberhard HJ: Human complement C3b inactivator: isolation, characterization, and demonstration of an absolute requirement for the serum protein beta1H for cleavage of C3b and C4b in solution. J Exp Med 146:257-70 (1977)
100. Popescu NI, Kluza J, Reidy MA, Duggan E, Lambris JD, Thompson LF, Coggeshall KM: Monocyte uptake of polymeric peptidoglycan is bimodal and governed by complement C3 and C4 opsonins. JCI Insight 10:e186346 (2024)

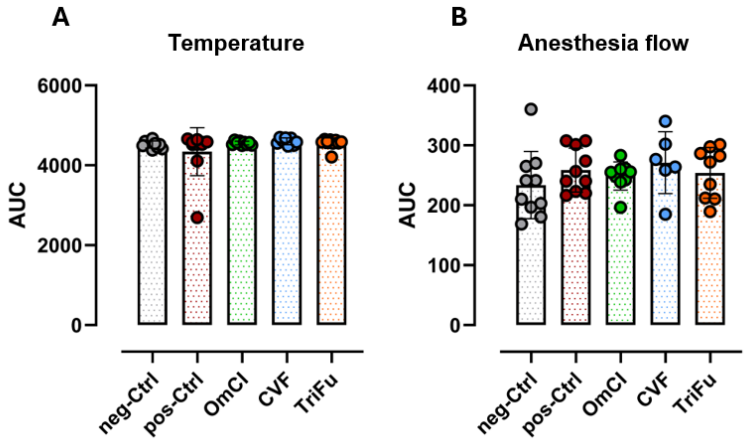
101. Poppelaars F, Holers VM, Thurman JM: Friend or foe: assessing the value of animal models for facilitating clinical breakthroughs in complement research. The Journal of Clinical Investigation 135:e188347 (2025)
102. Porto BN, Alves LS, Fernández PL, Dutra TP, Figueiredo RT, Graça-Souza AV, Bozza MT: Heme Induces Neutrophil Migration and Reactive Oxygen Species Generation through Signaling Pathways Characteristic of Chemotactic Receptors*. Journal of Biological Chemistry 282:24430-6 (2007)
103. Preissner KT, Podack ER, Müller-Eberhard HJ: The membrane attack complex of complement: relation of C7 to the metastable membrane binding site of the intermediate complex C5b-7. J Immunol 135:445-51 (1985)
104. Proctor LM, Moore TA, Monk PN, Sanderson SD, Taylor SM, Woodruff TM: Complement factors C3a and C5a have distinct hemodynamic effects in the rat. International Immunopharmacology 9:800-6 (2009)
105. Raynes JG. Acute-Phase Proteins. Encyclopedia of Life Sciences: John Wiley & Sons; 2015. p. 1-9.
106. Ricklin D: Complement-targeted therapeutics: Are we there yet, or just getting started? European Journal of Immunology 54 (2024)
107. Ricklin D, Hajishengallis G, Yang K, Lambris JD: Complement: a key system for immune surveillance and homeostasis. Nat Immunol 11:785-97 (2010)
108. Riedemann NC, Guo R-F, Bernacki KD, Reuben JS, Laudes IJ, Neff TA, Gao H, Speyer C, Sarma VJ, Zetoune FS, Ward PA: Regulation by C5a of Neutrophil Activation during Sepsis. Immunity 19:193-202 (2003)
109. Risitano AM, Notaro R, Marando L, Serio B, Ranaldi D, Seneca E, Ricci P, Alfinito F, Camera A, Gianfaldoni G, Amendola A, Boschetti C, Di Bona E, Fratellanza G, Barbano F, Rodeghiero F, Zanella A, Iori AP, Selleri C, Luzzatto L, Rotoli B: Complement fraction 3 binding on erythrocytes as additional mechanism of disease in paroxysmal nocturnal hemoglobinuria patients treated by eculizumab. Blood 113:4094-100 (2009)
110. Risitano AM, Peffault de Latour R, Marano L, Frieri C: Discovering C3 targeting therapies for paroxysmal nocturnal hemoglobinuria: Achievements and pitfalls. Seminars in Immunology 59:101618 (2022)
111. Rodríguez de Córdoba S, Esparza-Gordillo J, Goicoechea de Jorge E, Lopez-Trascasa M, Sánchez-Corral P: The human complement factor H: functional roles, genetic variations and disease associations. Mol Immunol 41:355-67 (2004)
112. Romejko K, Markowska M, Niemczyk S: The Review of Current Knowledge on Neutrophil Gelatinase-Associated Lipocalin (NGAL). International Journal of Molecular Sciences 24:10470 (2023)
113. Rossi V, Bally I, Ancelet S, Xu Y, Frémeaux-Bacchi V, Vivès RR, Sadir R, Thielens N, Arlaud GJ: Functional Characterization of the Recombinant Human C1 Inhibitor Serpin Domain: Insights into Heparin Binding. The Journal of Immunology 184:4982-9 (2010)
114. Röth A, Hock C, Konik A, Christoph S, Dührsen U: Chronic treatment of paroxysmal nocturnal hemoglobinuria patients with eculizumab: safety, efficacy, and unexpected laboratory phenomena. International Journal of Hematology 93:704-14 (2011)

115. Rother RP, Rollins SA, Mojcik CF, Brodsky RA, Bell L: Discovery and development of the complement inhibitor eculizumab for the treatment of paroxysmal nocturnal hemoglobinuria. Nat Biotechnol 25:1256-64 (2007)
116. Roumenina LT, Sène D, Radanova M, Blouin J, Halbwachs-Mecarelli L, Dragon-Durey M-A, Fridman WH, Fremeaux-Bacchi V: Functional Complement C1q Abnormality Leads to Impaired Immune Complexes and Apoptotic Cell Clearance. The Journal of Immunology 187:4369-73 (2011)
117. Roussel C, Morel A, Dussiot M, Marin M, Colard M, Fricot-Monsinjon A, Martinez A, Chambrion C, Henry B, Casimir M, Volle G, Dépond M, Dokmak S, Paye F, Sauvanet A, Le Van Kim C, Colin Y, Georgeault S, Roingeard P, Spitalnik SL, Ndour PA, Hermine O, Hod EA, Buffet PA, Amireault P: Rapid clearance of storage-induced microerythrocytes alters transfusion recovery. Blood 137:2285-98 (2021)
118. Roversi P, Johnson S, Caesar JJ, McLean F, Leath KJ, Tsiftsoglou SA, Morgan BP, Harris CL, Sim RB, Lea SM: Structural basis for complement factor I control and its disease-associated sequence polymorphisms. Proc Natl Acad Sci U S A 108:12839-44 (2011)
119. Ruminy P, Gangneux C, Claeyssens S, Scotte M, Daveau M, Salier JP: Gene transcription in hepatocytes during the acute phase of a systemic inflammation: from transcription factors to target genes. Inflammation Research 50:383-90 (2001)
120. Sánchez-Corral P, González-Rubio C, Rodríguez de Córdoba S, López-Trascasa M: Functional analysis in serum from atypical Hemolytic Uremic Syndrome patients reveals impaired protection of host cells associated with mutations in factor H. Molecular Immunology 41:81-4 (2004)
121. Savukoski S, Dettner AM, Schultze A, Gerber C, Steinberger MS, Halbgebauer R, Melter P, Dopler A, Palmer A, Braun CK, Hafner S, Nilsson B, Ekdahl KN, Mollnes TE, Heller R, Schrezenmeier H, Schmidt CQ, Huber-Lang MS, Mannes M: In vivo evidence of effective complement modulation by TriFu in comparison to C5 inhibition and complement depletion. Blood Adv (2026)
122. Schmidt CQ, Bai H, Lin Z, Risitano AM, Barlow PN, Ricklin D, Lambris JD: Rational engineering of a minimized immune inhibitor with unique triple-targeting properties. J Immunol 190:5712-21 (2013)
123. Schmidt CQ, Höchsmann B, Schrezenmeier H: The complement model disease paroxysmal nocturnal hemoglobinuria. European Journal of Immunology 54:2350817 (2024)
124. Schmidt CQ, Lambris JD, Ricklin D: Protection of host cells by complement regulators. Immunol Rev 274:152-71 (2016)
125. Schols S, Nunn MA, Mackie I, Weston-Davies W, Nishimura J-i, Kanakura Y, Blijlevens N, Muus P, Langemeijer S: Successful treatment of a PNH patient non-responsive to eculizumab with the novel complement C5 inhibitor coversin (nomacopan). British Journal of Haematology 188:334-7 (2020)
126. Schwaiger E, Wahrmann M, Bond G, Eskandary F, Böhmig GA: Complement Component C3 Activation: The Leading Cause of the Prozone Phenomenon Affecting HLA Antibody Detection on Single-Antigen Beads. Transplantation 97:1279-85 (2014)
127. Seegmiller JC, Bachmann LM: Urine Albumin Measurements in Clinical Diagnostics. Clinical Chemistry 70:382-91 (2024)
128. Seregina EA, Tsvetaeva NV, Nikulina OF, Zapariy AP, Erasov AV, Gribkova IV, Orel EB, Ataullakhanov FI, Balandina AN: Eculizumab effect on the hemostatic state

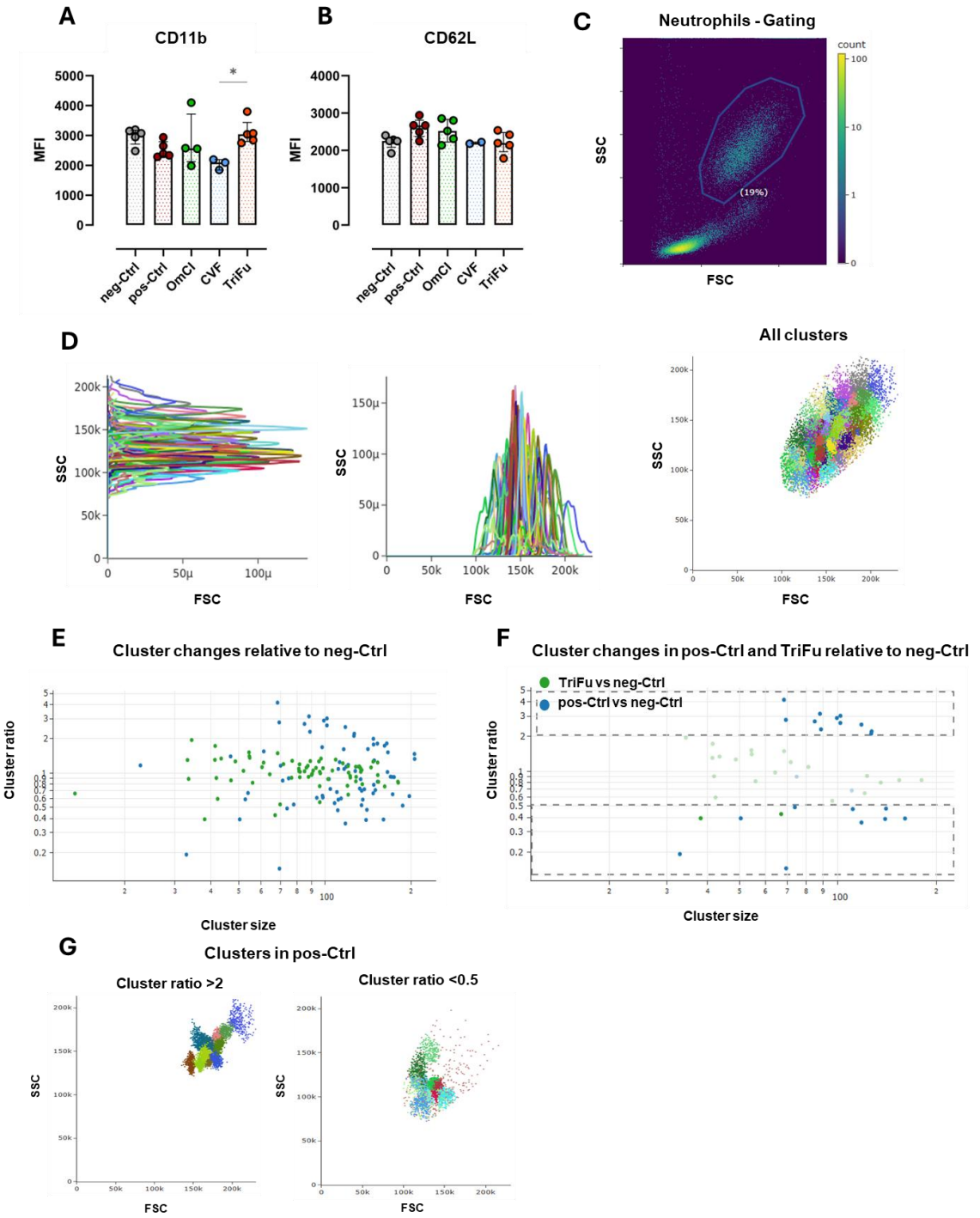
in patients with paroxysmal nocturnal hemoglobinuria. Blood Cells Mol Dis 54:144-50 (2015)
129. Settmacher B, Bock D, Saad H, Gärtner S, Rheinheimer C, Köhl J, Bautsch W, Klos A: Modulation of C3a activity: internalization of the human C3a receptor and its inhibition by C5a. J Immunol 162:7409-16 (1999)
130. Shah TA, Mauriello CT, Hair PS, Sharp JA, Kumar PS, Lattanzio FA, Werner AL, Whitley PH, Maes LA, Cunnion KM, Krishna NK: Complement inhibition significantly decreases red blood cell lysis in a rat model of acute intravascular hemolysis. Transfusion 54:2892-900 (2014)
131. Sica M, Rondelli T, Ricci P, De Angioletti M, Risitano AM, Notaro R: Eculizumab treatment: stochastic occurrence of C3 binding to individual PNH erythrocytes. Journal of Hematology & Oncology 10:126 (2017)
132. Sonnentag SJ, Dopler A, Kleiner K, Garg BK, Mannes M, Späth N, Akilah A, Höchsmann B, Schrezenmeier H, Anliker M, Boyanapalli R, Huber-Lang M, Schmidt CQ: Triple-fusion protein (TriFu): A potent, targeted, enzyme-like inhibitor of all three complement activation pathways. Journal of Biological Chemistry 300:105784 (2024)
133. Stahl D, Sibrowski W: Warm autoimmune hemolytic anemia is an IgM–IgG immune complex disease. Journal of Autoimmunity 25:272-82 (2005)
134. Steinberger M. Einfluss einer therapeutischen Komplementinhibition auf die akute Nierenschädigung nach induzierter Hämolyse. Ulm: University of Ulm; 2024.
135. Stevens LA, Levey AS: Measured GFR as a confirmatory test for estimated GFR. J Am Soc Nephrol 20:2305-13 (2009)
136. Stowell SR, Winkler AM, Maier CL, Arthur CM, Smith NH, Girard-Pierce KR, Cummings RD, Zimring JC, Hendrickson JE: Initiation and regulation of complement during hemolytic transfusion reactions. Clin Dev Immunol 2012:307093 (2012)
137. Stussi G, Huggel K, Lutz HU, Schanz U, Rieben R, Seebach JD: Isotype-specific detection of ABO blood group antibodies using a novel flow cytometric method. Br J Haematol 130:954-63 (2005)
138. Takabayashi T, Vannier E, Clark BD, Margolis NH, Dinarello CA, Burke JF, Gelfand JA: A new biologic role for C3a and C3a desArg: regulation of TNF-alpha and IL-1 beta synthesis. J Immunol 156:3455-60 (1996)
139. Tang G-Q, Tang Y, Dhamnaskar K, Hoarty MD, Vyasamneni R, Vadysirisack DD, Ma Z, Zhu N, Wang J-G, Bu C, Cong B, Palmer E, Duda PW, Sayegh C, Ricardo A: Zilucoplan, a macrocyclic peptide inhibitor of human complement component 5, uses a dual mode of action to prevent terminal complement pathway activation. Frontiers in Immunology Volume 14 - 2023 (2023)
140. Tosi MF, Zakem H, Berger M: Neutrophil elastase cleaves C3bi on opsonized pseudomonas as well as CR1 on neutrophils to create a functionally important opsonin receptor mismatch. J Clin Invest 86:300-8 (1990)
141. Tsioumpekou M, Krijgsman D, Leusen JHW, Olofsen PA: The Role of Cytokines in Neutrophil Development, Tissue Homing, Function and Plasticity in Health and Disease. Cells 12:1981 (2023)
142. Uribe-Querol E, Rosales C: Phagocytosis: Our Current Understanding of a Universal Biological Process. Front Immunol 11:1066 (2020)
143. Vandendriessche S, Cambier S, Proost P, Marques PE: Complement Receptors and Their Role in Leukocyte Recruitment and Phagocytosis. Front Cell Dev Biol 9:624025 (2021)

144. Wang H, van den Brink DJ, Heesters BA, Parren PWHI, Trouw LA: Local complement inhibition by selective precision-targeted therapies. Current Opinion in Immunology 98:102687 (2026)
145. Wang X, Cao L, Liu S, Zhou Y, Zhou J, Zhao W, Gao S, Liu R, Shi Y, Shao C, Fang J: The critical roles of IGFs in immune modulation and inflammation. Cytokine 183:156750 (2024)
146. Ward PA: The dark side of C5a in sepsis. Nature Reviews Immunology 4:133-42 (2004)
147. West EE, Kemper C: Complosome — the intracellular complement system. Nature Reviews Nephrology 19:426-39 (2023)
148. Wilken HC, Götze O, Werfel T, Zwirner J: C3a(desArg) does not bind to and signal through the human C3a receptor. Immunol Lett 67:141-5 (1999)
149. Wohlgemuth L, Stratmann AEP, Münnich F, Bernhard S, Thomaß BD, Münnich F, Mohamed AOK, Mannes M, Schmidt CQ, Nilsson Ekdahl K, Nilsson B, Fauler M, Föhr KJ, Huber-Lang M, Messerer DAC: Modulation of Neutrophil Activity by Soluble Complement Cleavage Products-An In-Depth Analysis. Cells 11 (2022)
150. Wood AJ, Vassallo AM, Ruchaud-Sparagano MH, Scott J, Zinnato C, Gonzalez-Tejedo C, Kishore K, D'Santos CS, Simpson AJ, Menon DK, Summers C, Chilvers ER, Okkenhaug K, Morris AC: C5a impairs phagosomal maturation in the neutrophil through phosphoproteomic remodeling. JCI Insight 5:e137029 (2020)
151. Xu R, Lin F, Bao C, Huang H, Ji C, Wang S, Jin L, Sun L, Li K, Zhang Z, Wang FS: Complement 5a receptor-mediated neutrophil dysfunction is associated with a poor outcome in sepsis. Cell Mol Immunol 13:103-9 (2016)
152. Yamada S, Asakura H: How We Interpret Thrombosis with Thrombocytopenia Syndrome? International Journal of Molecular Sciences 25:4956 (2024)
153. Zarantonello A, Revel M, Grunenwald A, Roumenina LT: C3-dependent effector functions of complement. Immunol Rev 313:120-38 (2023)
154. Zhang L, Dai Y, Huang P, Saunders TL, Fox DA, Xu J, Lin F: Absence of complement component 3 does not prevent classical pathway-mediated hemolysis. Blood Adv 3:1808-14 (2019)
155. Zipfel PF, Skerka C: Complement regulators and inhibitory proteins. Nat Rev Immunol 9:729-40 (2009)

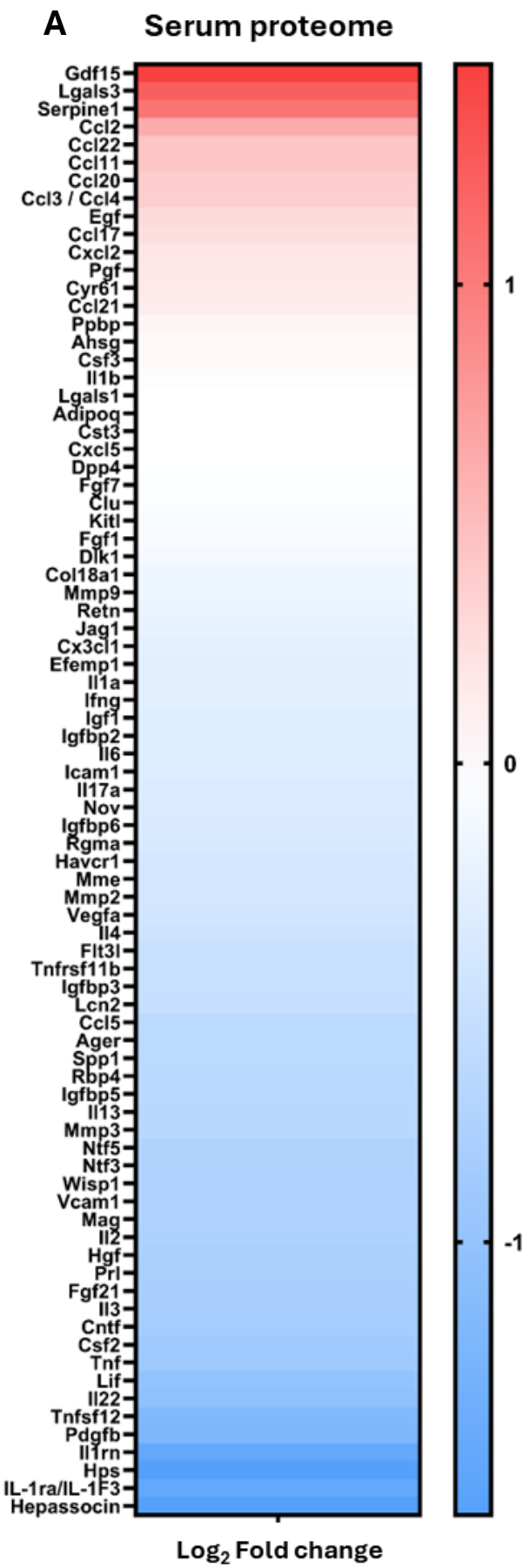
8. Appendix



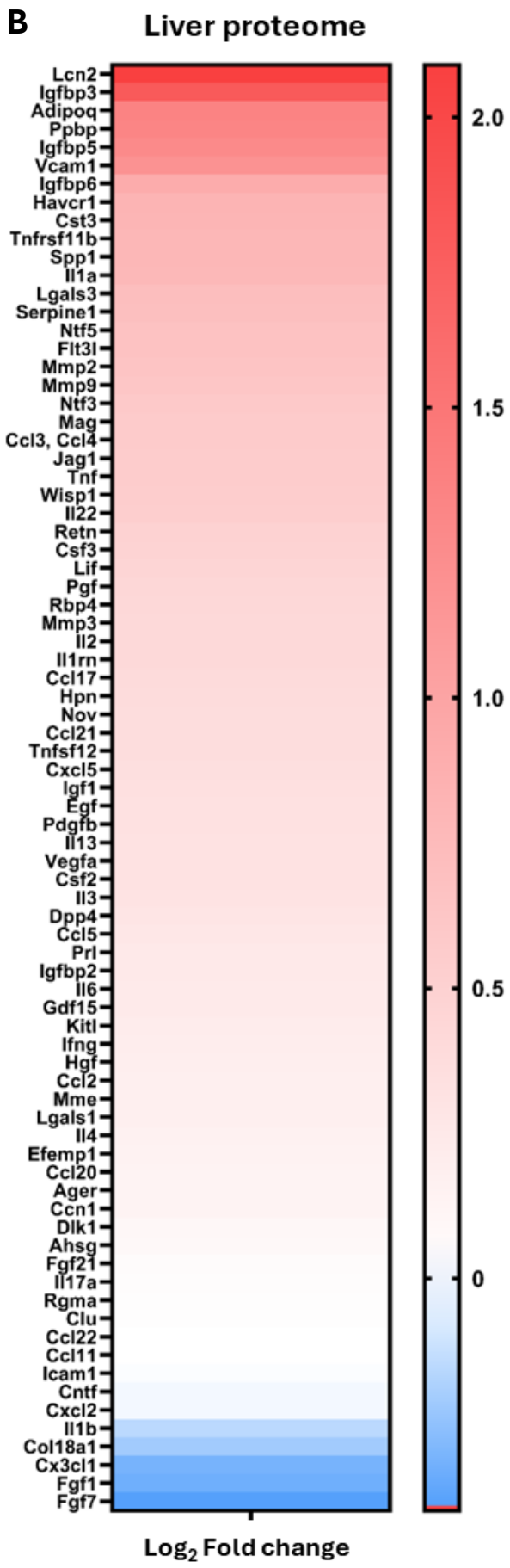
Supplemental figure 1. Analysis of area under the curve (AUC). Values plotted for A) temperature and B) anesthesia supply measured from all animals during the experimental timeline.



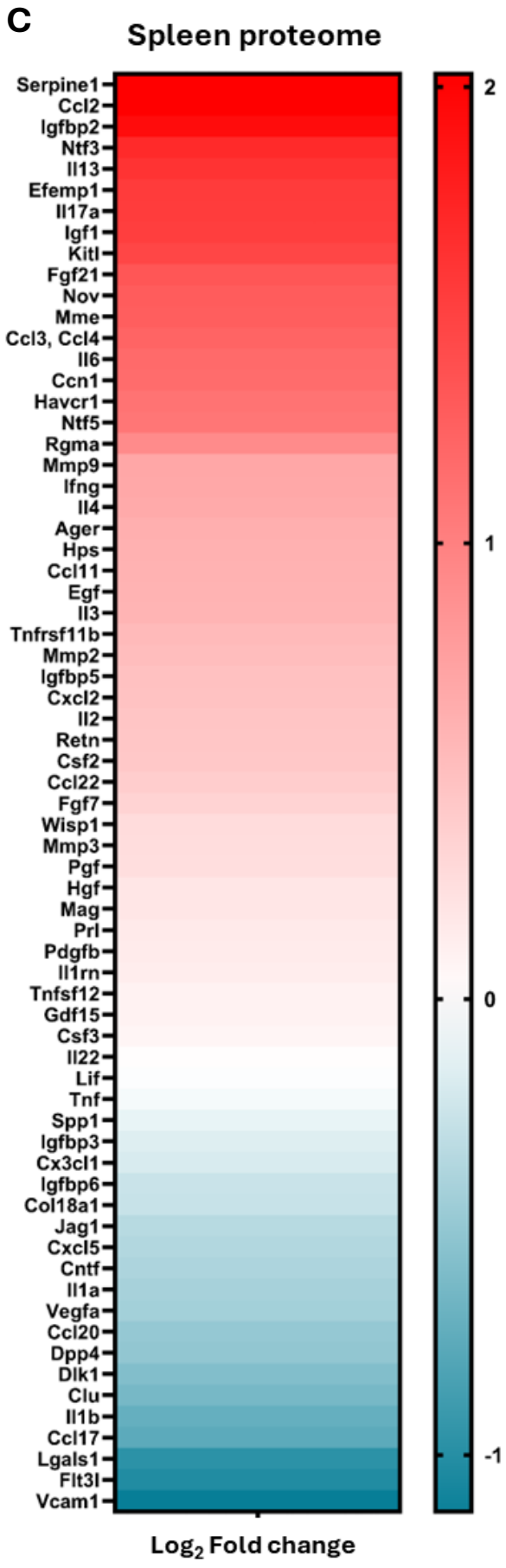
Supplementary figure 2. Analysis of rat neutrophils. Flow cytometric analysis of A) CD11b (MFI) and B) CD62L (MFI) on neutrophils. C-G) Subsequent machine-learning based analysis (Cytolution) of neutrophils subpopulations based on FSC, SSC, APC (CD11b), and PE (CD62L) markers. C) Gating strategy of neutrophils and their distribution based on D) SSC and FSC allowing cluster formation. E) Cluster changes in all animals or F) in pos-Ctrl and TriFu-treated animals in relation to neg-Ctrl animals (y=cluster ration and x=cluster size). G) Enriched clusters (cluster ratio >2) and reduced clusters (cluster ratio <0.5) in pos-Ctrl animals. Median with interquartile range is shown. Only statistically significant differences are indicated: $p \leq 0.05$ (*), $p \leq 0.01$ (**), $p \leq 0.001$ (***), $p \leq 0.0001$ (****). As author partially adapted from Savukoski et al., (2026) [121], CC BY-NC-ND 4.0, https://creativecommons.org/licenses/by-nc-nd/4.0/legalcode.en



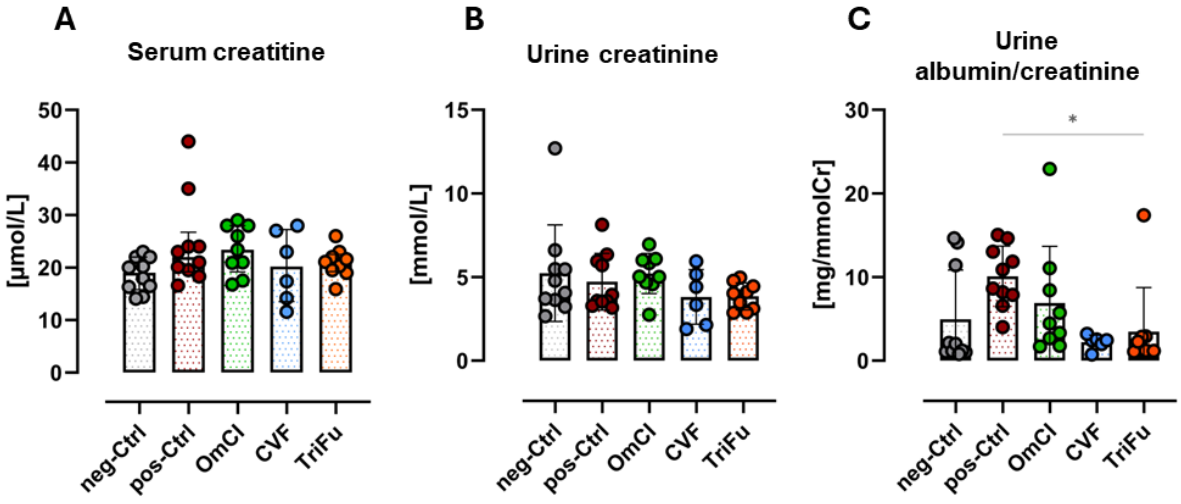
Supplemental figure 3A. Heatmap of rat serum proteins analyzed by Cytokine Proteome Profiler Rat XL Cytokine Array. Relative protein levels of the pos-Ctrl animal compared with the neg-Ctrl animal.



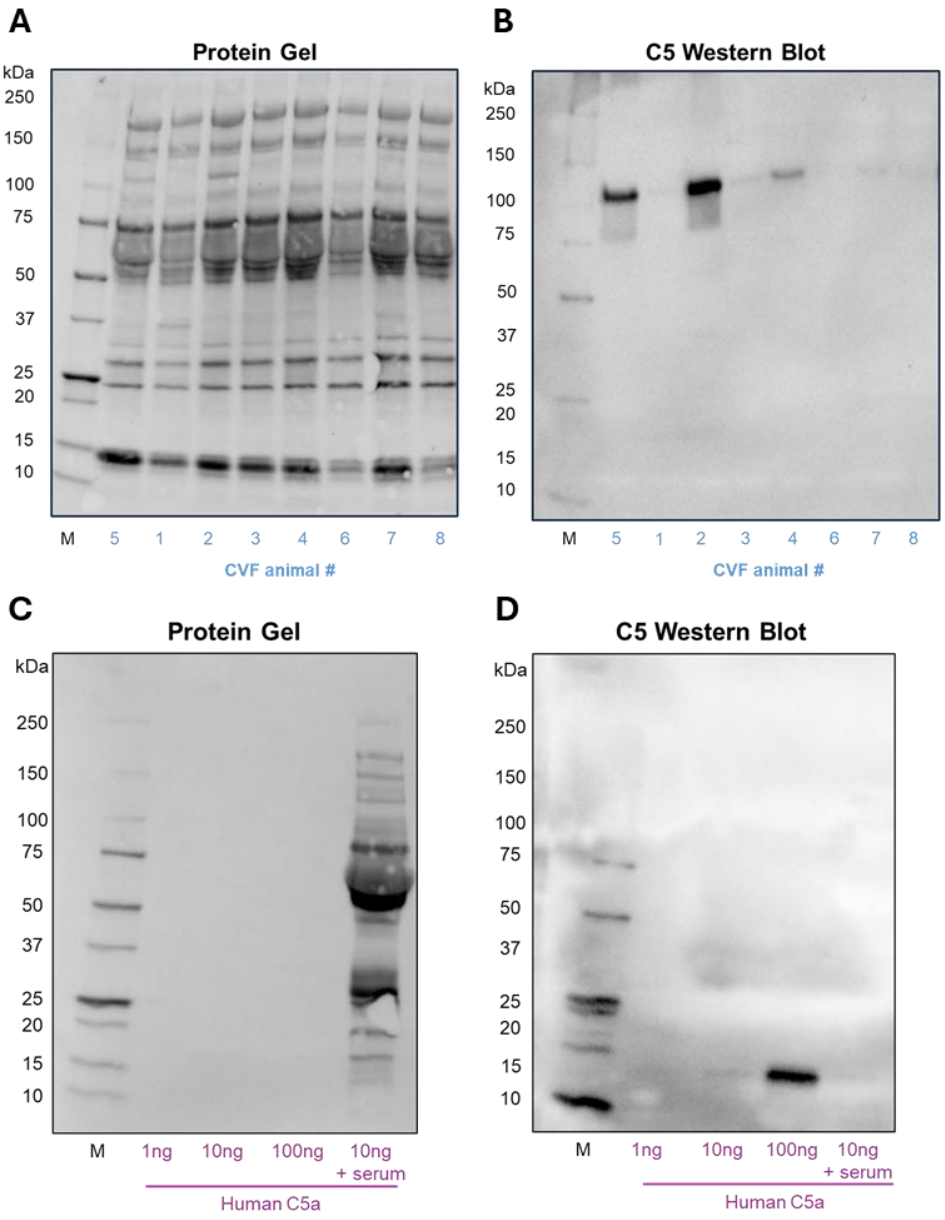
Supplemental figure 3B. Heatmap of rat liver proteins analyzed by Cytokine Proteome Profiler Rat XL Cytokine Array. Relative protein levels of the pos-Ctrl animal compared with the neg-Ctrl animal.



Supplemental figure 3C. Heatmap of rat spleen proteins analyzed by Cytokine Proteome Profiler Rat XL Cytokine Array. Relative protein levels of the pos-Ctrl animals compared with the neg-Ctrl animals.



Supplemental figure 4. Creatinine and albumin-creatinine-ratio. A) Serum creatinine (µmol/L), B) urine creatinine (mmol/L), and C) urine albumin/creatinine ratio (mg/mmol Cr). Median with inter-quartile range is shown. Only statistically significant differences are indicated: $p \leq 0.05$ (*), $p \leq 0.01$ (**), $p \leq 0.001$ (***), $p \leq 0.0001$ (****)**.** As author partially adapted from Savukoski et al., (2026) [121], CC BY-NC-ND 4.0, https://creativecommons.org/licenses/by-nc-nd/4.0/legalcode.en



Supplemental figure 5. Rat C5/C5a and human C5/C5a detection. A) Protein gel including plasma of CVF-treated animals and B) subsequent C5/C5a detection by western blot. Anti-rat C5a antibody (#PA5-78891, ThermoFischer Scientific) was used for detection. C) Protein gel for purified human C5a alone in different amounts (1, 10, 100 ng) or 10 ng C5 combined with 0,5 µl of human serum. D) C5 western blot analysis of C5a to determine the sensitivity of the method. Anti-human C5a antibody (#204889, CalbioChem) was used for detection. As author partially adapted from Savukoski et al., (2026) [121], CC BY-NC-ND 4.0, https://creativecommons.org/licenses/by-nc-nd/4.0/legalcode.en

Acknowledgements

This content has been removed for privacy reasons.

Declaration:

I hereby declare that I wrote the present dissertation with the topic:

TriFu effectively modulates the complement system activation in a rat xenotransfusion model

independently and used no other aids that those cited. In each individual case, I have clearly identified the source of the passages that are taken word for word or paraphrased from other works.

I also hereby declare that I have carried out my scientific work according to the principles of good scientific practice in accordance with the current „Satzung der Universität Ulm zur Sicherung guter wissenschaftlicher Praxis" [Rules of the University of Ulm for Assuring Good Scientific Practice].

Ulm, (date) 30.06.2026

(Signature)

Name, surname: Susa Savukoski

Statutory declaration

I hereby declare that I have carried out my scientific work independently and according to the principles of good scientific practice in accordance with the current „Satzung der Universität Ulm zur Sicherung guter wissenschaftlicher Praxis" [Rules of the University of Ulm for Assuring Good Scientific Practice]. I have used no sources or resources other than those specified, and have identified any passages taken verbatim or in substance as such.

During the preparation of this work, I used AI only in order to improve readability and language. After using AI, I reviewed and edited the content as needed and take full responsibility for the content in thesis.

The work has not been submitted in the same or a similar form for a doctoral degree program either in Germany or abroad. The data on which the dissertation is based has not been published as part of another doctoral degree program.

I am not currently enrolled in any other doctoral program, nor have I applied for one.

There are no criminal proceedings pending against me.

Ulm, 30.06.2026 Signature